ANALYSIS OF ICE AND METOCEAN MEASUREMENTS, CHUKCHI SEA, 2009-2010

Prepared for:

Shell Exploration and Production
Houston TX
Attn: Mark Hansen

By:

D.B. Fissel, T.D. Mudge, K. Borg, N. Kulan, D. Sadowy, K. Budd, J. Lawrence, J.R. Marko, A. Kanwar, D. Cowen and A. Bard

ASL Environmental Sciences Inc.
#1 - 6703 Rajpur Place,
Victoria, B.C.
Canada V8M 1Z5

ASL File: PR-701
May 2011
Final Version

The correct citation for this report is:

D.B. Fissel, T.D. Mudge, K. Borg, N. Kulin, D. Sadowy, K. Budd, J. Lawrence, J.R. Marko, A. Kanwar, D. Cowen and A. Bard, 2011. Analysis of Ice and Metocean Measurements, Chukchi Sea, 2009-2010. Report for Shell Exploration and Production by ASL Environmental Sciences Inc., Victoria, B.C. Canada. xi + 118 p.

EXECUTIVE SUMMARY

A program of ice keel depth and ice velocity measurements was carried out off northwestern Alaska in support of oil and gas exploration by Shell in the Chukchi Sea from September 2009 to July 2010. The data collection program involved the deployment and operation of two underwater, internally recording instruments at two sites (Crackerjack and Burger) in 45 to 46 m depth for nearly a year. The 2009 to 2010 data sets represent the second year of a multiyear measurement program planned for the two offshore sites in the Chukchi Sea, offshore of Wainright, Alaska.

Key results of the 2009 to 2010 measurement program included:

Ocean Wave measurements

In October 2009, there were three storms when the significant wave heights approached or exceeded 4 m. The largest wave heights (Oct. 21 to 24) at the Crackerjack site reached a maximum significant wave height value of 5.6 m (10.9 m maximum individual wave height) with a corresponding peak period of 10s. At the Burger site, during this same event, the largest significant wave height was 5.1 m. During this event, wind speeds at Point Lay exceeded 19 knots for several hours. For all non-ice measurement times, the average significant wave heights were 1.2 m at Burger and 1.4 m at Crackerjack.

Large Ice Keels

Very deep ice keels were observed at both Burger and Crackerjack with 9 keels at Burger and 18 keels at Crackerjack measuring over 20 m ice draft. The deepest keels at Burger and Crackerjack were 26.1 m and 23.7 m respectively.

Keels exceeding 12 m ice draft were measured in all months from December 2009 to May 2010 at both sites and in June 2010 at Crackerjack. The total number of ice keels having ice drafts exceeding 5, 8 and 11 m were 7345, 2273 and 626 respectively for Burger and 8363, 2726 and 808 for Crackerjack. The average widths of the individual ice drafts with thresholds of 5, 8 and 11 m were 30.9, 35.1 and 40.3 m for Burger and 29.0, 33.4 and 39.4 m for Crackerjack, respectively.

By comparison to the first year of measurements, 2008-2009, there was a notable reduction at both sites for the total number of keels and the total distance of ice measured (in 2008-2009, the number of keels > 5 m ice draft were 13,628 and 12,924 at Burger and Crackerjack, respectively). The 2008-2009 maximum keel ice draft was 27.0 and 27.7 m, at Burger and Crackerjack.

There were occurrences of ice keels with very large horizontal dimensions of up to a few hundred meters. The widest keels, using a threshold of 5 m, were 273 m for Burger and 262 m for Crackerjack.

Ice Velocities

The region has a very dynamic ice regime with ice movement occurring 97% of the time at both Burger and Crackerjack from November 2009 to June 2010. The greatest percentage of no-motion events for a month in this measurement period was 12% at Burger in March 2010.

Over ten occurrences of large ice velocities were measured throughout the year. Over a 30 minute ensemble averaging period, peak ice velocities of 87 cm/s at Burger and 64 cm/s at Crackerjack were observed. The episodes of large ice velocities were associated with strong wind events having peak speeds of 5 to 9 m/s (10 to 18 knots). At both sites, the median ice drift was generally highest in November and December (17-28 cm/s) and lower (~10 cm/s) from January to July. The lone exception of a 28 cm/s ice velocity occurred in June at Crackerjack

Ocean Currents

Ocean currents were also measured over a 30 minute period. During major events, current speeds exceeded 40 cm/s at Burger. Whereas currents at Crackerjack were weaker than those observed at Burger with events rarely exceeding 40 cm/s. From September to late December, current speeds were typically large and associated with strong wind events that were at times greater than 8 m/s as measured at Wainwright. During January the currents were typically lower except for a large event late in the month. Currents then generally remained weak for the rest of the ice season.

Surface current directions at Burger were aligned along an E-W axis, and were more variable than the surface currents at Crackerjack, which were predominantly to the NE. Mid-depth and near-bottom current directions were less variable than the surface and were predominately towards the ESE and NE for Burger and Crackerjack respectively.

Inertial oscillations are present in the ocean current data during the times of reduced or zero ice concentrations. These twice-daily ocean current variations produced a peak to trough current variation of up to 35 cm/s, and they appeared to be more prevalent at Crackerjack.

ACKNOWLEDGEMENTS

Many persons and organizations contribute to making a project of this scope possible, including:

Our Client, Shell Exploration and Production:

Mark Hansen, Project Manager, Shell

The Captain and Crew of the vessels CCGS Sir Wilfred Laurier (deployment) and MV Norseman II (recovery)

Dr. Humfrey Melling, Chief Scientist on the CCGS Laurier, Department of Fisheries and Oceans, Canada

Sheyna Wisdom, Project Coordinator, Greeneridge Sciences Inc.

Logistical support and vessel for recovery provided by:

Jeff Hastings, Project Manager, Olgoonik Fairweather LLC

Carley Hastings and Tom Ainsworth of Olgoonik Fairweather LLC

Technical Support from:

Dave English and Rick Birch of ASL Environmental Sciences Inc.

Program Management Support from:

Bernadette Fissel and Des Buermans of ASL Environmental Sciences Inc.

TABLE OF CONTENTS

DATA ARCHIVE SECTION

A complete set of data files, along with additional data products, in the form of plots and tables such as JFTs are provided in this Data Archive Section (available on the project ftp site or via DVD discs).

LIST OF FIGURES

LIST OF TABLES

1 INTRODUCTION

1.1 STUDY OBJECTIVES

The Shell Alaska (Shell) team is examining geotechnical and environmental forcing issues related to offshore production systems for the Chukchi Sea exploration lease areas off northwestern Alaska. As part of the study, ASL Environmental Sciences (ASL) was contracted to collect and analyze data on ice drafts and ice velocities in the lease areas. Additionally, ocean current profiles, non-directional waves, salinity and temperature of seawater were also measured and analyzed. This report presents the results of the measurements obtained in the second year of the Shell Chukchi Sea measurement program.

Measurements of ice drafts and velocities were obtained with upward looking sonar instrumentation in taut-line moorings at two sites in Chukchi Sea (Figure 1-1). The measurement program was first started in October 2008 at two sites, one in the Crackerjack lease block and the other in the Burger lease block. For this second year of the program, measurements began in late September 2009. It is part of a series of sea ice and oceanographic programs conducted by ASL for Shell that started in September 2005 in Camden Bay and later expanded into Chukchi Sea in September 2008.

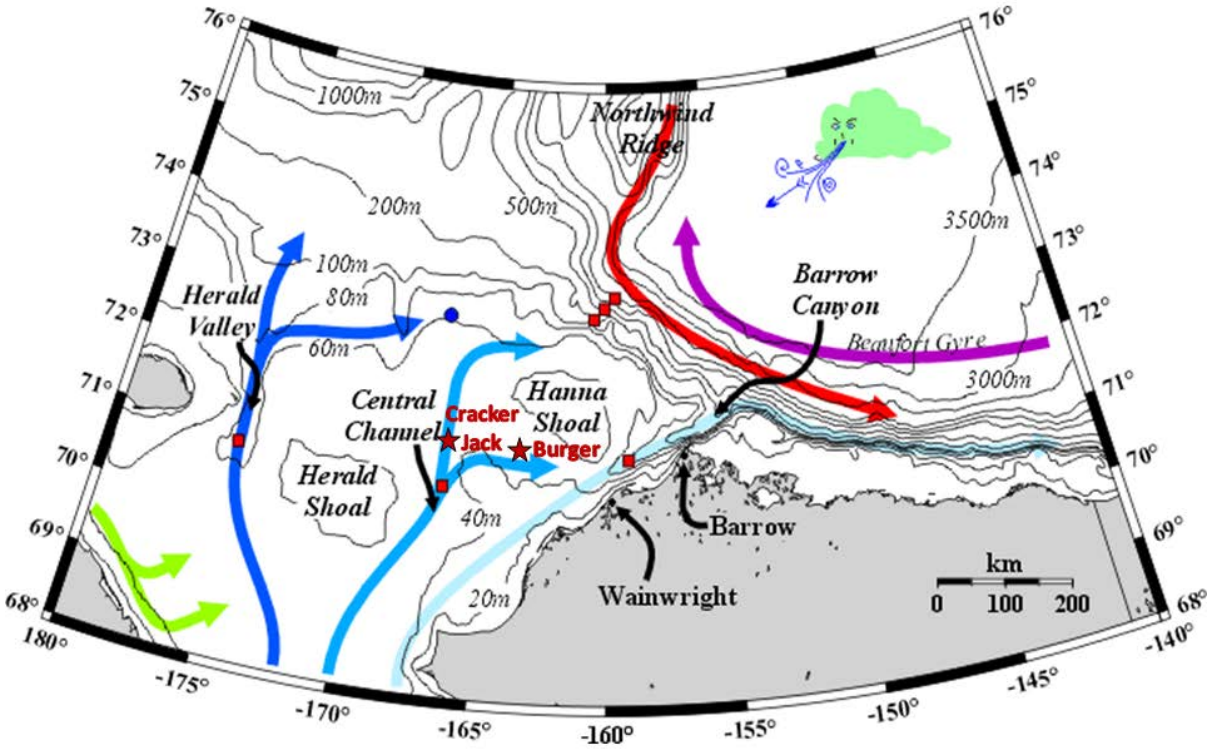

Figure 1-1. The location of the two measurement sites (dark red stars), Crackerjack and Burger, are plotted on a map by University of Alaska Institute of Marine Science (Weingartner et al., 2009) of the Chukchi and Beaufort Seas. Also plotted are the main currents and the depth contours from 20 to 3500 m. Pacific waters (3 shades of blue) originating in Bering Strait to the south at 170W, Siberian Coastal Current (green), Atlantic Water on the continental slope (red) and the anticyclonic circulation of the Beaufort Gyre surface waters (purple). The red squares represent the locations of previous oceanographic moorings operated by the U. of Alaska.

The field portion of the project was conducted for Shell through a contract with ASL to provide the scientific instruments and equipment, provide assistance in deployment and recovery of the equipment, and provide processing and analysis of the collected data sets.

The 2009-2010 measurement program was carried out within two different logistical arrangements for the deployment and recovery stages. For the deployment, a collaborative agreement was entered into with the Canadian Department of Fisheries and Oceans (under the supervision of Dr. Humfrey Melling, Institute of Ocean Sciences) to provide access to the Canadian Coast Guard icebreaker, CCGS Sir Wilfrid Laurier. The equipment recovery (to conclude the 2008-2009 measurement program) and re-deployment (to start the data collection for the 2009-2010 measurement program) was carried out as the CCGS Laurier traveled westward through the Beaufort and Chukchi Seas (Figure 1-2) in September and October of 2009 as part of its summer operations in Arctic waters.

At the end of 2009-2010 measurement program, Olgoonik Fairweather LLC (Fairweather) was contracted to provide support personnel, equipment and services for the recovery of the instrumentation. After the retrieval of the data, the instruments were serviced and re-

deployed to start the third consecutive year (2010-2011) of the Chukchi Sea measurement program for Shell. Recovery and re-deployment operations were conducted on board the vessel MV Norseman II.

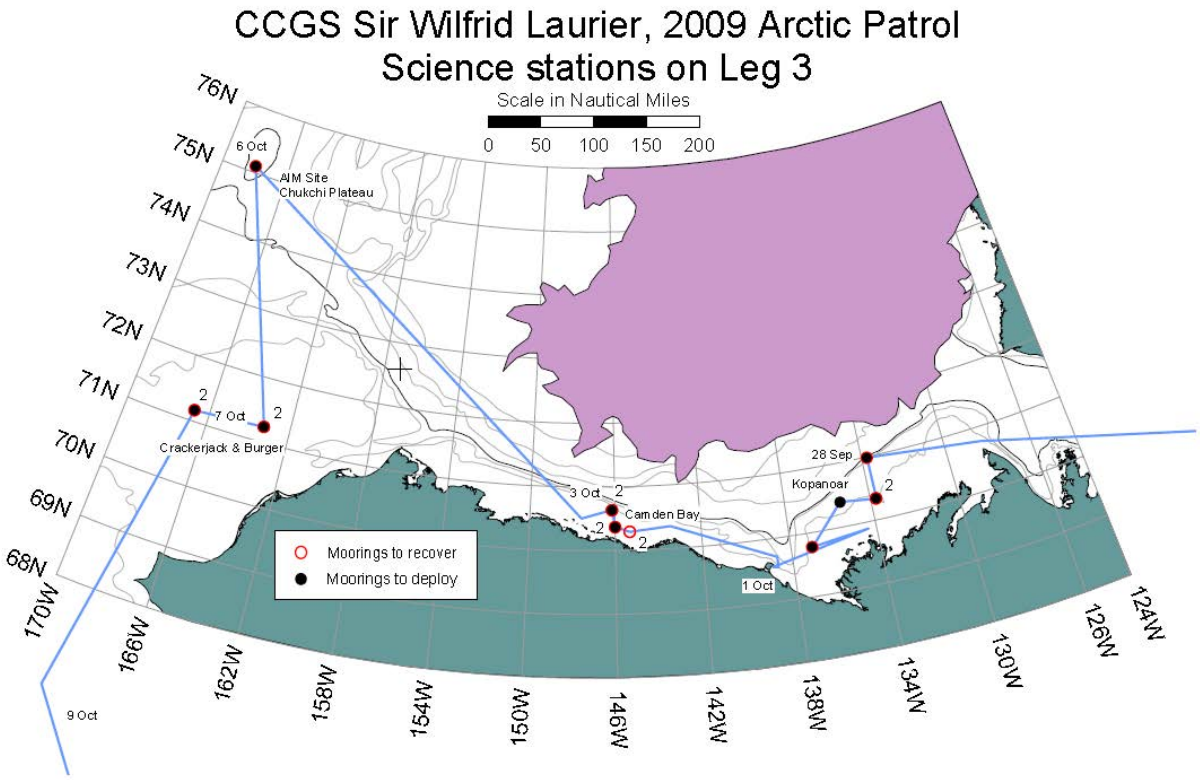

Figure 1-2. The locations of the Shell measurement sites in Chukchi Sea and Camden Bay (red circles, filled with black for redeployed near 71°N 166°W for Chukchi Sea sites and just north of 70°N 146°W for Camden Bay sites) shown on the ship track of the CCGS Laurier as it travelled westward through the Beaufort Sea from Sept. 28 to Oct. 9, 2009 (Melling, 2009).

1.2 OVERVIEW OF THE STUDY AREA AND SEASONAL ICE CONDITIONS

The Chukchi Sea is an Arctic shelf sea with water depths of less than 200 m representing part of the western Arctic Ocean. However, it is closely linked to the Pacific Ocean both atmospherically (through Aleutian Low) and oceanographically (through Bering Strait). The water masses in the study area are dominated by the inflow of Pacific waters that enter the Arctic Ocean through Bering Strait (Figure 1-1). The three branches of Pacific waters are color-coded with dark blue being the most nutrient-rich waters and light blue being the least nutrient-rich (Weingartner et al., 2009).

The Crackerjack measurement site lies in a 45m deep region west of Hanna Shoal and north of where the central channel flow has split into a predominately northerly flow. Burger is located south of Hanna Shoal and in the other branch of the bifurcated central channel flow. On average, the flow direction in the vicinity of Burger site is eastward and weaker than the flow at Crackerjack. While the average current speed of the central channel flow is approximately 8 cm/s, short-term wind forced currents can dominate with observed currents of up to 50 cm/s.

The sea ice in the region is characterized by three major categories: the offshore, mobile polar pack ice of the Arctic Ocean, a narrow region of landfast ice and a poorly studied area of highly mobile coastal zone ice (Norton and Gaylord 2004). The landfast ice zone is typically on the order of 10 km wide. Sea-ice is for the most part consolidated in the region over winter. By March, the on-average, anti-cyclonic (clockwise) pattern of ice movement known as Beaufort Gyre produces a semi-permanent polynya (Chukchi flaw zone) within about 100 km of the coast. At the Burger location, 120 km west-northwest of Wainwright, is generally within the flaw zone while at Crackerjack, about 240 km west-northwest of Wainwright, is dominated by a coherent pack ice. Figure 1-3 provides a schematic of the ice zones.

New ice formation in the Chukchi Sea begins in nearshore areas in early October while the outer edge of the offshore ice pack edge can be several hundred kilometers north of the coastline. Growth is characterized by outward extension and thickening of the nearshore ice cover. Simultaneously, new growth also appears in the offshore pack, primarily in areas of open water and thin ice.

Breakup of landfast ice near Barrow since 2000 has occurred in a period from mid June to early July. The 2010 breakup of sea ice in the Shell lease areas began in late May at Burger and was evident at Crackerjack in early June. Occasional ice floes originating to the north from the pack ice edge (just north of 72°N) continued to pass the measurement sites until well into July. The clearing of the sea ice in the eastern Chukchi Sea was approximately 3 to 5 weeks earlier in 2010 than in the year 2009.

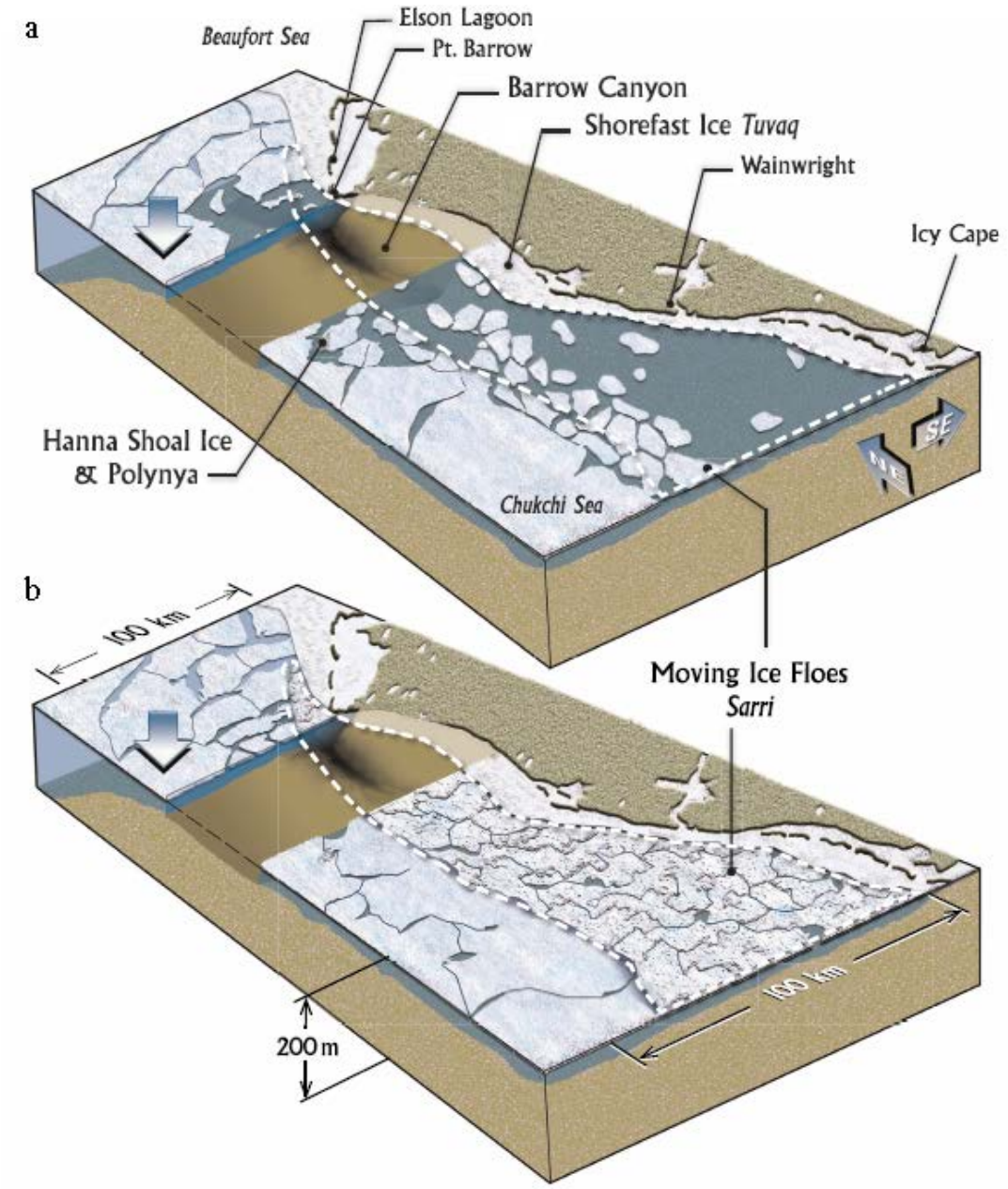

Figure 1-3. Ice dynamics in the Chukchi Sea (Norton and Gaylord, 2004). The dashed white line indicates Alaska's northern Chukchi Sea flaw zone from Icy Cape to the western edge of the Beaufort Sea. a) Ice moving to the southwest and b) ice moving to the northeast.

The coastal ice zone (sometimes referred to as the transition zone), located between the near-shore landfast ice and the offshore polar pack zone, is characterized by very dynamic ice conditions. This zone is characterized by interactions involving incursions of the polar pack-ice along with the mobile locally grown sea ice with the outer edge of the landfast ice which results in the formation of ridges, leads, and polynyas. The large ridge fragments, when grounded, are referred to as *stamukhi*. A system of leads or long narrow bands of open water, also occur intermittently along the edge of the landfast ice. Under offshore

movements of the mobile ice, large areas of open water can also occur as polynyas or large-scale flaw leads offshore of the coastline and its adjoining landfast ice.

In the adjoining Beaufort Sea where stamukhi have been studied since the 1970's, they are known to establish the seaward boundary of the immobile landfast ice through contact between their keels and sea floor.

Floeberg is another ice feature that is observed in the Beaufort Sea but is not as well documented in the Chukchi Sea. A floeberg is a massive hummock sea ice or a group of hummock sea ice frozen together. Hummock sea ice is formed when individual ice floes impinge upon each other or push against weaker ice resulting in the "haphazard accumulation of ice blocks of a most irregular and formidable appearance" (Kovacs and Mellor, 1974). In the Alaskan Beaufort Sea floebergs have been observed to extend over distances of many kilometers parallel to the coastline with sail heights of 5 to 25 m. In the Chukchi Sea, Stinger and Groves (1991) observed a similar process at Hanna's Shoal where a seamount (71.94°N,161.48°W) extends to within 20 m of the sea surface; and at Herald Shoal which is within 10 m of the sea surface (70.37°N, 170.85°W). The wedge of ice grounded on Hanna's Shoal, known as Katie's Floeberg, has been observed on occasion to have a cross section of about 10 km and a length of 8 to 38 km (Barrett and Stringer, 1978). The wedge of ice has been observed to break loose with changes in the direction of ice motion.

The presence of a semi-permanent flaw zone in northern Chukchi Sea due to an abrupt change in landmass distribution resisting the westward movement of polar pack ice past Point Barrow is the reason for coastal ice regimes to differ between the Beaufort and Chukchi Seas. Individual ice floes in the Chukchi Sea flaw zone move differently than the polar pack ice. The dominant direction of motion for ice floes in the northern Chukchi Sea flaw zone is East-Northeast, while polar pack ice moves westward on-average. The maximum speed attained by individual ice floes in the flaw zone can be ten times as fast as the polar pack ice, according to a study by Norton and Gaylord (2004) based on analysis of satellite imagery. They also found that fastest ice floes were moving to the West-Southwest, opposite to the dominant ice floe motion. Floes less than 10 km in diameter can reach speeds as large as 140 cm/s (Norton and Gaylord, 2004).

1.3 ORGANIZATION OF THE REPORT

This report is organized into several sections reflecting the various phases of the study.

- Section 2 presents a summary of the data collection program, including the field operations (Deployment and Recovery) and the instrumentation and methodology used for data collection.
- Section 3 presents summaries of the data processing results for each type of data collected.

- Section 4 presents the results of an analysis of the ice draft data set involving detailed statistical summaries, and the width of very large observed ice features. Analysis results are also presented for ice velocities and ocean waves.

- Finally, a summary of the study and analyses of the largest observed ice keels are presented in Section 5, followed by literature and report citations in Section 6.

More detailed information, key study data sets and results derived from the data processing tasks of this study are provided in a Data Archive via an FTP site.

2 DATA COLLECTION

2.1 INSTRUMENTATION

The primary instruments utilized in this study were the Ice Profiling Sonar (IPS-5), manufactured by ASL Environmental Sciences Inc (ASL), which allows detailed measurements of ice keel depths, and the Teledyne RDI Acoustic Doppler Current Profiler (ADCP), which measures ice and ocean current velocities.

The IPS and ADCP instruments were deployed using separate near-bottom taut line moorings at Sites Crackerjack and Burger (Figure 2-1). The IPS and ADCP moorings were located within 200 meters of each other, for each site, and their configurations were as shown in Figure 2-2.

To provide additional speed of sound information, a self-contained conductivity/temperature sensor, a RBR XR420 CT data logger, was attached to the IPS-5 mooring frame only at Site Crackerjack (Figure 2-3).

Recovery was carried out through use of acoustic release devices, which are activated by sonar signals transmitted from a command unit operated from the deck of the deployment/recovery vessel. Mooring details, including their location, depth, and deployment and recovery times are shown in Table 2-1.

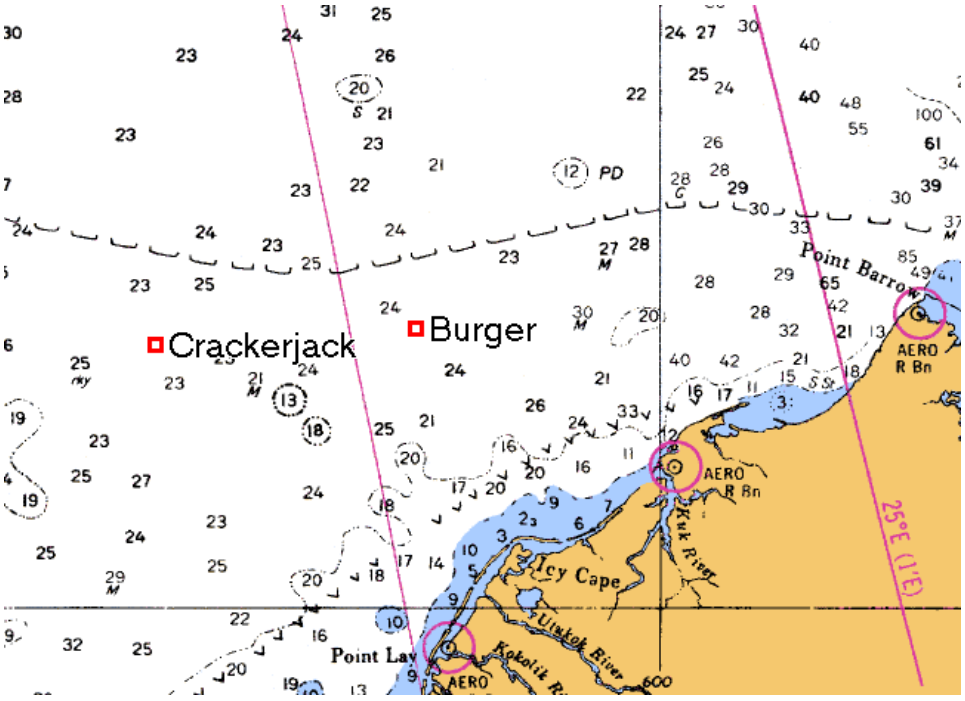

Figure 2-1. Map of mooring locations for Crackerjack and Burger, 2009-2010 field program.

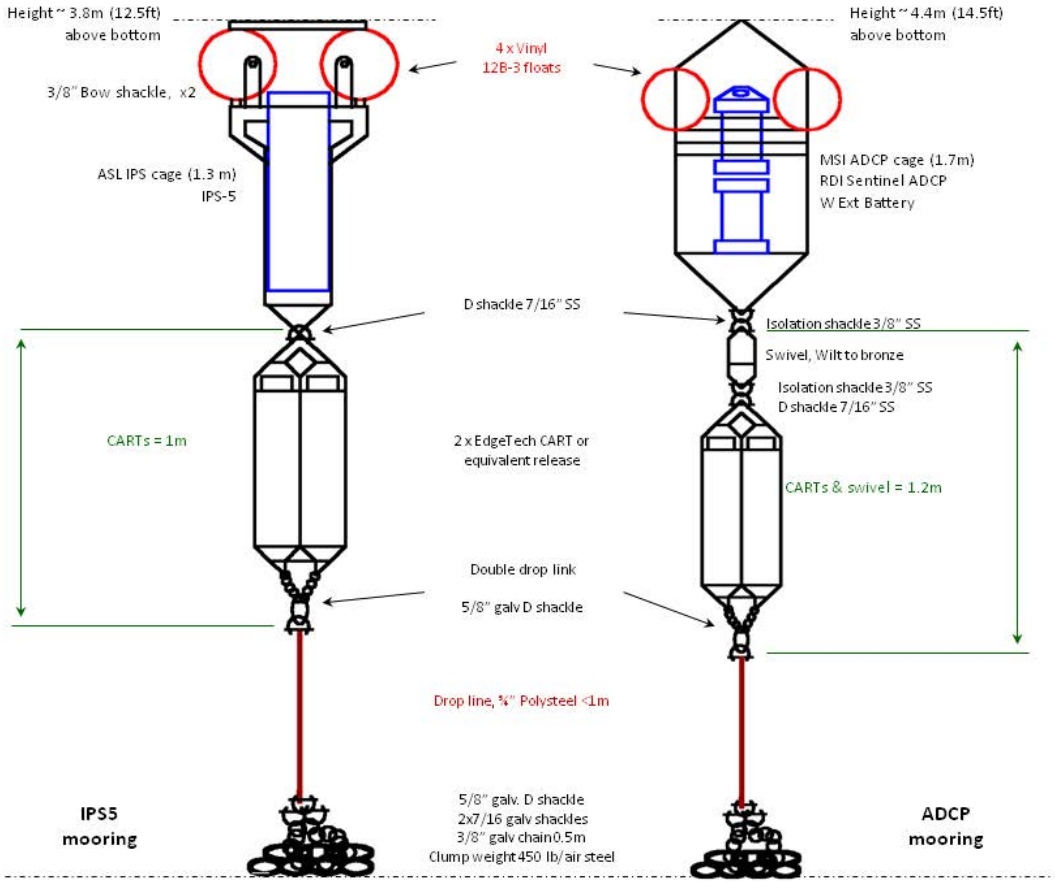

Figure 2-2. A schematic diagram of the taut line moorings used for deployment of the IPS and ADCP instruments. Each instrument is at the upper end of the mooring supported by four plastic Vinyl floats. Two acoustic releases (EdgeTech CART units) are located below.

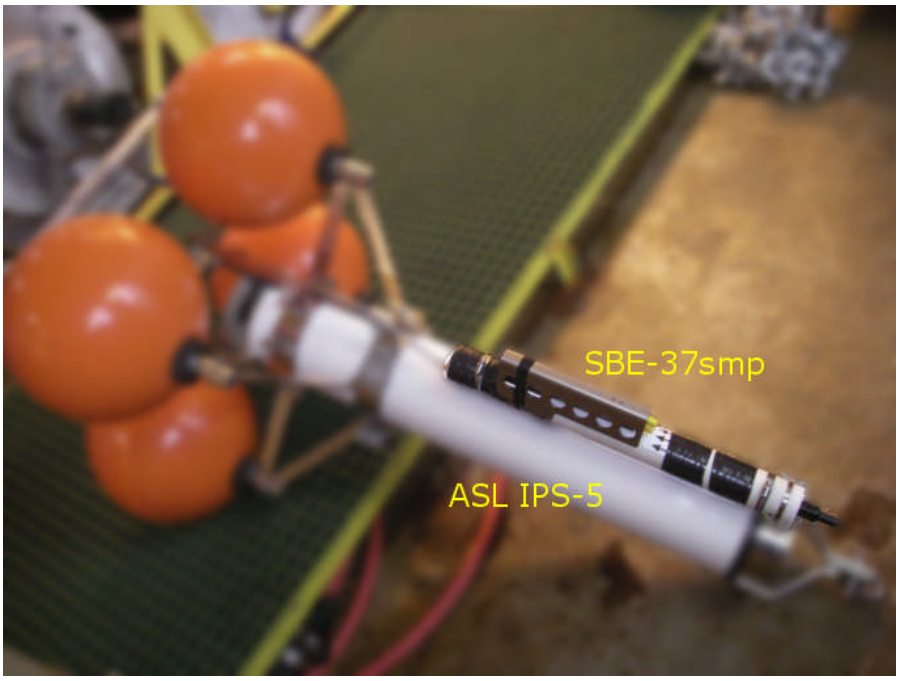

Figure 2-3. SBE 37-SMP mounted on IPS-5 frame. All of the image but the SBE 37 has been intentionally blurred.

The ASL IPS-5 provides a continuous full-year record of ice draft at sampling rates of once every 1 or 2 seconds. In combination with ADCPs, used to measure ice velocities, ice draft time series acquired with IPS instruments can be converted to a distance series equivalent. The IPS-5 also provided 2 Hz wave bursts during the ice-free season.

The instrumentation used in this study has been widely used in other parts of the world, including the greater Arctic Ocean region, where sea ice is present for nearly the entire year (Melling et al., 1995), and in marginal seasonal ice zones (Fissel, Marko and Melling, 2008).

Table 2-1. Instrumentation, locations, and deployment and recovery times for the moorings operated in the Chukchi Sea from October 2009 to July 2010. Further details are available in the Cruise Report (Borg et al., 2010).

Site	Instr. Type	Latitude	Longitude	Water Depth (m)	Deployment Date	Recovery Date
Crackerjack	IPS-5	71°10.2021' N	166°45.0071' W	45.3	Oct 8, 2009	Jul 27, 2010
	ADCP	71°10.1815' N	166°44.9315' W	45.6	Oct 8, 2009	Jul 27, 2010
Burger	IPS-5	71°14.3723' N	163°16.8523' W	44.7	Oct 7, 2009	Jul 29, 2010
	ADCP	71°14.3922' N	163°16.8120' W	44.7	Oct 7, 2009	Jul 29, 2010

The use of two separate moorings at each monitoring site was dictated by a need to keep the instruments as close to the seabed as possible, whereas, in deeper waters, the IPS-5 is often located above the ADCP on a single taut line mooring. It was expected that the largest sea-ice keels could have keels nearly as deep as the water depth at the measurement locations, raising concerns that collisions with sea-ice could lead to loss of the instruments as well as of the collected data sets.

2.1.1 ICE PROFILING SONAR (IPS)

The IPS instrument is an upward-looking ice profiling sonar, which provides the high-quality ice thickness, or more correctly ice draft, data required for engineering and environmental assessment applications. Originally, this instrument was designed by the Institute of Ocean Sciences, Sidney, BC, Canada, and has been subsequently manufactured, and further developed, by ASL Environmental Sciences Inc. of Victoria, BC, Canada. The ice keel depth is determined from the return travel time of an acoustic pulse (420 kHz; 1.8° beam at -3 dB) reflected off the underside of the sea ice. The return time is converted to an acoustic range value through use of the speed of sound in seawater.

The IPS-5 units were setup to run through various configurations (phases) to acquire the best data based on climatological conditions. Crackerjack and Burger IPS-5 samplings were done in three phases. The initial phase had 2048 seconds of 2 Hz wave bursts every two hours for wave sampling from October 7, 2009 to November 15, 2009. No wave sampling was done in the second phase as there is no or very little open water during this period (November 16 to July 15). The last phase began on July 16, 2009 and lasted until the recovery with the same wave sampling rates as phase one. Ice profiling was done during all three phases with the range data being sampled at 2 second intervals at both sites.

A pressure sensor (Paroscientific Digiquartz), installed on each IPS-5 unit, was used to measure water level changes due to tidal and wind forcing, as well as apparent water level changes arising from depression/tilt of the mooring. The measured acoustic range, after correction for instrument tilt, is subtracted from the water level in order to get an accurate computation of ice keel drafts. The IPS-5 contains pitch/roll sensors, to permit additional data compensation for instrument tilt and also collects near-bottom ocean temperature measurements.

The newer generation of IPS instruments can take compact-flash cards (8 GB as deployed and a max. 16 GB as of the date of writing). This increased data storage allows for the recording of up to 5 targets per individual ping and a subset of the raw acoustic backscatter profiles. The IPS-5 also has a wave mode, allowing bursts of wave data to be collected at up to 2 Hz. The 122 Alkaline D-cell batteries provided the necessary power to collect over 32 million pings over a 1 year period.

Instrument specification sheets for the IPS-5 instruments used in this project are included in the Data Archive.

2.1.2 ACOUSTIC DOPPLER CURRENT PROFILER (ADCP)

The Acoustic Doppler Current Profiler (ADCP), Sentinel Workhorse series, manufactured by Teledyne RD Instruments of Poway, California, USA was used at Sites Crackerjack and Burger. The ADCP technology is widely used for oceanic environmental monitoring applications. Mounted near the sea bottom, the ADCP unit provides precise measurements of ocean currents (both the horizontal and vertical components) at levels within the water column, from near surface to near-bottom. In addition, the ADCP provides time series measurements of the velocity of the pack ice moving on the ocean's surface, as well as near-bottom ocean temperature data.

The ADCP instruments measure velocity by detecting the Doppler shift in acoustic frequency, arising from water current (or ice) movements, of the backscattered returns of upward (20° from vertical) transmitted acoustic pulses. The Doppler shift of the 300 kHz acoustic signals is used to determine water velocities at a vertical spacing of 4 m at Sites Crackerjack and Burger. The Sentinel ADCPs were modified by RDI in 1996 to use the Doppler shift from the ice bottom surface to measure ice velocity as well [this is now a standard option]. The sampling scheme involved 30-minute ensembles composed of water-column pings, interleaved with ten bottom-track pings.

The data measurements are stored internally on a PCMCIA recorder card(s). Because of the extended 12-month deployment, the internal alkaline battery packs were supplemented with external battery packs (doubles).

2.1.3 CTD AND CT SENSOR

A profile of conductivity and temperature *versus* pressure (water depth) was obtained using a Seabird Electronics model SBE 9 CTD profiler during the 2009 cruise. Adverse weather and sea state conditions precluded the possibility of acquiring a profile at Crackerjack during the 2009 cruise. No CTD casts were done during the recovery operations in 2010. The primary purpose of the CTD data is to obtain speed of sound profiles, which represent optional inputs to processing the IPS data. In a more traditional role, the CTD also provides accurate measurement of temperature, conductivity, salinity, and density throughout the water column.

The CTD profiler uses very accurate temperature, conductivity and pressure sensors, which are sampled at approximately 24 Hz as the instrument is lowered through the water column. The pressure measurements are used to determine the instrument depth during the profile. From the temperature, conductivity, and pressure data, vertical profiles of the salinity and density were computed and recorded, along with the measured profiles of temperature and conductivity.

A RBR CT internal recording conductivity and temperature (CT) sensor was mounted on the IPS-5 frame at Site Crackerjack. This CT provided continuous measurements of salinity and temperature for use in adjusting the speed of sound to provide more accurate acoustic ranges (section 3.1).

Refer to the Data Archive for further specifications on the CTD and CT sensors.

2.2 DEPLOYMENT AND RECOVERY

Mooring deployments were carried out using the vessel *CCGS Sir Wilfrid Laurier* (Figure 2-4), operated by the Canadian Coast Guard under the command of Captain Norman Thomas. This vessel is primarily used for the tending of navigation buoys and for Arctic Ocean scientific research.

Sea ice, which had retreated further in 2009 than the climatological average, had no direct impact to any operations during the cruise. However, strong winds (30-40 knots) were blowing from both the east and west, generating wave heights of 3-4m due to the large fetch produced by the extraordinarily large degree of sea ice retreat. Individual wave heights of up to 4-6 m were estimated for Crackerjack on October 7, 2009.

Figure 2-4. A photograph of the Canadian Coast Guard Ship *Sir Wilfrid Laurier* in Victoria Harbor.

Recovery of the data collected by the moored instruments was carried out in July 2010 from MV Norseman II (Figure 2-5). The ORE Coastal Acoustic Release Transponders (CARTs) were used to bring the IPS-5 and ADCP moorings to the surface. With a release load of 500 kg, a maximum depth rating of 1000 m and battery lifetime of 1.5 years, they are ideal for the deployments in the Chukchi Sea. However, during recovery operations, corrosion was noted on some of the CART acoustic releases. Similar corrosion issues had previously been encountered with these releases, and it was thought that these had been addressed by the manufacturer. This issue will be taken up again with them before the 2011 recovery cruise.

Figure 2-5. MV Norseman II in Nome.

The recovery operations started at Crackerjack on the evening of July 26 (local time) and completed early morning in July 27, 2010. The recovery operations started at the Burger site on the evening of July 28 (local time) and completed early morning in July 29, 2010.

2.2.1 PRE-DEPLOYMENT INSTRUMENTATION CHECKOUT

All the instrumentation had undergone extensive testing at ASL facilities in Canada prior to shipment to the Arctic. The orientations of the ADCP-measured currents were determined at each instrument by using an internal magnetic flux-gate compass. Because of the close

proximity of the measurement locations to the north magnetic pole in the Canadian Arctic Islands, and the consequent weakness of the earth's horizontal magnetic field component, regional calibrations of the instrument compass must be carried out. These calibrations were carried out in Herschel Island, Yukon on October 1, 2009. The compass calibrations were carried on again for the replacement ADCP instruments in Nome, Alaska on July 20, 2010.

Refer to the Data Archive for further specifications on the Sentinel Workhorse ADCP's.

2.2.2 ON-SITE DATA DOWNLOADING

All 2009-2010 data sets were downloaded from the retrieved instruments onboard the vessel (MV Norseman II), with timing checks made on the instrument clocks to measure the clock drift over the period of the deployment. A preliminary examination of the data indicated that the IPS-5 and ADCP instruments recorded full datasets at Site Crackerjack. The IPS-5 at Site Burger recorded a full dataset, while the ADCP stopped recording data prematurely on July 9, 2010 due to an external battery problem.

All data downloaded during the July 2010 cruise were initially inspected, and found to be of uniformly high quality.

2.2.3 CTD PROFILE – OCTOBER 2009 AT SITE BURGER

Following the deployment of the mooring at Burger, a single CTD profile was obtained near the site by lowering the CTD through the water column. The times and locations for the CTD profile measurements are provided in Table 2-2 for the deployment in 2009. The weather and sea conditions prevented a CTD cast being performed at Crackerjack. Additional CTD casts were not required and hence not performed during the recovery operation in July 2010.

Table 2-2. Time and location of the CTD profile made in October 2009 at Burger.

Date / Time	Station Name	Depth (m)	Latitude	Longitude	Maximum Pressure (dbar)
October 7, 2009 19:13	Burger	45	71º 14.32'	163º 17.64'	41.6

3 DATA PROCESSING

3.1 ICE DRAFT

3.1.1 INTRODUCTION

The processing of the Ice Profiling Sonar (IPS) data involves the conversion of the time-of-travel measurements recorded internally by the IPS unit into a calibrated time-series of ice draft in units of meters, at 1 or 2 second intervals. The ice draft time-series is then converted to a spatial (or distance) data series, i.e. the time coordinate is transformed to distance using the measured ice velocities (section 3.1.2.3). The general approach to the data processing follows that of Melling et al. (1995). The implementation of the procedures, along with many further refinements, have been developed and carried out by ASL personnel over the past 12 years.

The raw data recorded by the IPS instrument consists of two measured parameters: the time-of-travel to the selected target echo and the amplitude and persistence (duration above a threshold amplitude level) of the target echo. The basic operation of the IPS instrument is outlined briefly below (more details are provided in the *IPS-5 Users Manual*). Essentially, the IPS operates in a pulsed mode with its acoustic beam directed toward zenith. A multi-faceted algorithm (Melling et al., 1995) identifies the echo, which is intended to be that of the bottom of the sea-ice, if present, or in the absence of sea-ice, from the ocean-atmosphere interface. The following describes the target selection algorithm:

- Select those echoes that are returned from beyond a minimum range but within a maximum range whose amplitudes and durations (persistence) exceed chosen minimum values (i.e. the echo start amplitude and the minimum persistence).
- From this initial selection, the echoes of longest duration (persistence) are chosen (up to 5 targets). Choice of the control parameters must be carried out with a view to minimizing the likelihood that the algorithm will select echoes from sources within the water-column as opposed to the ice under-surface.

The time of travel value was converted to a one-way range by applying a first estimate of the speed of sound of seawater, c, in m s^{-1}. For this study the initial value of c was chosen to be 1440 ms^{-1}.

The IPS units when recovered had range data sets of approximately ten months duration. At a sampling interval of 2 seconds, the total data record for an IPS unit over this time has over 13,000,000 logical records of acoustic range and amplitude data. The IPS units also provided measurements of near-bottom pressure, two-components (x and y) of instrument tilt, and the near-bottom ocean temperature.

As expected, the raw IPS data contain “drop-outs” for pings in which an acoustic target exceeding the threshold amplitude was not found. The number of occurrences of such

dropouts was very small. The Ice Profiler model IPS5 instruments have a feature where the range to the maximum amplitude value (index target) is also recorded. When drop-outs occur, the index target range value is then used. Less frequently, other types of erroneous values occurred in the form of 'spikes', i.e. one or a few data points that were markedly inconsistent with the measured neighboring values. These were removed through automated programs that detected and replaced the erroneous values using linear interpolation. In the IPS datasets, some segments of consecutive "drop-outs" were found. These segments contained more points than the threshold for allowing automatic interpolation during automated despiking. A method for removing most of these segments was developed (see following section) and a small number of segments that could not be edited automatically were reviewed manually.

3.1.2 PROCESSING IPS DATA

Steps in the IPS data processing, as developed from processing many dozens of IPS data sets, consisted of:

1. Converting raw IPS data from binary form in instrument units to nominal engineering units.
2. Preparing time-series plots of the raw range measurements. Sample plots are shown in Figure 3-1 and Figure 3-2. Note that the plots show 'raw' data presented exactly as measured without any corrections or changes. In addition to the 'spikes' evident in the raw data, the data have not been corrected for variations in water levels due to tides and other effects, nor for changes in the speed of sound in the water column or the effects of instrument tilt.
3. Manual examination of the time-series plots of range to determine where editing is required. Segments of the data set characterized by level ice errors, recurrent spikes to a specific range, and 'missing' ice echoes were noted. The portion of the data sets where the instrument was not in measurement position (i.e. before and during deployment and following release of instrument from bottom mooring) were also noted and checked against log sheets. A first order assessment of occurrences of open water conditions was also made during this first examination and review of the data.
4. Editing IPS range data using automated data editing algorithms.
5. The times in the data file are corrected for the effects of instrument clock time drift (as derived from comparison of instrument start and stop times with times recorded on start-up and shut-down of the instrument). Clock drifts are typically small – 0 to 10 minutes over deployments of several months.
6. Remove unwanted data at the beginning or end of each data record (obtained during deployment and recovery operations).
7. Identify, and set to flag values (-9999), data segments where false subsurface acoustic targets, likely bubbles associated with strong winds and large waves, were detected rather than the underside of the sea ice or the water surface. Occasionally, the amplitude values were useful as a guide in detecting these scattering events, as the

onset of such events were characterized by reduced amplitudes. More commonly, the detection of these events was based on large variations in successive range measurements, which clearly were inconsistent with surface wave effects.

8. Automated removal of erroneous values that occur with the following attributes:
   - range values < 0.01 m to remove range dropouts
   - range values that exceed a reasonable value computed as: high tide = instrument depth + 8.0 m
9. The erroneous values, identified in the steps immediately above, are replaced through linear interpolation. On completion of the automated editing, longer sequences of consecutive data values (10 points or more) that were removed were examined manually to ensure that the error detection algorithm had functioned as expected.
10. The boundary points of segments of consecutive null range records were compared. If the range values of these points differed by less than 10 cm then the range values of these records were calculated by linear interpolation of the boundary points. The remaining segments were investigated and edited manually.
11. Replot the edited data set and review for any additional spikes or suspect values. Manually replace any further spikes (usually occurrences over 5 to 10 consecutive data values) using linear interpolation; occasionally, longer segments of suspect data are replaced with 'flag' values at this stage.

The numbers of erroneous data values detected and removed using the procedures described above are summarized in Table 3-1 and Table 3-2.

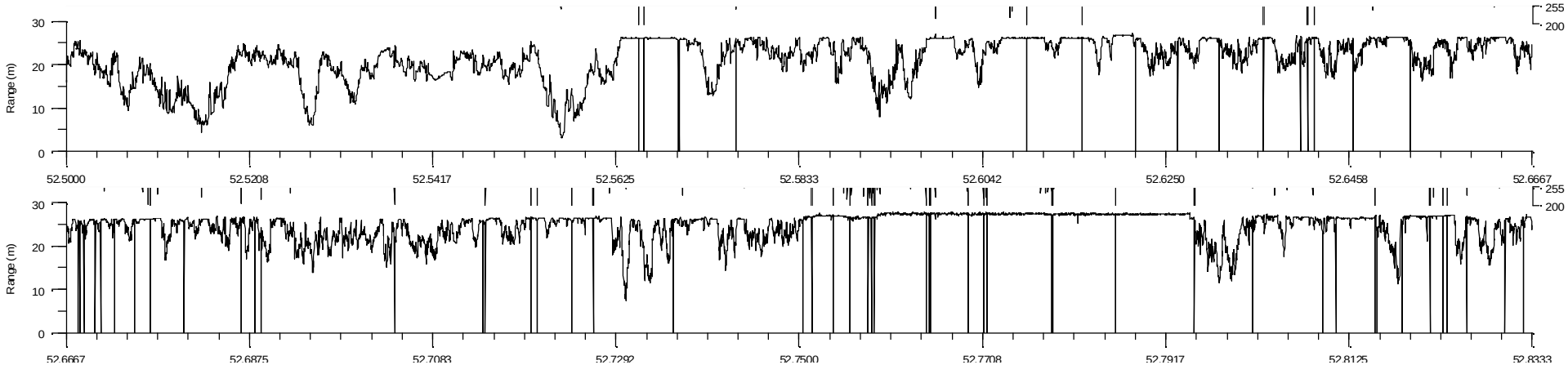

Figure 3-1. An example of the unedited range and amplitude data measured by an IPS showing a period characterized by sea-ice floes and some range “drop-outs”.

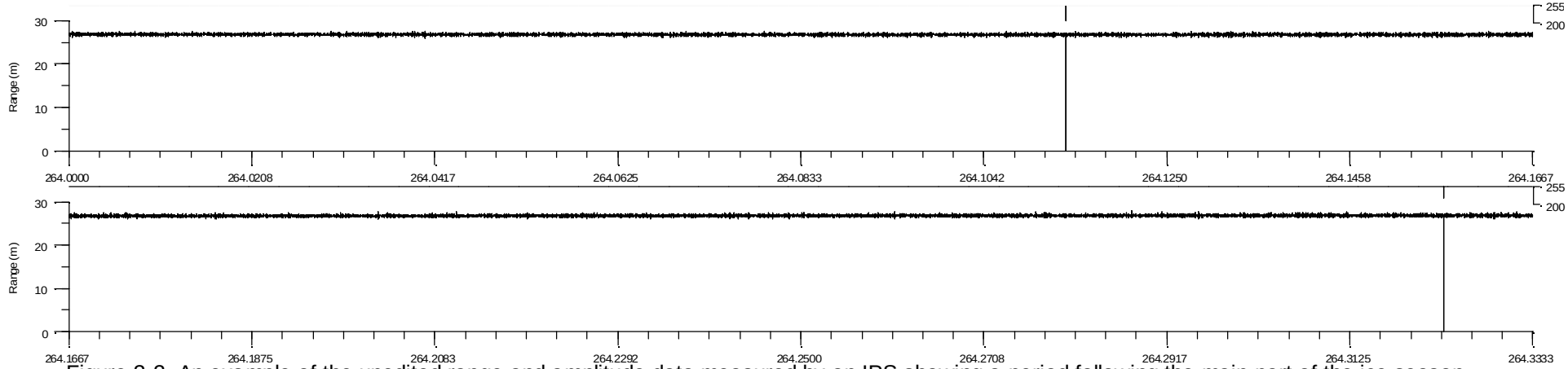

Figure 3-2. An example of the unedited range and amplitude data measured by an IPS showing a period following the main part of the ice season. This is an example of ‘rough open water’ in which the returns obtained from targets below mean sea level are believed to result from the troughs of ocean waves and from bubbles located beneath the surface

Table 3-1. Summary of the two main stages of ice draft data processing for Burger, giving number of data records having errors that were detected and replaced or flagged. Where applicable, the number of segments of edited data and/or the percentage of the total number of points is provided in parentheses.

		Burger		
	Phase	**1**	**2**	**3**
	Start date/time	07-Oct-2009 00:00:02	16-Nov-2009 00:00:54	16-Jul-2010 00:06:07
	Stop date/time	16-Nov-2009 00:00:52	16-Jul-2010 00:06:06	30-Jul-2010 00:09:48
	Sample interval	2.0000459	2.0000459	2.0000439
Range data	**# records as lower out-of-bound**	16	49	55
	# records as upper out-of-bound	0	0	0
	# records as single negative spikes	0	1,657	3
	# records as single positive spikes	1	1,654	1
	# records as double negative spikes	0	100	0
	# records as double positive spikes	0	92	0
	# records as triple spikes	0	39	0
	# records as quadruple spikes	0	20	0
	# records replaced by manual editing	0	15	1
Ice draft data	**# records flagged as bad**	21	51	3
	# records replaced manually	0	413	9
	# records flagged as open water/thin ice	1,693,728 (100.0%)	2,548,733 (24.38%)	565,583 (99.63%)
	Total # of records	1,693,728	10,454,082	567,662
	Final # of replaced data records (excluding open water/thin ice)	38 (0.002%)	4,090 (0.039%)	72 (0.013%)

Table 3-2. Summary of the two main stages of ice draft data processing for Crackerjack, giving number of data records having errors that were detected and replaced or flagged. Where applicable, the number of segments of edited data and/or the percentage of the total number of points is provided in parentheses.

		Crackerjack		
	Phase	**1**	**2**	**3**
	Start date/time	07-Oct-2009 00:00:00	16-Nov-2009 00:01:12	16-Jul-2010 00:08:27
	Stop date/time	16-Nov-2009 00:01:10	16-Jul-2010 00:08:25	27-Jul-2010 23:17:52
	Sample interval	2.0000406	2.0000412	2.0000296
Range data	**# records as lower out-of-bound**	2	2	0
	# records as upper out-of-bound	0	0	0
	# records as single negative spikes	1	1,794	0
	# records as single positive spikes	0	2,221	0
	# records as double negative spikes	0	164	0
	# records as double positive spikes	0	180	0
	# records as triple spikes	0	36	0
	# records as quadruple spikes	0	0	0
	# records replaced by manual editing	3	81	18
Ice draft data	**# records flagged as bad**	0	50	0
	# records replaced manually	0	1	0
	# records flagged as open water/thin ice	1,681,275 (100.0%)	2,052,862 (19.63%)	485,264 (100.0%)
	Total # of records	1,681,275	10,454,389	485,267
	Final # of replaced data records (excluding open water/thin ice)	6 (0.000%)	4,529 (0.043%)	18 (0.004%)

3.1.2.1 COMPUTATION OF ICE DRAFT

The next stage of data processing deals with converting the measured ranges into ice drafts. The ice draft, *d*, is derived from the edited ice ranges, *r*, and the water level, η. η is computed from the measured ocean bottom pressure, P_{btm}, and atmospheric pressure, P_{atm}, as follows:

$$\eta = \frac{(P_{btm} - P_{atm})}{\rho \cdot g} \qquad (1)$$

where g is the calculated local acceleration due to gravity and ρ is the density of sea water. Table 3-3 lists the values of these parameters for the IPS measurement sites. Measurements of P_{atm} were obtained from Wainwright, Alaska. The ice draft, *d*, is then computed from the edited range data as:

$$d = \eta - \beta \cdot r - \Delta D \qquad (2)$$

where β is a calibration factor for the actual mean speed of sound in sea-water, *c*, relative to the initially assumed value of 1440 ms-1 and ΔD is the distance of the pressure sensor below the acoustic transducer as shown in Table 3-3. Note that the sign convention for ice draft is positive downwards, i.e. a draft of +5 m represents an ice keel, which extends 5 m below sea level.

Table 3-3. Values used in the calculation of water level for Burger and Crackerjack.

Site	ρ (kg m^{-3})	g (m s^{-2})	ΔD (m)
Burger	1026.19	9.826792	0.200
Crackerjack	1026.09	9.826753	0.200

The density values were derived from historical temperature-salinity-density data sets available for the Chukchi Sea and from the measured density values, as derived from the Conductivity-Temperature (CT) instrument data available at the Crackerjack site (section 3.5). The CT derived densities represent an upper bound of the actual water column density values due to density stratification of the water column, especially during summer and fall.

Corrections were also made for the effect of instrument tilt on the measured ranges. Generally, if not corrected for, this source of uncertainty would result in errors of a few centimeters or less on the ice drafts.

3.1.2.2 RANGE CORRECTION FACTOR

The factor, β, applied to the measured range in equation (2) represents the ratio of the actual sound speed to the nominal value of 1440 ms^{-1}. To determine β, open water segments in the range data set were selected (i.e. *d = 0* in equation 2 above) and β was empirically computed. The empirical values of β seem to follow reasonably well the variation

in the local speed of sound as computed from the measured near-bottom temperatures obtained from the IPS values at the measurement locations.

A fit was made to determine the time varying β values over the full duration of the time-series data based on:

- the empirical computations of β realized from periods of open water;
- the computed effect of near-bottom temperatures on c (using a fixed salinity and the speed of sound algorithm of Urick, 1983).

Plots of the time varying $\Delta\beta$ values are shown in Figure 3-3 and Figure 3-4 where:

$$\Delta\beta = (\beta - 1) \times 1000 \qquad (3)$$

The empirically derived values of β were applied through equation 2 to the edited range data to compute ice drafts.

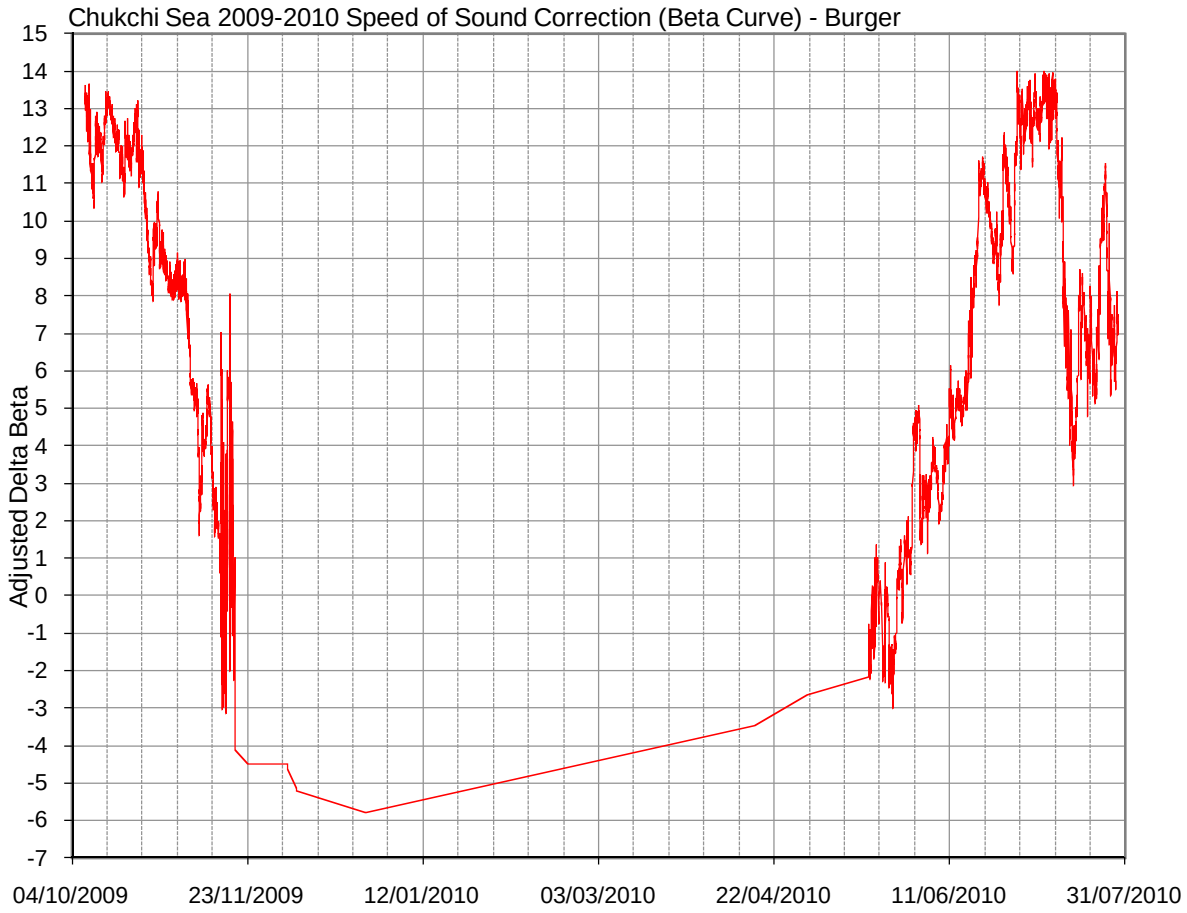

Figure 3-3. Plot of the time varying $\Delta\beta$ values for Burger.

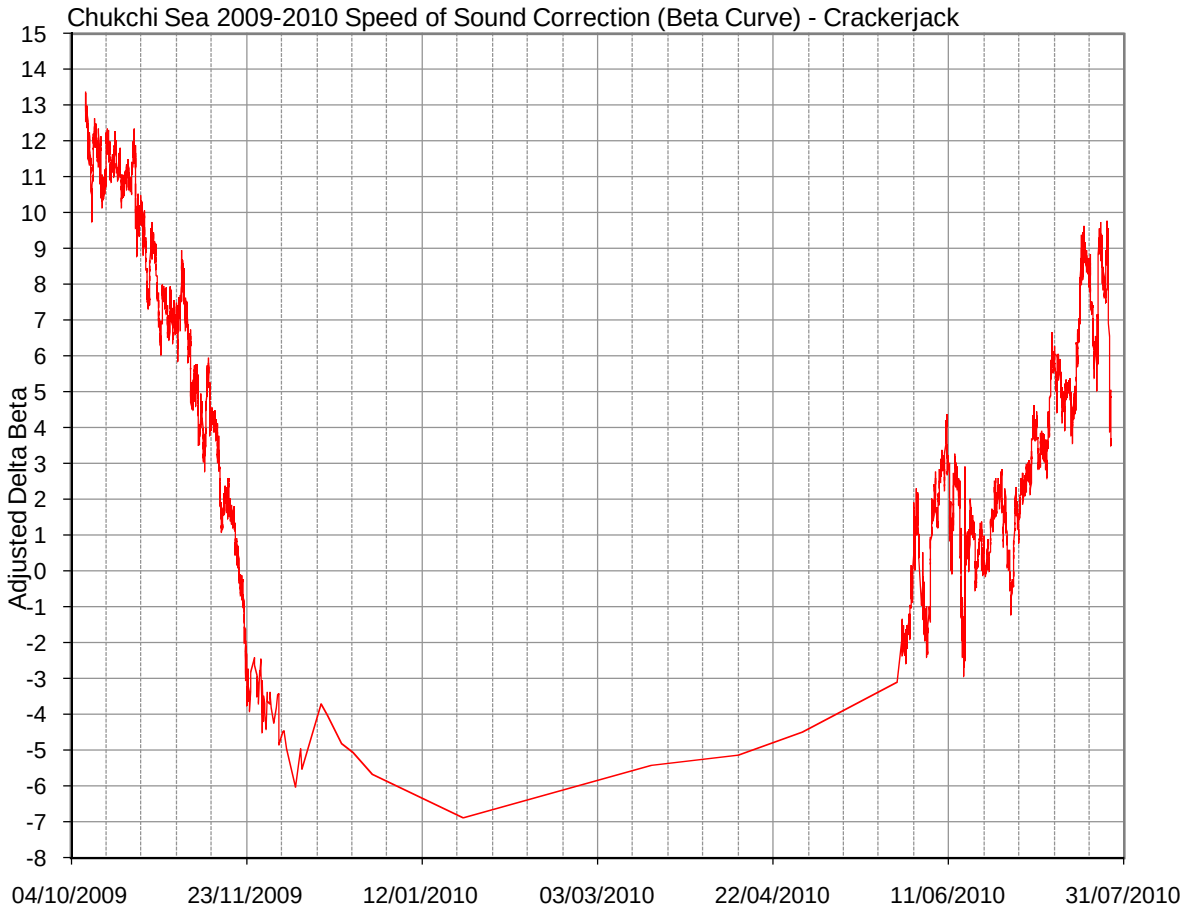

Figure 3-4. Plot of the time varying $\Delta\beta$ values for Crackerjack.

3.1.2.3 Conversion of Time-Series to Distance-Series for Ice Draft Data Sets

The ice draft time-series data sets were converted to a distance (or spatial) series using the processed ADCP ice velocities (Section 3.3). The resulting spatial data file contained east and north displacements and ice drafts beginning at zero east and north displacement incrementing until the end of the file. The cumulative ice path length, or distance, was then calculated using the east and north displacements for each sample.

The ice draft was sampled at regular time intervals, but due to the irregular motion of the ice the resulting distance-series was unevenly spaced in distance. The distance-series was interpolated to regular increments using a double-weighted double-quadratic interpolation scheme. As shown in Figure 3-5, the value Y_1 represents the value obtained from a quadratic interpolation using two points to the left and one to the right of x_i {($y(u_{i-1})$, $y(u_i)$ and $y(u_{i+1})$} and Y_2 represents the interpolated value using two points to the right and one to the left of x_i {($y(u_i)$, $y(u_{i+1})$ and $y(u_{i+2})$}. In the figure, the desired regularly spaced interpolation point is x_i, and the measurement locations are given by u_{i-1}, u_i, u_{i+1} and u_{i+2}. The two interpolated values were then averaged using a weight based on the distance between

points and on the change in draft between points. The double weighting scheme, as shown in equation 4, was adopted to avoid overshoots in areas of sudden draft changes.

In order to represent the ice drafts at low ice velocities, the draft data file was interpolated to 0.10 m distances then block averaged to 1.0 m distances. The 1.0 m spacing represents a distance slightly less than the width of the IPS sonar footprint at an average 30 m water depth and the smallest resolvable distance.

As part of reviewing the data for open water occurrences, a manual review was conducted to identify data segments, which contain both thin ice and waves (denoted as "waves in ice"). The flagging of long sections of open water occurred at times when air temperatures rose above 0 degrees, and low concentrations of sea-ice with only occasional large keel occurrences were detected.

The final step in reviewing the spatial series was to search for unrealistic features. These features were generally located where the uncertainty in the ice velocities was largest. Modifications were made to the ice velocities, and the spatial series were recalculated.

$$y(x_i) = \frac{Y_1[y(u_{i+2}) - y(u_{i+1})][x_i - x(u_{i+1})] + Y_2[y(u_i) - y(u_{i-1})][x_i - x(u_i)]}{[y(u_{i+2}) - y(u_{i+1})][x_i - x(u_{i+1})] + [y(u_i) - y(u_{i-1})][x_i - x(u_i)]} \quad (4)$$

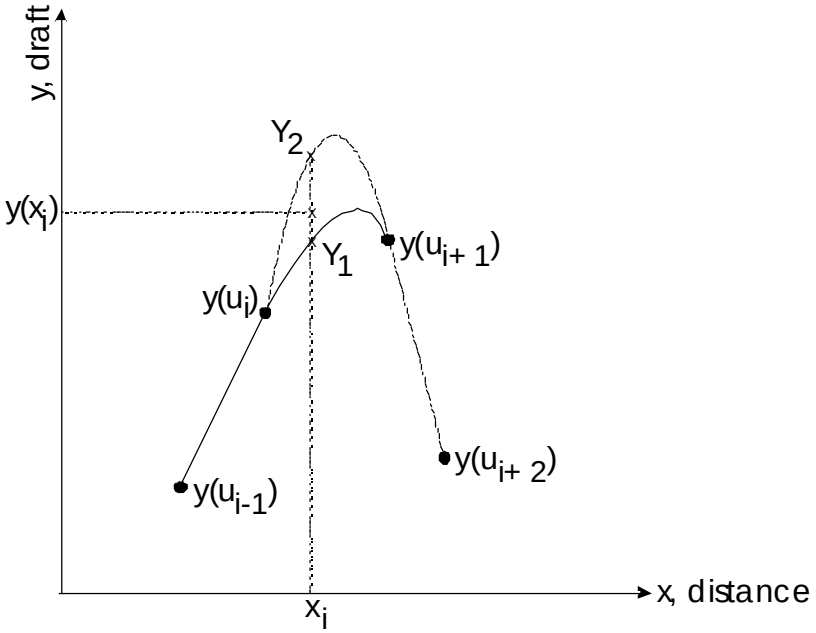

Figure 3-5. The double quadratic interpolation method used to convert the ice draft time series into a spatial series.

3.1.3 SUMMARY OF ICE DRAFT

The measured acoustic range, pressure, and tilt data channels recorded by the IPS5 instrument, combined with sea level pressure measurements were processed and analyzed to compute time- and distance-series of ice keel drafts. Following a careful and thorough review of the ice drafts, final edited versions of ice draft time- and distance-series were created and plotted. The duration of the ice draft records with time and distance at the measurement sites are shown in Table 3-4 and Table 3-5. Sea ice was first detected on November 18 at Burger and November 22 at Crackerjack. The ice had mostly disappeared after May 20 and after June 5 at Burger and Crackerjack respectively, but ice was present on an intermittent basis until July 20 at Burger and June 15 at Crackerjack. The clearing dates for sea ice in summer are 4 to 5 weeks earlier than median value of break-up dates, derived from ice charts for the years of 1971 to 2000. The earlier clearing dates are consistent with the general trend of reduced ice concentrations in the summer over the past decade.

The distance-series of ice drafts have interruptions in May and June 2010 due to reduced ice concentrations, which makes ice velocity measurements unreliable.

Table 3-4. Final time-series and distance-series segments of valid data for Burger.

Burger		
Time-Series		
Phase	**Start Date / Time**	**Stop Date / Time**
1	07-Oct-2009 00:00:02	16-Nov-2009 00:00:52
2	16-Nov-2009 00:00:54	16-Jul-2010 00:06:06
3	16-Jul-2010 00:06:07	30-Jul-2010 00:09:48
Distance-Series		
Segment	**Start Date/Time**	**Stop Date/Time**
1	18-Nov-2009 22:31:25	20-May-2010 10:07:01

Table 3-5. Final time-series and distance-series segments of valid data for Crackerjack.

Crackerjack		
Time-Series		
Phase	**Start Date / Time**	**Stop Date / Time**
1	07-Oct-2009 00:00:00	16-Nov-2009 00:01:10
2	16-Nov-2009 00:01:12	16-Jul-2010 00:08:25
3	16-Jul-2010 00:08:27	27-Jul-2010 23:17:52
Distance-Series		
Segment	**Start Date/Time**	**Stop Date/Time**
1	22-Nov-2009 15:00:15	05-Jun-2010 19:00:54
2	14-Jun-2010 16:01:15	15-Jun-2010 13:01:01

The final versions of the ice draft data series (Data Archive) are considered to be generally accurate to within 0.3 m for the largest keel features and to somewhat better accuracies, to as good as 0.05 to 0.1 m, for thinner ice, based on the estimated uncertainties in the various stages of data processing. These accuracy estimates are consistent with inspections of the final edited data sets for data segments consisting of open water intervals when the ice draft, after allowing for any ocean wave effects, should be identically zero.

The processed ice draft data files are provided as part of the Data Archive, both as time-series data and as distance-series data. Plots of the distance-series ice drafts are also provided in the Data Archive for each of the segments of continuous good ice velocities. In the ice draft plots, segments containing waves in ice were flagged to -500 and segments containing open water were flagged to -200 but were plotted as values slightly above the abscissa. Segments of bad data were flagged to -9999.

3.2 OCEAN WAVE DATA DERIVED FROM ICE PROFILER

The range data from ASL Ice Profiler was used to derive information on ocean waves when sea ice was not present. The processing of the IPS-5 data sets involved the conversion of the time-of-travel measurement recorded internally by the instrument, to an edited time series of wave heights. Wave autospectra were computed using the Fast Fourier Transform (FFT) technique. Two quantities, or non-directional wave parameters, were then computed from the autospectra: the significant wave height (H_s), calculated as four times the square root of the area under the autospectral curve; and the peak period (T_p), calculated as the corresponding period at which the autospectra reaches its maximum. At Crackerjack, the maximum wave height (H_{max}) was computed from the largest crest to trough distance in the segment.

The data was collected in three phases consisting of different sampling intervals. Wave data for phases 1 (Oct 7/09 to Nov 16/09) and 3 (Jul 16/10 to Jul 29/10) were collected in wave burst mode at 2 Hz (4096 points every 2 hours). The significant wave height (Hs) and the peak period (Tp) were computed from the autospectra using cutoffs of 20 seconds (0.05 Hz) to 1 second (1 Hz) and 4096 points.

Phase 2 (Nov 16/09 to Jul 16/10) was sampled every 2 seconds (0.5 Hz) and the smallest resolvable period was 4 seconds (0.25 Hz). Ocean waves occurred only during the last month or so during phase 2; as discussed above the sea ice cleared earlier than normal, so waves occurred earlier than expected and, in particular, prior to the end of Phase 2.The significant wave height (Hs) and the peak period (Tp) were computed from the autospectra using cutoffs of 20 seconds (0.05 Hz) to 4 sec (0.25 Hz) and 3600 points. For this phase, the data was not sampled frequently enough to represent the wave data as accurately as in Phases 1 and 3.

For both data sets, the acoustic travel time was converted to a one-way range (distance from the IPS-5 to the air/water interface) by applying an estimate of the speed of sound in seawater of 1440 m/sec. Steps in the data processing consisted of:

1. Automated removal by linear interpolation of erroneous values that occur with the following attributes:
    - Out-of-range values
    - Null values
    - Statistical outliers
2. Trimming the start and end dates corresponding to the start and end of good data.
3. Applying a tilt correction using the recorded tilt values. For phases 1 and 3, the range and tilt were measured at 0.5s intervals and each range was corrected using the corresponding tilt value. In Phase 2, the tilt values were recorded at 30 second intervals and were smoothed using a 31 point running average and then interpolated to the 2-second range sampling interval.

4. Preparing time series plots of the edited wave data showing 12 hours of data per page.
5. Manual examination of the time series plots for remaining spikes that are replaced by linear interpolation and bubble clouds (erroneous data) that are replaced with 'flag' values (-9999). Ice data was also flagged.
6. Computing and plotting the autospectra using the 4096 point bursts (~34 minute) for phases 1 and 3 at 2 hour intervals. For phase 2, 3600 points (2 hours) were used to compute the autospectra. The significant wave height (H_s) and the peak period (T_p) were computed from the autospectra. If more than 50% of the data in a burst was flagged, the H_s and T_p values are set to –9999. For all phases, the peak period was flagged if the significant wave height was less than 0.1 m.
7. Manually reviewing each autospectral curve and the computed values for H_s and T_p.

Detailed processed results for each of the study sites are presented in Section 4.5 and are also included in the Data Archive.

3.3 ICE VELOCITY

3.3.1 INTRODUCTION

Ice velocity measurements were made with an Acoustic Doppler Current Profiler (ADCP) operated from the seabed (section 2.1.2), using the "Bottom-Track Upgrade" feature of the RD Instruments Sentinel Workhorse. The ADCP's at Burger and Crackerjack recorded ice velocities at 30 minute sample intervals. Each measurement was derived using the observed Doppler shifts as realized from the four individual acoustic beams (each beam was oriented at a 20 degree angle from the vertical). Each 30 minute water velocity sample is an ensemble average of multiple acoustic water column pings. Each 30 minute ice velocity sample is an ensemble average of special "bottom tracking" pings which are used only for ice tracking and not for water column ocean current profiles. The details of the number of ADCP pings for each measurement ensemble are given in Table 3-6.

Table 3-6. Summary of ADCP configurations indicating the number of pings used for calculating ice and current velocity measurements over the 30 minute ensemble sampling interval.

	Burger	**Crackerjack**
	2009-2010	
Water Pings	100	100
Bottom Pings	10	10
Cell Size (m)	4	4
Processing Bandwidth	Narrow Band	Narrow Band

According to the manufacturer, the accuracy of the "bottom track" velocity measurements is: 0.7 cm s^{-1}/(no. of pings per ensemble)$^{1/2}$. The accuracy of ice velocity measurements may be degraded because of the weak scattering coefficient from sea ice (Garrison et al., 1991); scattering energy from the seabed, which the manufacturers' specification is based on, is expected to be generally larger than that from sea-ice. However, the ADCP instruments have been demonstrated to effectively track ice velocities under at least some ice conditions (Belliveau et al., 1990; Melling et al., 1995).

Use of the ADCP for ice velocity measurements presents some special problems not encountered when used for bottom tracking (Melling et al., 1995):

Open water conditions: poorer accuracies for measurements of ice velocities under largely open-water conditions; under these conditions, the ADCP measurements are too noisy to be meaningful due to the rapid movement of the new targets (air bubbles and very short, capillary waves on the ocean surface) in response to the energetic motion of ocean waves. Due to the separation of the four acoustic beams, the wave-dominated velocities are unlikely to be equal within each beam. The assumption of uniform velocities among the four beams is fundamental to the operation of the ADCP instrument. As a result, the derived velocity is very noisy and has little information content. Such occurrences of noisy velocities associated with open water conditions are generally indicated by marked increases in the values of the vertical and error velocity components (the error velocity component is indicative of the degree of divergence in the Doppler velocities from each of the four acoustic beams).

Smooth ice: the occurrence of very weak echoes from smooth first year ice providing poor signal-to-noise ratio for velocities, so that the precision of the ice velocities is degraded. Uncertainties from smooth ice were not found to be a problem in the present ice velocity data set. However, episodes of open water or very low ice concentrations were often apparent in the ice velocity data set.

3.3.2 PROCESSING ICE VELOCITIES

The procedures for processing the ice velocity data (using the oceanographic direction convention of motion towards rather than the wind direction convention) involved the following sequence of tasks:

1. Prepare plots of raw east, north, vertical and error velocity channels.
2. Identify periods of probable open water for each data record using the plots from step (1) and other available information, including ice profiling sonar records supplemented by ice charts, and satellite imagery. For these periods, set the values of the horizontal velocity components to flag values of –9999. The first part of the time series records, when sea ice had not yet entered the area, or was of very low concentration, is also flagged.
3. Identify horizontal velocity values exceeding 150 cm s^{-1} in absolute value.

4. Identify horizontal velocity values associated with error velocities exceeding 10 cm/s in absolute value.
5. Identify single point 'spikes' in each component of the horizontal velocities. A single point spike is where two successive first difference values exceed 6 cm/s and are opposite in sign.
6. Identify 'double spikes' exceeding a double spike threshold of 8 cm/s in each component of the horizontal velocities. A double spike consists of two consecutive points, both of which are either larger or smaller than the preceding and following points by more than the double spike threshold.
7. Identify 'triple spikes' exceeding a triple spike threshold of 10 cm/s in each component of the horizontal velocities. A triple spike consists of three consecutive points which are smaller than the preceding and following points by more than triple spike threshold, but whose middle points may not change by more than one third of the triple spike threshold from their respective leading neighbors.
8. Identify 'quadruple spikes' exceeding a quadruple spike threshold of 12 cm/s in each component of the horizontal velocities. A quadruple spike consists of four consecutive points which are smaller than the preceding and following points by more than quadruple spike threshold, but whose middle points may not change by more than one third of the quadruple spike threshold from their respective leading neighbors.
9. For all suspect values found as above in items 3 to 8, the values are replaced by linear interpolation, over all individual segments with durations of less than three hours (one eighth the duration of the tidal signal which is predominantly diurnal). For longer segments of erroneous or suspect data, the values are replaced with flag values (-9999) and reviewed again in step 10.
10. Plots of the edited data sets (following step 9) are prepared and manually reviewed. Any remaining suspect values are manually edited using the ASL_EDIT display/editing software package. These suspect values are generally determined as being anomalous from adjoining values at nearby times and at nearby velocity bins containing data consistent with measurements on either side of the values in question.
11. Identify data segments where low ice concentrations increase the uncertainties in the ice velocities to unacceptable levels by further examination of the now-edited ice velocity time series, ice profiling sonar range plots and ice charts.
12. Reconstruct these sections, if possible, using nearby ice velocities or upper level ocean current measurements from the same site. If the ice velocities cannot be reconstructed, then flag the values as unreliable using –9999.
13. Plot the fully edited ice velocity data file to evaluate and continue editing, as required.
14. The final step before starting the analysis of the data was to convert the ice velocities from magnetic coordinates to geographic coordinates.

At Burger and Crackerjack, open water was encountered until the ice finally set in November. Afterwards, open water was not encountered again until the early summer break-up. A summary by site of the start and end times of the periods of valid ice velocity measurements is given in Table 3-7.

Time series plots of the ice velocities are presented in Figure 3-6 and Figure 3-7. The plots show the major and minor components at Burger and Crackerjack, respectively. Segments of bad data are denoted by vertical lines. The direction of the major ice drift component, including the positive major component, is tabulated in Table 3-8. At Burger, the ice motion was oriented from 77° to 257° (77º positive), at Crackerjack the motion was oriented from 26° to 206° (26º positive). This rotation is optimized to maximize the variance in the major current component. The minor current component is perpendicular to the major current component.

Table 3-7. Summary of segments of the ice velocity data sets that were judged to be reliable or unreliable. Unreliable data includes open water.

Burger			
Valid Date Start	**Valid Data End**	**Bad Data Start**	**Bad Data End**
		07-Oct-2009 19:00	18-Nov-2009 22:01
18-Nov-2009 22:31	20-May-2010 09:37	20-May-2010 10:07	24-May-2010 15:37
24-May-2010 16:07	24-May-2010 18:07	24-May-2010 18:37	28-May-2010 05:37
28-May-2010 06:07	28-May-2010 10:37	28-May-2010 11:07	29-May-2010 06:07
29-May-2010 06:37	30-May-2010 20:07	30-May-2010 20:37	02-Jun-2010 14:37
02-Jun-2010 15:07	02-Jun-2010 17:37	02-Jun-2010 18:07	07-Jun-2010 17:07
07-Jun-2010 17:37	08-Jun-2010 17:37	08-Jun-2010 18:07	28-Jun-2010 16:08
28-Jun-2010 16:38	28-Jun-2010 23:38	29-Jun-2010 00:08	04-Jul-2010 06:38
04-Jul-2010 07:08	04-Jul-2010 08:08	04-Jul-2010 08:38	09-Jul-2010 01:08
4242 bad data points out of 13165 total for entire record (32.2%)			
1993 bad data points out of 10916 total from first ice to last ice (18.3%)			
Crackerjack			
Valid Date Start	**Valid Data End**	**Bad Data Start**	**Bad Data End**
		08-Oct-2009 02:00	22-Nov-2009 14:30
22-Nov-2009 15:00	05-Jun-2010 18:31	05-Jun-2010 19:01	14-Jun-2010 15:31
14-Jun-2010 16:01	15-Jun-2010 12:31	15-Jun-2010 13:01	27-Jul-2010 05:01
4613 bad data points out of 14023 total for entire record (32.9%)			
426 bad data points out of 9836 total from first ice to last ice (4.3%)			

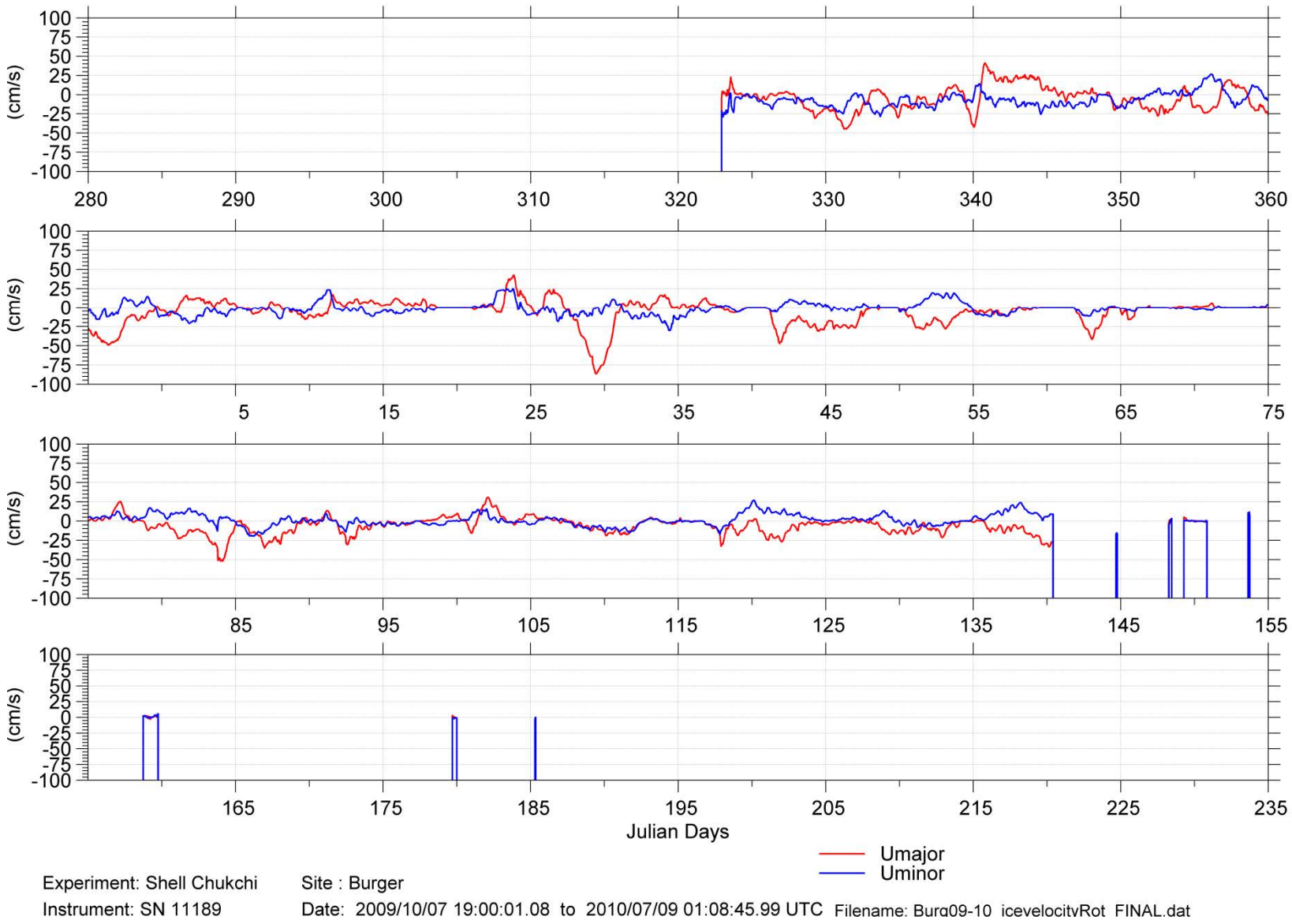

Figure 3-6. Plot of the edited ice velocity for Burger as a time series of the major and minor components of the ice velocity. Segments of bad data are denoted by vertical lines.

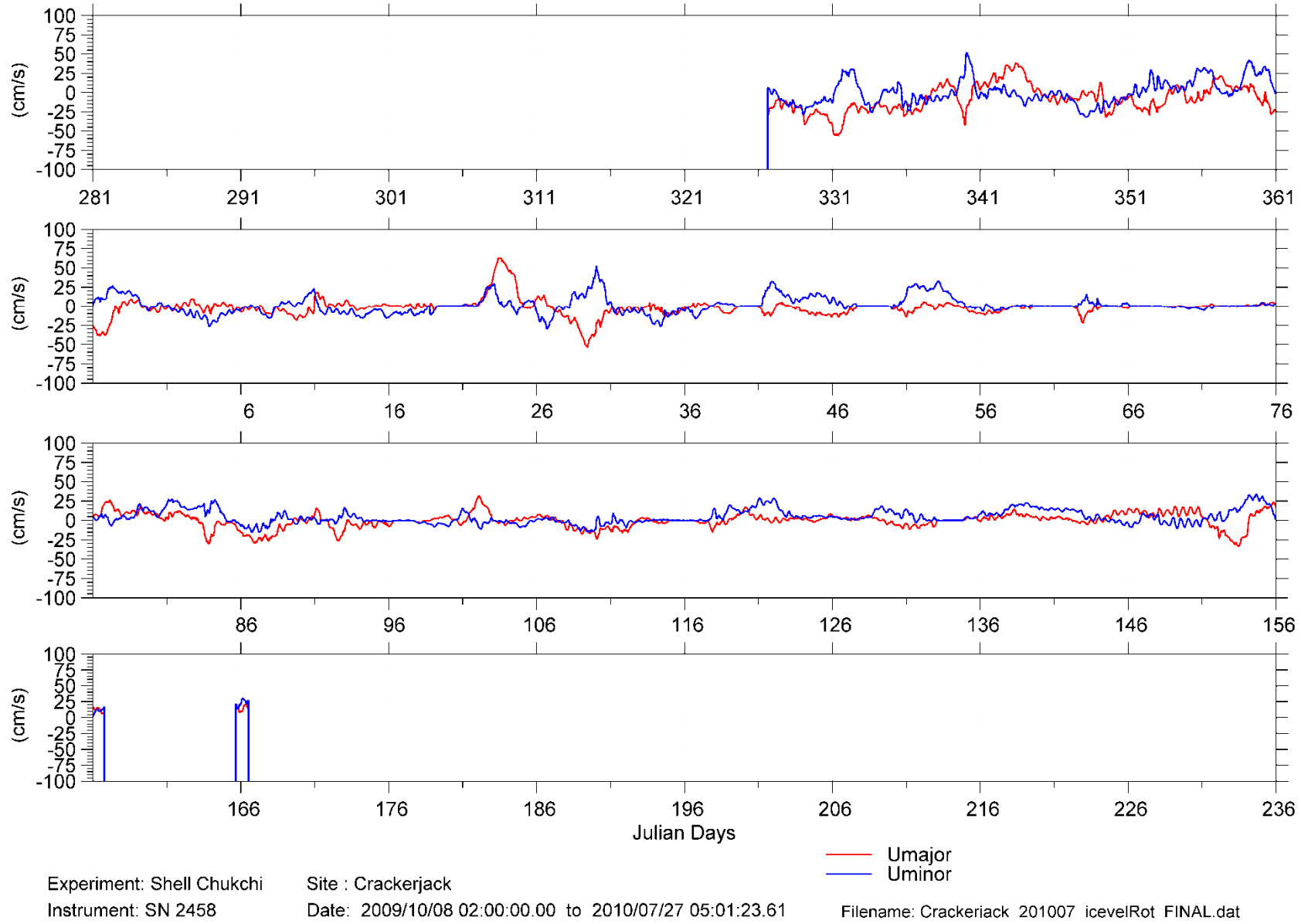

Figure 3-7. Plot of the edited ice velocity for Crackerjack as a time series of the major and minor components of the ice velocity. Segments of bad data are denoted by vertical lines.

Table 3-8. Summary of the major current direction for each site.

Site	Current Direction (°)	Heading of Positive Umajor (°)
Burger	77-257	77
Crackerjack	26-206	26

Table 3-9. Summary of the number of ice velocity points that were edited.

	Burger		Crackerjack	
	East/ West	**North/ South**	**East/ West**	**North/ South**
Out of Range	0	1	1	4
Single Spike	100	91	97	89
Double Spike	40	45	25	37
Triple Spike	2	3	3	3
Quad. Spike	0	1	0	0
Manual Edit	1155	1234	1690	1444
% Edit	8.8%	9.4%	12.1%	10.3%
# Flags in Raw Data (%)	87 (0.7%)		155 (1.1%)	
# New Flags (%)	4155 (31.6%)		4458 (31.8%)	
Total Pts	13165		14023	

Table 3-10. Statistical summary of measured 30 minute ice velocities by month at Burger.

Burger		min	1%	5%	25%	50%	mean	75%	95%	99%	std	max	# valid	total #
Time	cm/s													
07-Oct-2009	Umajor	0.0	0.0	0.0	0.0	0.0	0.0	0.0	0.0	0.0	0.0	0.0		
-	Uminor	0.0	0.0	0.0	0.0	0.0	0.0	0.0	0.0	0.0	0.0	0.0		
31-Oct-2009	Speed	0.0	0.0	0.0	0.0	0.0	0.0	0.0	0.0	0.0	0.0	0.0	0	1162
01-Nov-2009	Umajor	-44.8	-44.5	-37.8	-20.7	-5.3	-10.2	0.9	5.7	14.2	13.9	23.6		
-	Uminor	-29.4	-27.0	-23.7	-15.9	-10.6	-11.0	-5.3	-0.2	1.8	7.4	2.5		
30-Nov-2009	Speed	0.6	1.3	2.8	8.7	18.6	18.6	24.9	40.2	48.3	11.3	50.1	579	1440
01-Dec-2009	Umajor	-49.5	-46.6	-39.5	-16.6	-5.8	-5.6	5.6	23.0	32.3	17.6	41.7		
-	Uminor	-25.9	-20.0	-16.6	-11.2	-5.6	-3.9	1.7	13.7	23.3	9.7	27.0		
31-Dec-2009	Speed	0.0	0.2	3.7	11.8	17.2	18.6	23.4	40.9	47.4	10.2	50.9	1488	1488
01-Jan-2010	Umajor	-86.9	-81.1	-51.3	-3.6	2.5	-1.4	7.0	18.7	37.8	19.6	43.2		
-	Uminor	-21.6	-18.8	-14.1	-7.0	-2.8	-2.2	0.0	19.2	23.6	8.3	25.3		
31-Jan-2010	Speed	0.0	0.0	0.0	4.8	9.0	14.0	16.8	50.9	81.0	16.2	86.9	1488	1488
01-Feb-2010	Umajor	-47.5	-41.7	-28.1	-17.8	-4.0	-8.1	0.0	7.7	15.4	12.1	17.4		
-	Uminor	-30.5	-24.9	-13.8	-5.5	-0.2	-1.0	2.5	15.1	19.0	8.3	20.0		
28-Feb-2010	Speed	0.0	0.0	0.0	3.4	11.5	13.0	23.0	29.9	40.7	10.6	47.5	1344	1344
01-Mar-2010	Umajor	-52.2	-49.2	-30.3	-13.5	-0.3	-6.8	0.2	5.0	20.9	12.5	25.8		
-	Uminor	-19.8	-18.7	-11.5	-1.7	0.0	0.6	3.7	11.9	15.7	6.4	17.6		
31-Mar-2010	Speed	0.0	0.0	0.0	1.0	5.3	10.5	17.3	31.5	49.2	11.6	52.5	1488	1488
01-Apr-2010	Umajor	-33.2	-29.3	-17.7	-8.4	-1.6	-2.8	1.9	11.6	25.5	9.4	30.9		
-	Uminor	-17.8	-13.9	-11.3	-4.7	-1.4	-0.8	1.6	13.9	22.1	7.0	27.3		
30-Apr-2010	Speed	0.0	0.0	0.4	3.3	6.5	9.3	15.0	23.5	31.4	7.7	35.5	1440	1440
01-May-2010	Umajor	-33.5	-31.0	-25.0	-13.4	-6.9	-8.5	-1.5	0.6	1.9	8.2	5.7		
-	Uminor	-17.3	-7.9	-5.8	-0.1	2.5	4.1	8.9	16.7	22.2	6.7	24.6		
31-May-2010	Speed	0.0	0.1	0.3	3.2	10.1	11.1	17.5	28.5	31.3	8.8	34.2	1023	1488
01-Jun-2010	Umajor	-57.5	-57.5	-55.0	-0.3	0.7	-4.0	1.8	2.6	3.6	15.9	3.9		
-	Uminor	-2.3	-2.3	-1.7	-0.4	0.5	1.6	2.7	10.8	11.6	3.3	12.2		
30-Jun-2010	Speed	0.3	0.3	0.5	1.3	2.1	6.8	3.8	56.1	57.6	15.3	57.8	70	1440
01-Jul-2010	Umajor	-5.3	-5.3	-5.3	-5.3	-3.3	-3.2	-3.3	-0.9	-0.9	2.2	-0.9		
-	Uminor	-1.9	-1.9	-1.9	-1.9	-0.8	-0.6	-0.8	0.9	0.9	1.4	0.9		
09-Jul-2010	Speed	1.3	1.3	1.3	1.3	3.4	3.4	3.4	5.7	5.7	2.2	5.7	3	387
Entire	Umajor	-86.9	-51.0	-30.0	-12.7	-2.2	-5.6	1.5	14.7	25.6	14.4	43.2		
-	Uminor	-30.5	-21.9	-15.3	-6.2	-0.9	-1.5	2.3	13.7	22.5	8.5	27.3		
Record	Speed	0.0	0.0	0.1	3.9	11.0	13.2	19.7	33.0	50.9	11.8	86.9	8923	13165

Table 3-11. Statistical summary of measured 30 minute ice velocities by month at Crackerjack.

Crackerjack		min	1%	5%	25%	50%	mean	75%	95%	99%	std	max	# valid	total #
Time	cm/s													
08-Oct-2009	Umajor	0.0	0.0	0.0	0.0	0.0	0.0	0.0	0.0	0.0	0.0	0.0		
-	Uminor	0.0	0.0	0.0	0.0	0.0	0.0	0.0	0.0	0.0	0.0	0.0		
31-Oct-2009	Speed	0.0	0.0	0.0	0.0	0.0	0.0	0.0	0.0	0.0	0.0	0.0	0	1148
01-Nov-2009	Umajor	-56.0	-55.6	-53.1	-28.3	-21.8	-24.8	-17.7	-12.2	-8.7	11.0	-7.6		
-	Uminor	-28.1	-27.8	-21.7	-15.2	-9.8	-4.5	3.6	27.5	30.4	14.8	30.9		
30-Nov-2009	Speed	9.0	9.8	16.6	21.2	27.6	29.3	33.6	54.0	56.1	10.8	56.8	402	1440
01-Dec-2009	Umajor	-43.0	-37.5	-28.6	-13.7	-3.7	-3.4	6.9	24.3	35.4	15.7	39.0		
-	Uminor	-32.4	-29.5	-22.5	-6.0	1.1	3.4	12.3	30.4	41.5	15.3	52.3		
31-Dec-2009	Speed	0.2	1.6	4.1	10.7	19.1	19.7	28.3	37.4	45.2	10.6	55.6	1488	1488
01-Jan-2010	Umajor	-53.5	-46.0	-22.1	-5.5	-0.2	-0.2	2.3	33.9	59.3	16.2	63.4		
-	Uminor	-29.9	-25.6	-17.0	-9.5	-3.8	-1.7	2.3	23.9	37.0	12.1	53.0		
31-Jan-2010	Speed	0.0	0.0	0.1	5.9	10.4	14.6	17.2	49.5	59.5	14.0	63.7	1488	1488
01-Feb-2010	Umajor	-14.9	-13.5	-11.6	-7.6	-2.2	-3.5	0.0	3.2	5.0	4.7	6.2		
-	Uminor	-26.7	-23.3	-13.2	-2.4	0.1	3.6	9.9	26.1	31.7	11.5	33.1		
28-Feb-2010	Speed	0.0	0.0	0.0	3.2	8.6	10.2	16.1	26.7	32.2	8.6	34.3	1344	1344
01-Mar-2010	Umajor	-30.5	-28.1	-22.1	-2.1	0.0	-0.9	2.9	12.5	23.3	9.6	26.5		
-	Uminor	-15.4	-13.5	-6.9	-0.2	0.2	3.3	5.0	20.5	25.6	7.8	28.2		
31-Mar-2010	Speed	0.0	0.0	0.0	0.5	4.7	8.8	16.2	27.3	30.4	9.4	32.3	1488	1488
01-Apr-2010	Umajor	-27.0	-23.0	-14.9	-5.5	-0.6	-1.4	2.3	13.9	26.0	8.4	31.8		
-	Uminor	-15.4	-13.6	-8.8	-2.7	-0.2	0.3	1.4	14.2	19.2	6.3	26.2		
30-Apr-2010	Speed	0.0	0.0	0.1	2.4	5.8	8.0	12.9	20.8	27.5	7.0	33.3	1440	1440
01-May-2010	Umajor	-12.0	-10.0	-6.5	-0.1	2.6	3.0	6.2	13.6	16.9	5.7	18.9		
-	Uminor	-10.5	-8.5	-5.0	0.9	4.6	6.5	12.3	20.9	27.4	7.8	29.3		
31-May-2010	Speed	0.0	0.0	0.2	5.4	9.5	10.2	14.5	22.6	27.5	6.4	29.9	1488	1488
01-Jun-2010	Umajor	-34.0	-32.8	-30.7	-19.8	8.5	0.2	15.1	20.5	22.6	18.2	24.3		
-	Uminor	-1.6	-1.5	1.5	10.7	16.7	17.7	26.4	31.1	33.6	9.4	34.6		
30-Jun-2010	Speed	9.0	12.1	14.1	20.2	28.1	26.1	31.8	34.4	35.9	6.9	36.6	272	1440
01-Jul-2010	Umajor	0.0	0.0	0.0	0.0	0.0	0.0	0.0	0.0	0.0	0.0	0.0		
-	Uminor	0.0	0.0	0.0	0.0	0.0	0.0	0.0	0.0	0.0	0.0	0.0		
27-Jul-2010	Speed	0.0	0.0	0.0	0.0	0.0	0.0	0.0	0.0	0.0	0.0	0.0	0	1259
Entire	Umajor	-56.0	-38.5	-24.3	-7.3	-0.2	-2.0	3.2	15.5	34.6	12.5	63.4		
-	Uminor	-32.4	-24.1	-14.3	-3.4	0.2	2.7	8.0	25.2	32.5	11.4	53.0		
Record	Speed	0.0	0.0	0.1	4.4	10.5	13.1	19.3	33.5	52.5	11.2	63.7	9410	14023

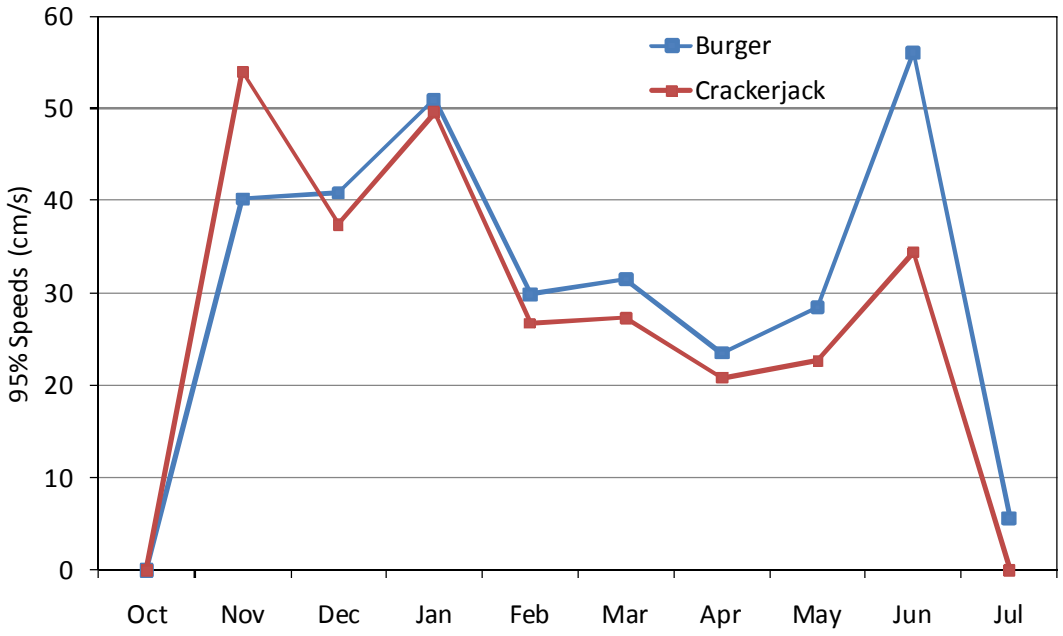

Figure 3-8. The 95 percentile 30 minute ice speeds (cm/s) by month at both sites.

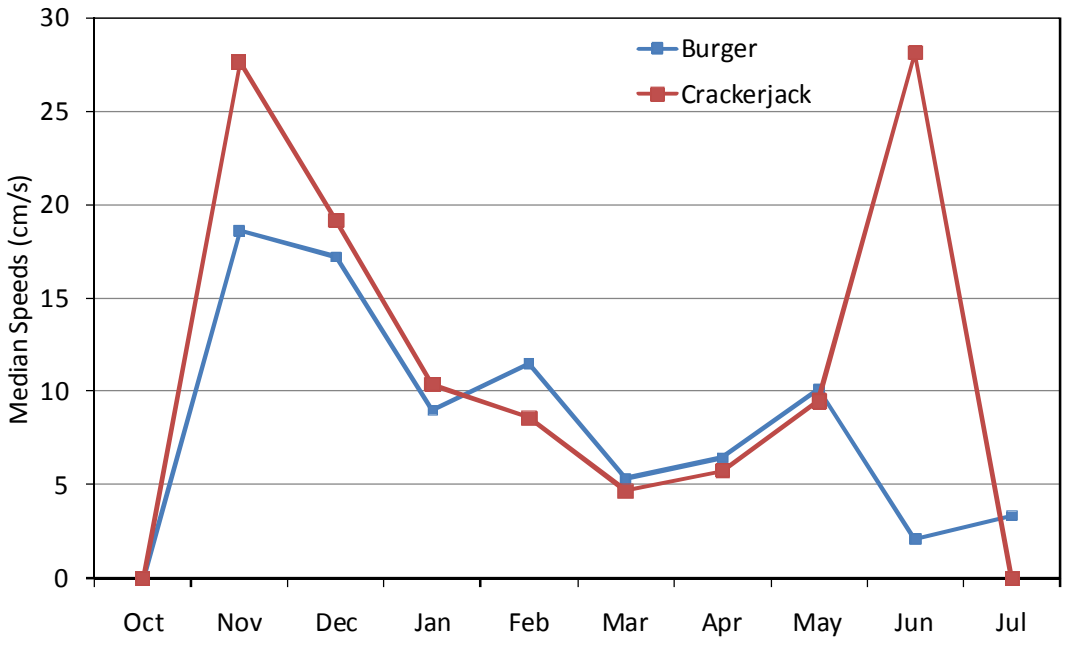

Figure 3-9. The median ice speeds (cm/s) by month at both sites.

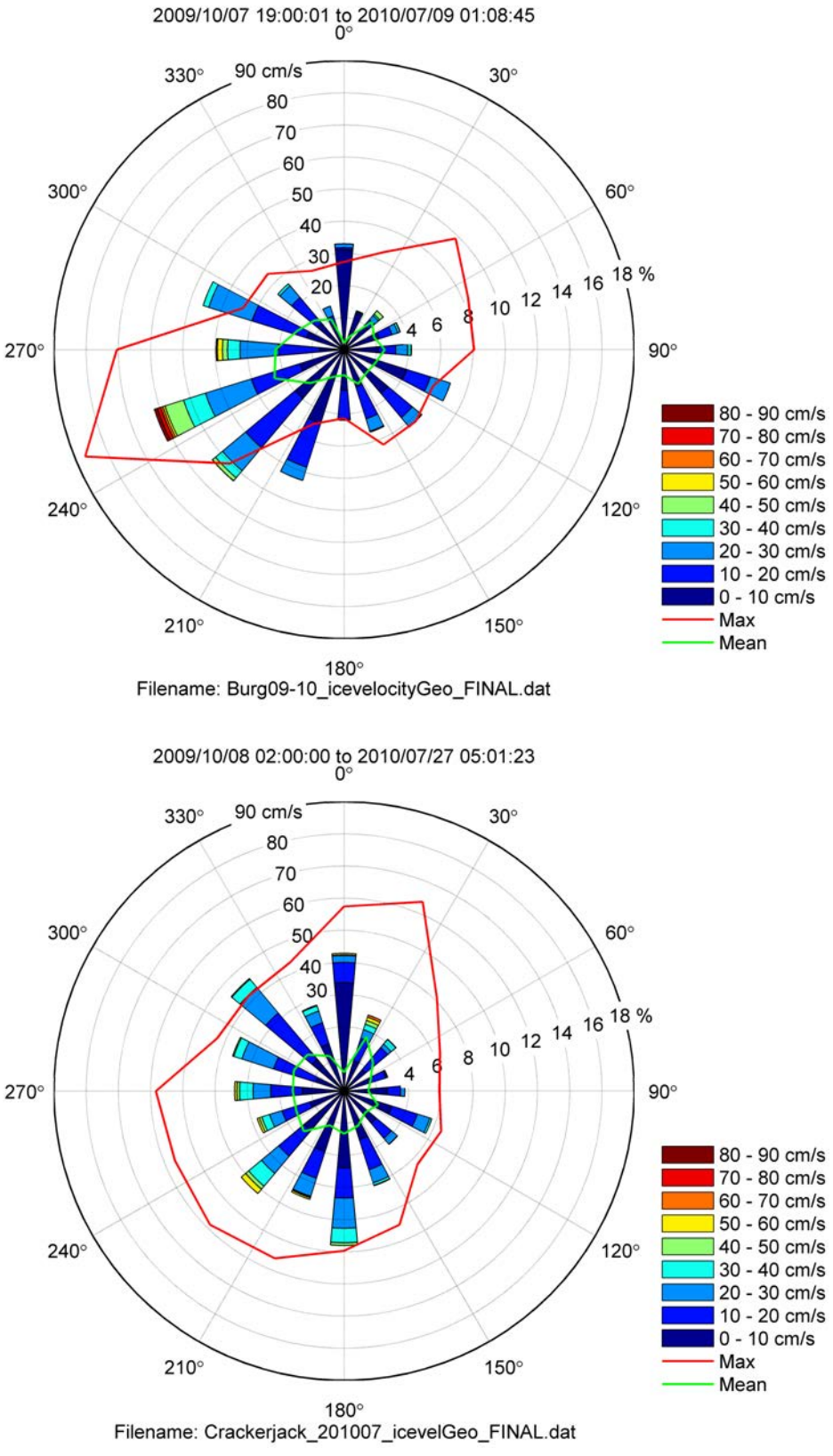

Figure 3-10. Compass plots of the directional (towards) distribution of the observed ice velocity over the full deployment for Burger (top) and Crackerjack (bottom). The next pages contain the monthly compass plots for each site.

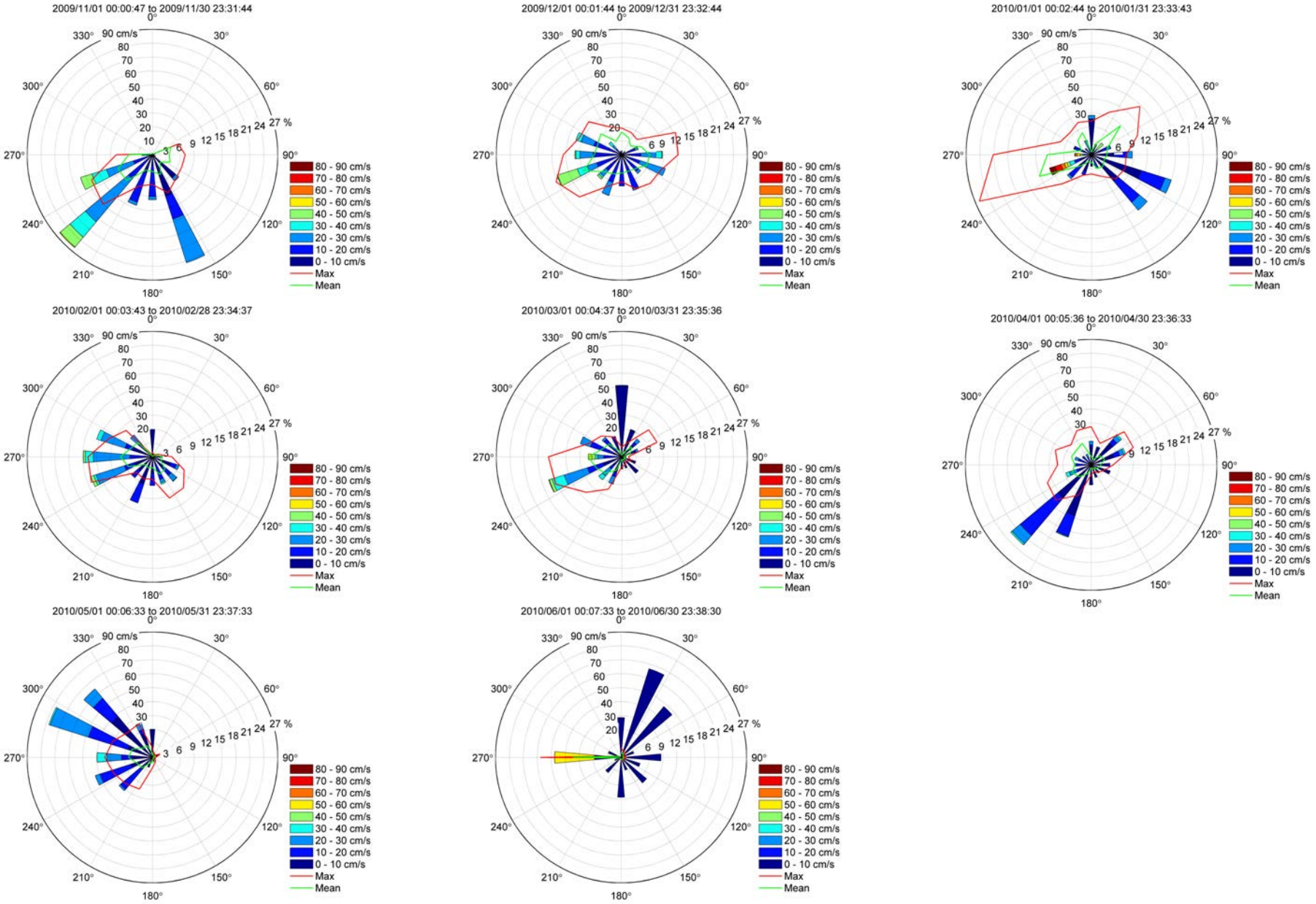

Figure 3-11. Monthly compass plots of the directional (towards) distribution of ice velocities from Burger, November 2009 to June 2010.

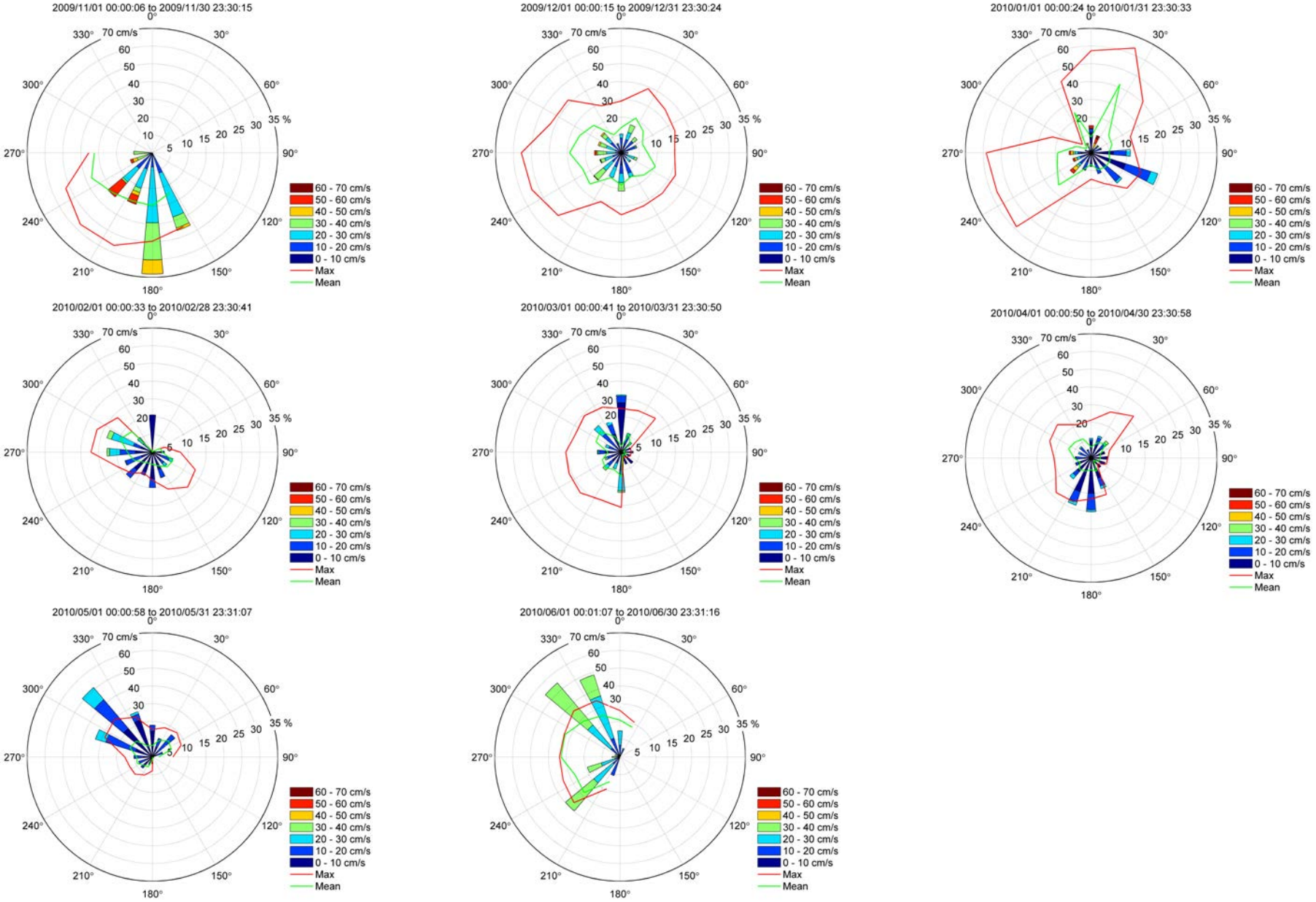

Figure 3-12. Monthly compass plots of the directional distribution of ice velocity at Crackerjack from November 2009 to June 2010.

3.3.3 SUMMARY OF ICE VELOCITY

Starting in December, there were periods where the ice would stop moving, in effect becoming locked up. The number of no-motion points in each month is summarized in Table 3-12. The proportion of no-motion observations reaches a maximum of 11.5% in March at Burger. For the same month, 7.4% of the time there was no-motion at Crackerjack.

Table 3-12. Summary of the number of no-motion points encountered at each site from October 2009 to July 2010.

	Burger			Crackerjack		
Month	# points	# zero points	% zero points	# points	# zero points	% zero points
Oct-09	1162	0	0.0%	1148	0	0.0%
Nov-09	1440	0	0.0%	1440	0	0.0%
Dec-09	1488	9	0.6%	1488	0	0.0%
Jan-10	1488	108	7.3%	1488	65	4.4%
Feb-10	1344	70	5.2%	1344	140	10.4%
Mar-10	1488	171	11.5%	1488	110	7.4%
Apr-10	1440	34	2.4%	1440	11	0.8%
May-10	1488	1	0.1%	1488	6	0.4%
Jun-10	1440	0	0.0%	1440	0	0.0%
Jul-10	387	0	0.0%	1259	0	0.0%

Ice velocity measurements were obtained at both measurement sites starting from November 2009, when new sea-ice formation began. The data at both sites ends when the resulting lower sea ice-concentrations led to unusable sea-ice velocity measurements.

The full set of joint frequency tabulations of Ice Speed vs. Ice Direction for each site (full record plus each individual month) are provided as part of the Data Archive on ASL's FTP site.

3.4 OCEAN CURRENT DATA

3.4.1 PROCESSING CURRENT PROFILER DATA

The Acoustic Doppler Current Profiler (ADCP) instrument, operating in the conventional water column data acquisition mode, provided time series measurements of three dimensional ocean currents, at 30 minute sampling intervals and with a vertical resolution of 4 m at Burger and Crackerjack.

The ADCP measurements nearest the bottom, at bin 1, correspond to measurements at about 34 m water depth or about 11 m above the seabed due to the length of the taut line

mooring, and the blanking distance associated with the instrument. The measurement depths, sampling intervals and number of data values, are summarized in Table 3-13. The mid-depth current measurements were taken from bin 4 at about 22 m water depth. The near-surface currents were recovered from various bins as outlined below. The data recovered from the instrument at Burger spans the entire deployment from October 7th, 2009 until July 9th, 2010 with some gaps where the instrument rejected inconsistent data. The instrument at Crackerjack also spans the entire deployment from October 8th, 2009 to July 27, 2010.

The ADCP currents in bins near the water-air interface are at time contaminated by waves. Similarly, the currents in the upper-most bins near the ice-water interface are at times contaminated by the presence of ice keels. A semi-automated methodology was developed to identify the first uncontaminated bin nearest the air-water interface for open water conditions or nearest the ice-water interface for ice covered conditions. This involved the use of the ADCP's pressure and bottom track channels in the following way:

1. The data was viewed in WinADCP, and for large wave events, the nearest surface bin that contained acceptable data was chosen.
2. The pressure record and the pressure standard deviation record were extracted from the ADCP.
3. The depth of water in each beam at which the bottom track was located was extracted from the ADCP (i.e. the vertical component of the bottom track range in each beam).
4. Due to the possibility of acceptable three beam solutions of the ice velocity, an assumption was made that if ice was present in one of the beams, but not the other three, the built-in data rejection algorithms of the ADCP would discard the data in the blocked beam, and generate an acceptable solution. Therefore, the second deepest depth by beam was extracted.
5. The pressure was converted to approximate depth by multiplying by a density of 1.025 and the time series was plotted.
6. The second deepest bottom track depth time series was overlaid on the same plot.
7. In a segment that was deemed to have no ice present, near the beginning of the record, the offset between the pressure record and the second deepest bottom track depth was determined to be 2.02m at Crackerjack and 2.13m at Burger. This was likely the result of accumulated errors in density of sea water and speed of sound that are used in converting pressure and bottom tracking measurements into actual depth.
8. The pressure standard deviation time series was plotted, and a noise floor of 0.05m was found. This amount was subtracted from the pressure standard deviation.
9. The modified pressure standard deviation was then multiplied by a factor and subtracted from the pressure signal, and overlaid on the plot of bottom track, and (now also modified) pressure sensor.

10. For each ensemble, the deepest of either the second deepest bottom track depth or the (pressure-factor*Press_std_dev) was chosen as the nearest surface.

11. For each of the ranges chosen in the previous step, a factor of range*cos(20) was subtracted to account for surface contamination. Due to the 20 degree angle of the ADCP beams from the vertical, the data from bins immediately below the water surface can be contaminated by the strong direct reflection from the water surface through the first side lobe in each beam. This effect of side-lobe returns could occur within 6% of the distance from the transducer to the water surface.

12. The factor by which the pressure standard deviation was multiplied was increased until the bin chosen visually in step one was picked by this algorithm for large wave events. Note that 4*Press_std_dev ≤ significant wave height. The actual factor used was 24 for Burger and 32 for Crackerjack.

13. If the bin picking algorithm described here chose a bin deeper than (20m for Crackerjack) or (25m for Burger), then the ensemble was flagged.

14. During large wave events, smoothing was applied manually as necessary.

The ADCP's *false target rejection* algorithm calculates a three-beam solution if the intensity from a single beam differs by a significant amount from the other beams. However, if more than one beam's intensity was significantly different from the other values or too small, no measured value was recorded.

Table 3-13. Summary of current measurement parameters.

	Burger	Crackerjack
Latitude	N 71° 14.3973'	N 71° 10.1832'
Longitude	W 163° 16.8112'	W 166° 44.9305'
Water Depth (m)	45	45
Bin Size (m)	4	4
Sample Interval (min)	30	30
Number of Data Values	13165	14023
Instrument Bin Number	Measurement Depth (m)	
1	34	34
2	30	30
3	26	26
4	22	22
5	18	18
6	14	14
7	10	10
8	6	6
9	2	2

Each time series data set was subjected to quality control procedures. The steps in the error detection and removal procedures were applied as follows:

1. Plots of all the raw data sets were prepared and reviewed, including the ADCP vertical and error velocities.
2. Values of measured horizontal components of current that had absolute values exceeding 200 cm s^{-1} were selected.
3. Values of measured horizontal components of current with accompanying error velocities that exceeded 10 cm s^{-1} were selected.
4. Single point 'spikes' in each component of the horizontal velocities were identified. A single point spike consisted of two successive first difference values exceeding 6 cm s^{-1} and opposite in sign.
5. 'Double spikes' exceeding a double spike threshold of 8 cm s^{-1} in each component of the horizontal velocities were identified. A double spike consisted of two consecutive points, both of which were either larger or smaller than the preceding and following points by more than the double spike threshold.
6. 'Triple spikes' exceeding a triple spike threshold of 10 cm s^{-1} in each component of the horizontal velocities were identified. A triple spike consisted of three consecutive points which were smaller than the preceding and following points by more than the triple spike threshold, but whose middle points could not change by more than one third of the triple spike threshold from their respective leading neighbors.
7. 'Quadruple spikes' exceeding a quadruple spike threshold of 12 cm s^{-1} in each component of the horizontal velocities were identified. A quadruple spike consisted of four consecutive points which were smaller than the preceding and

following points by more than the quadruple spike threshold, but whose middle points could not change by more than one third of the quadruple spike threshold from their respective leading neighbors.

8. For all suspect values found as above in items 2 to 7, the values were replaced by linear interpolation, over all individual segments with durations of less than three hours (approximately one eighth of the tidal signal which was predominantly diurnal). For longer segments of erroneous or suspect data, the values were replaced with flag values (-9999) and reviewed again in step 9.
9. Plots of the edited data sets (following step 8) were prepared and manually reviewed. Any remaining suspect values were manually edited. These suspect values were generally determined as being anomalous from adjoining values at nearby times or at adjacent bins above and below.
10. In cases where there were flags (from step 8), velocity data from neighboring bins were used to reconstruct the segments.

The number of data points which were identified as suspect in accordance with the above methodology is summarized in Table 3-14. The final step before starting the analysis of the data was to convert the currents from magnetic coordinates to geographic coordinates. This step included the application of the compass calibration information measured prior to the deployment of the ADCP's.

Table 3-14. Summary of the number of points modified at Burger and Crackerjack for selected bins.

	Veast			Vnorth		
	Near Surface	22m	34m	Near Surface	22m	34m
	Burger					
Out of Range	3	2	2	3	2	2
Single Spike	439	2	3	301	4	2
Double Spike	85	1	0	42	0	0
Triple Spike	4	0	0	4	0	0
Quad. Spike	0	0	0	1	0	0
Manual Edit	1567	2	0	1313	0	0
Total # Edited (%)	2191 (16.64%)	8 (0.06%)	5 (0.04%)	1717 (13.04%)	6 (0.05%)	4 (0.03%)
# Flagged	1	0	0	1	0	0
Total Pts	13165			13165		
	Veast			**Vnorth**		
	Near Surface	**22m**	**34m**	**Near Surface**	**22m**	**34m**
	Crackerjack					
Out of Range	1	1	1	1	1	1
Single Spike	386	11	4	308	6	1
Double Spike	71	1	0	54	0	0
Triple Spike	2	0	0	0	0	0
Quad. Spike	0	0	0	0	0	0
Manual Edit	1778	0	0	1650	0	0
Total # Edited (%)	2313 (16.49%)	14 (0.10%)	5 (0.04%)	2067 (14.74%)	7 (0.05%)	2 (0.01%)
# Flagged	0	0	0	0	0	0
Total Pts	14023			14023		

3.4.2 PLOTS AND STATISTICAL SUMMARIES FOR NEAR-SURFACE, MID-DEPTH AND NEAR-BOTTOM MEASUREMENT LEVELS

A major/minor coordinate system (Umajor and Uminor) was used, similar to the one already presented for the ice velocities in the previous section (Table 3-15). At Burger, the currents near the bottom were oriented along 93° to 273° (93º positive), near the middle oriented along 97° to 277° (97° positive), and near the surface oriented along 99° to 279° (99° positive). At Crackerjack, the currents near the bottom and near the middle were oriented along 37° to 217° (37º positive) and near the surface oriented along 32° to 212° (32° positive).

Table 3-15. Summary of the rotation applied at the near-surface, mid-depth, and near-bottom bins of each site to obtain the major/minor velocity components.

Burger	Current Direction (°)	Heading of Positive Umajor (°)
Bin 1	93-273	93
Bin 4	97-277	97
Near Surface	99-279	99
Crackerjack	Current Direction (°)	Heading of Positive Umajor (°)
Bin 1	37-217	37
Bin 4	37-217	37
Near Surface	32-212	32

The final versions of the edited current meter data sets for the two sites are presented for the near-surface, mid-depth, and near-bottom as time series plots (Figure 3-13 through Figure 3-20). Note that the measurement depth of the variable depth near-surface currents are generally between 6 and 10 m with the occasional time when the measurement depth can be 14 or 18 m (see Figure 3-14 and Figure 3-18)/

Statistical summaries of the near-surface, mid-depth and near-bottom current speeds are given for the entire deployment period in Table 3-16. Quarterly statistical tables are given in Table 3-17 through Table 3-22. The compass plot version of the ocean current directions and current speeds are presented for the full measurement record at each site in Figure 3-21.

The full set of joint frequency tabulations of current speed vs. current direction for each depth at each site (full record plus each individual month) are provided in Appendix 2 to this report (on DVD/CD ROM media).

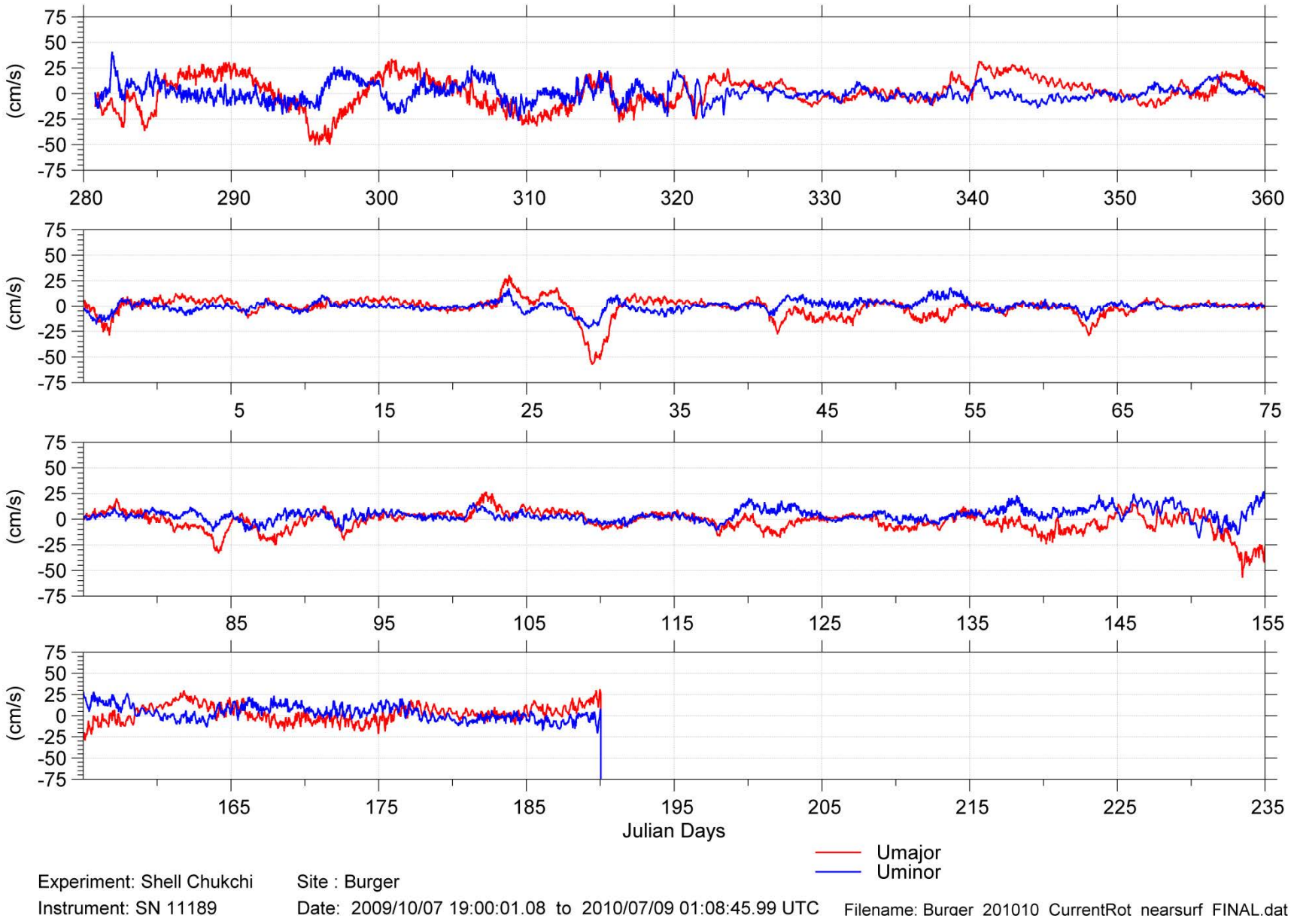

Figure 3-13. Plot of variable near surface 30 minute current measurements at Burger.

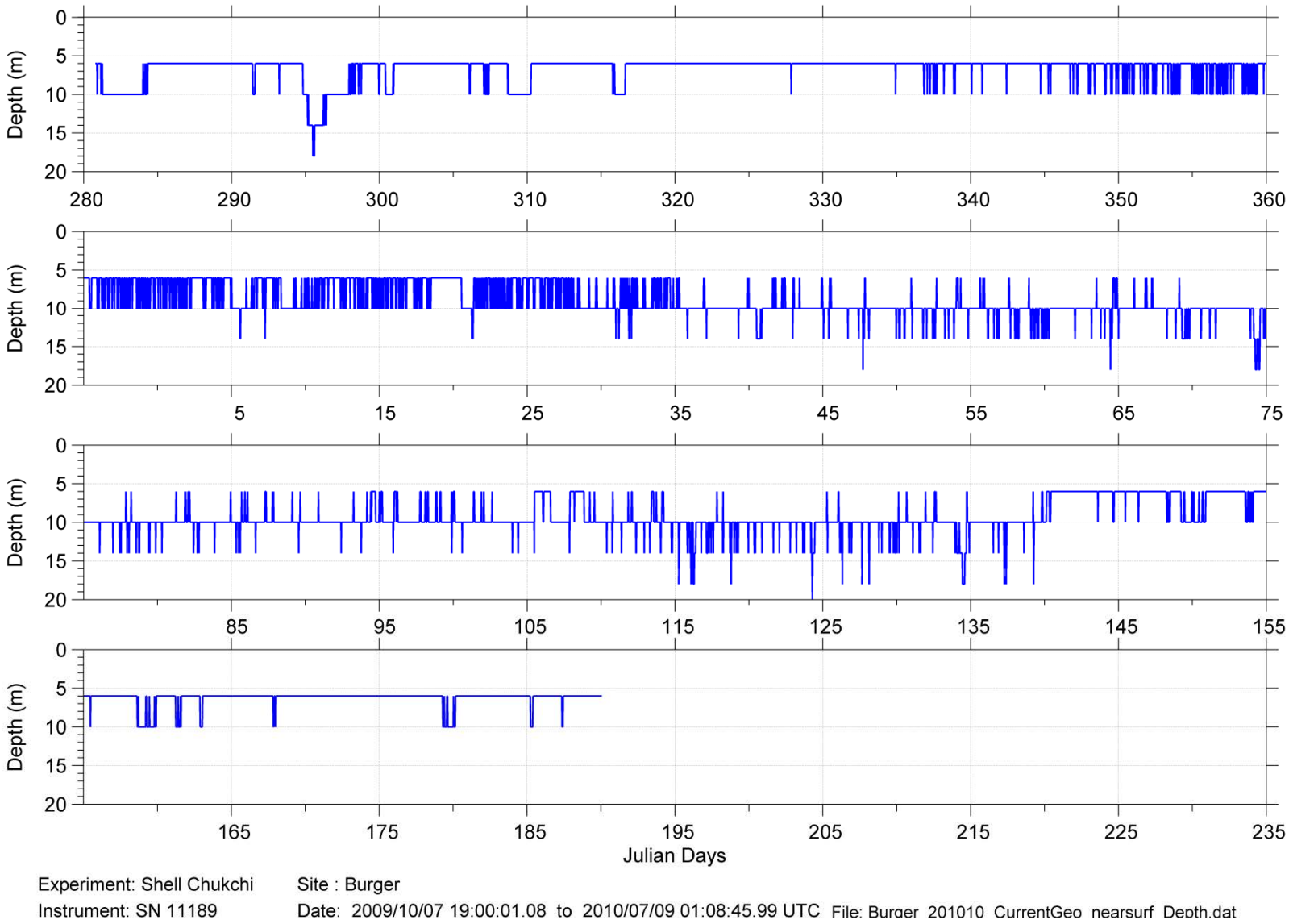

Figure 3-14: Time series plot of the depth chosen for the near surface bin at Berger.

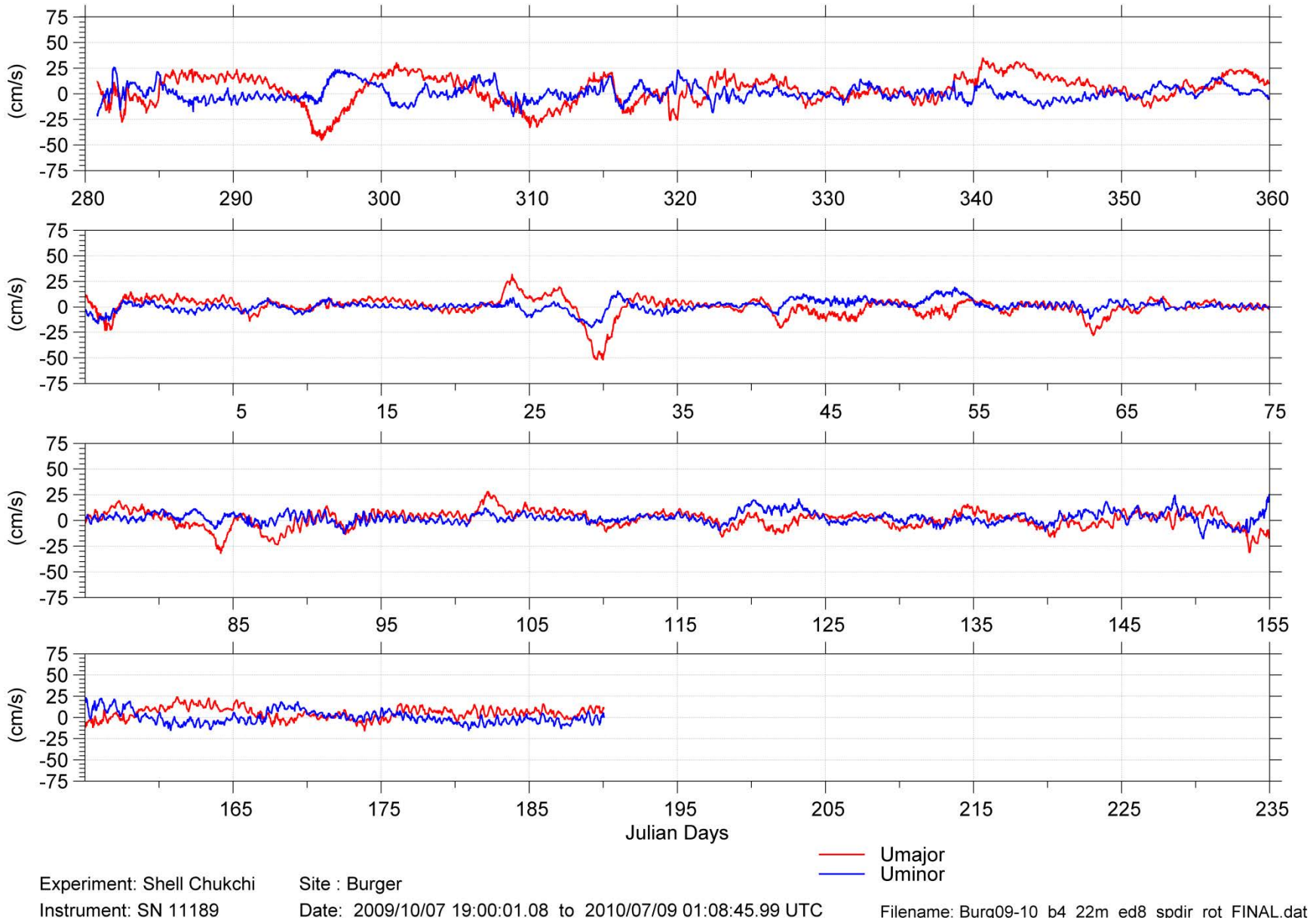

Figure 3-15. Plot of mid-depth (22m) 30 minute current measurements at Burger.

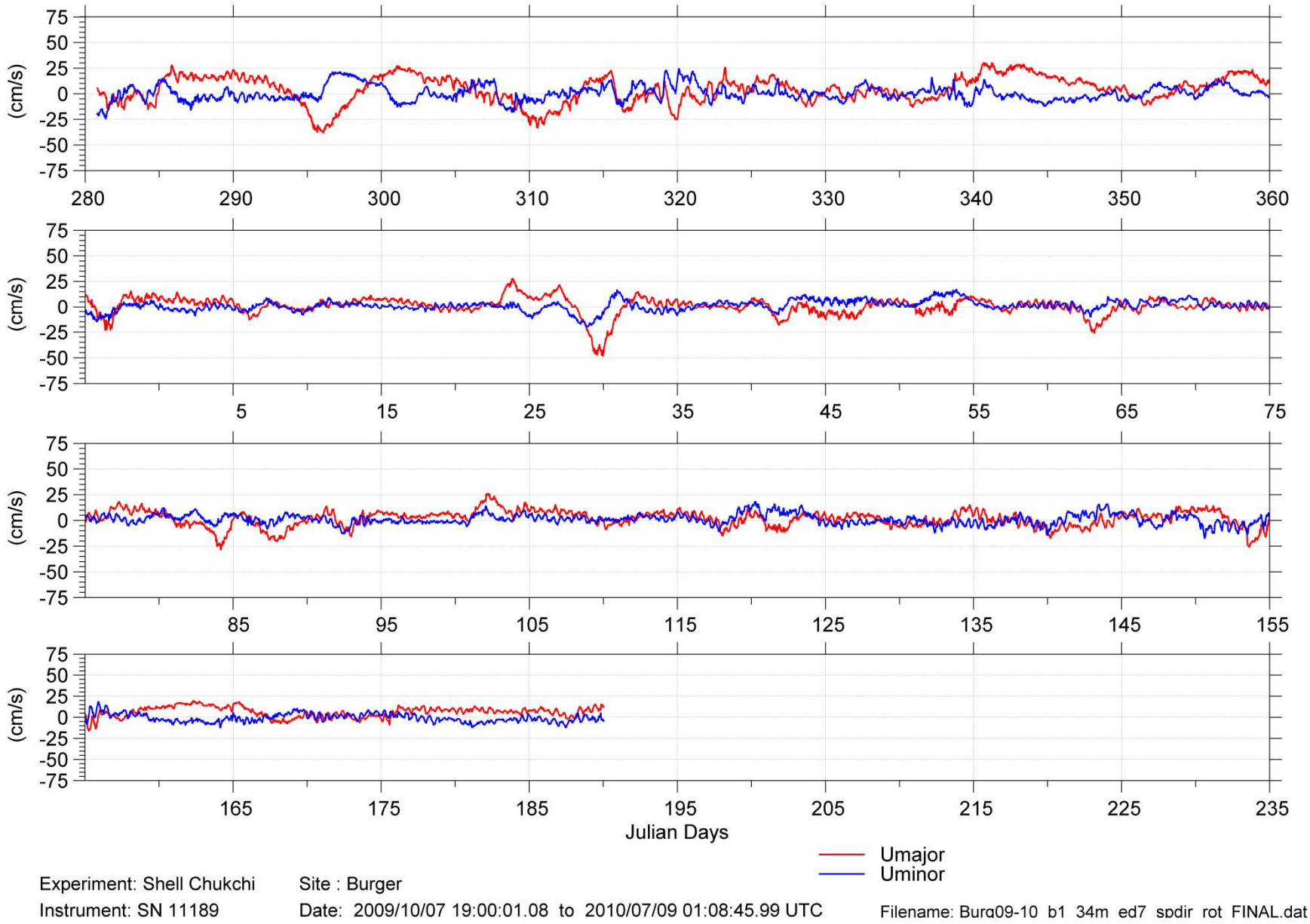

Figure 3-16. Plot of near bottom (34m) current measurements at Burger.

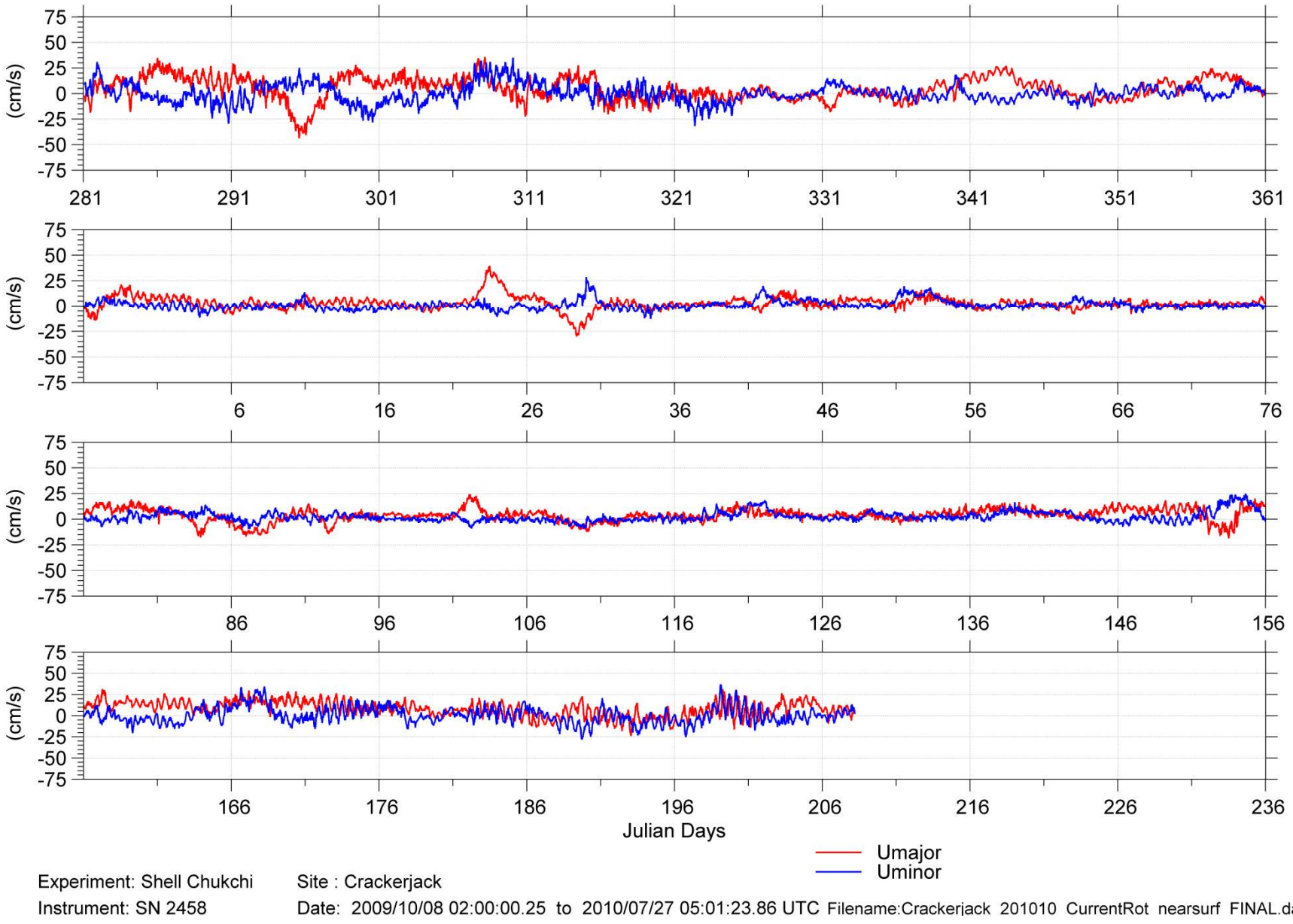

Figure 3-17: Plot of variable near surface 30 minute current measurements at Crackerjack.

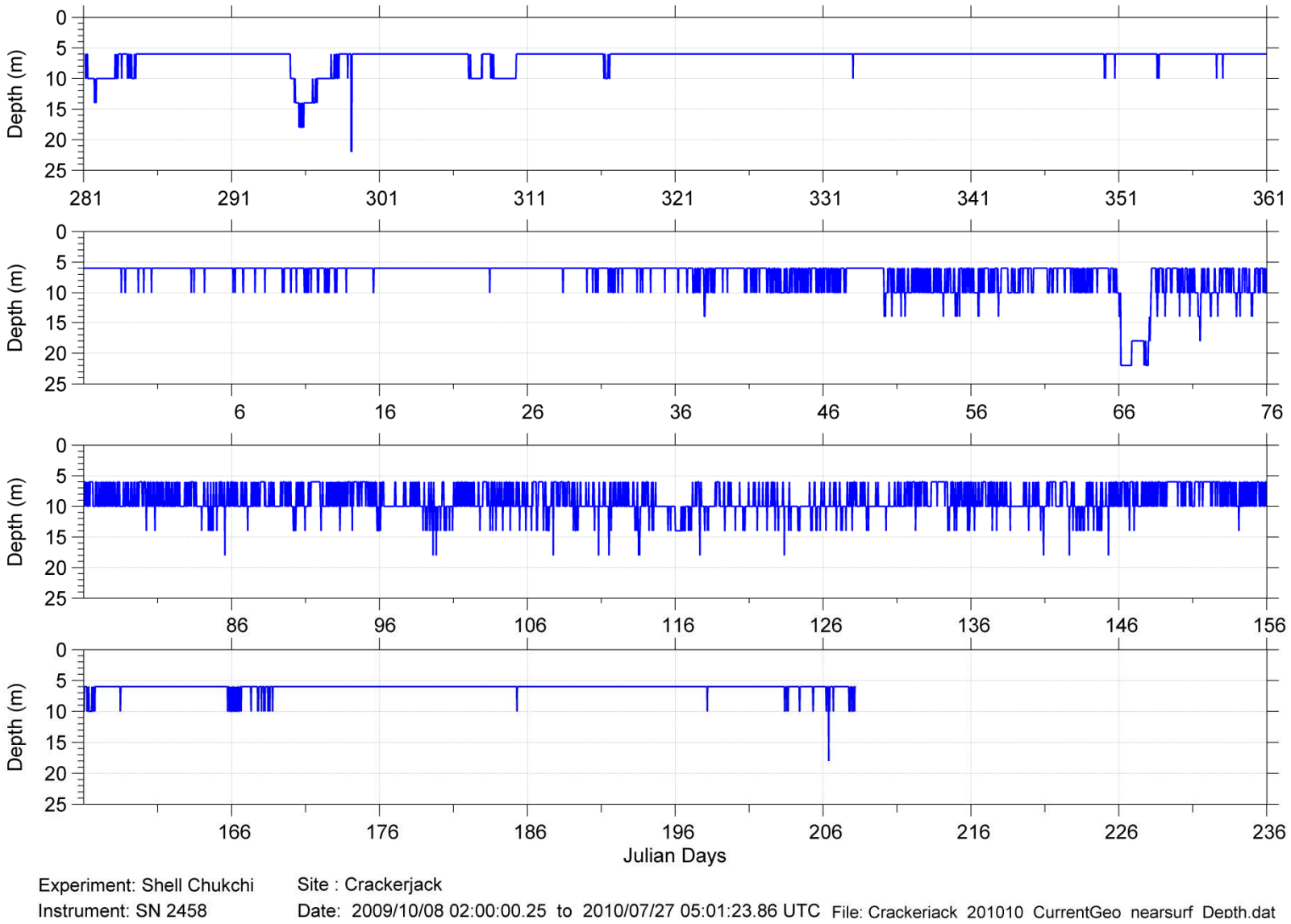

Figure 3-18: Time series plot of the depth chosen for the near surface bin at Crackerjack.

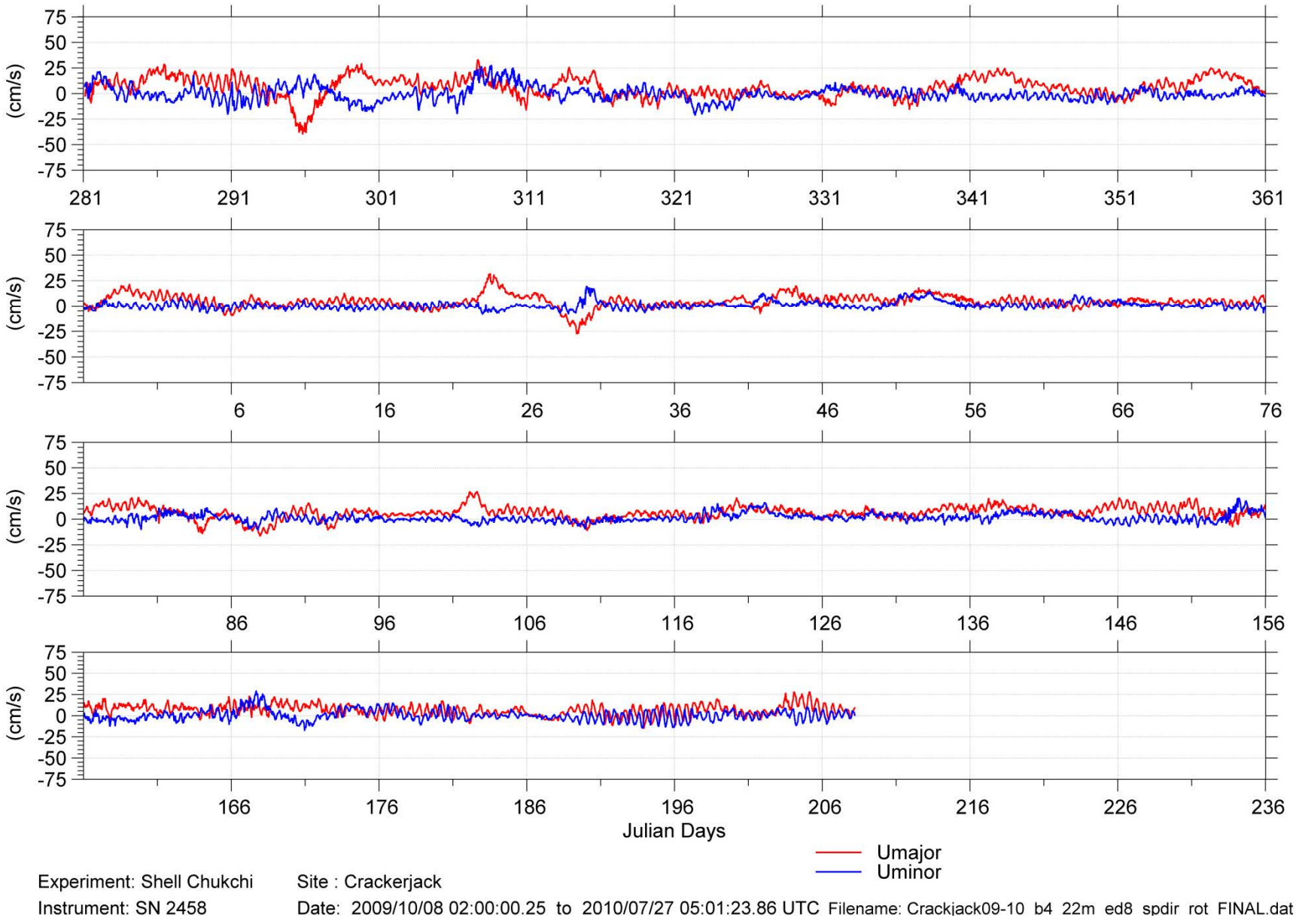

Figure 3-19: Plot of mid-depth (22m) 30 minute current measurements at Crackerjack.

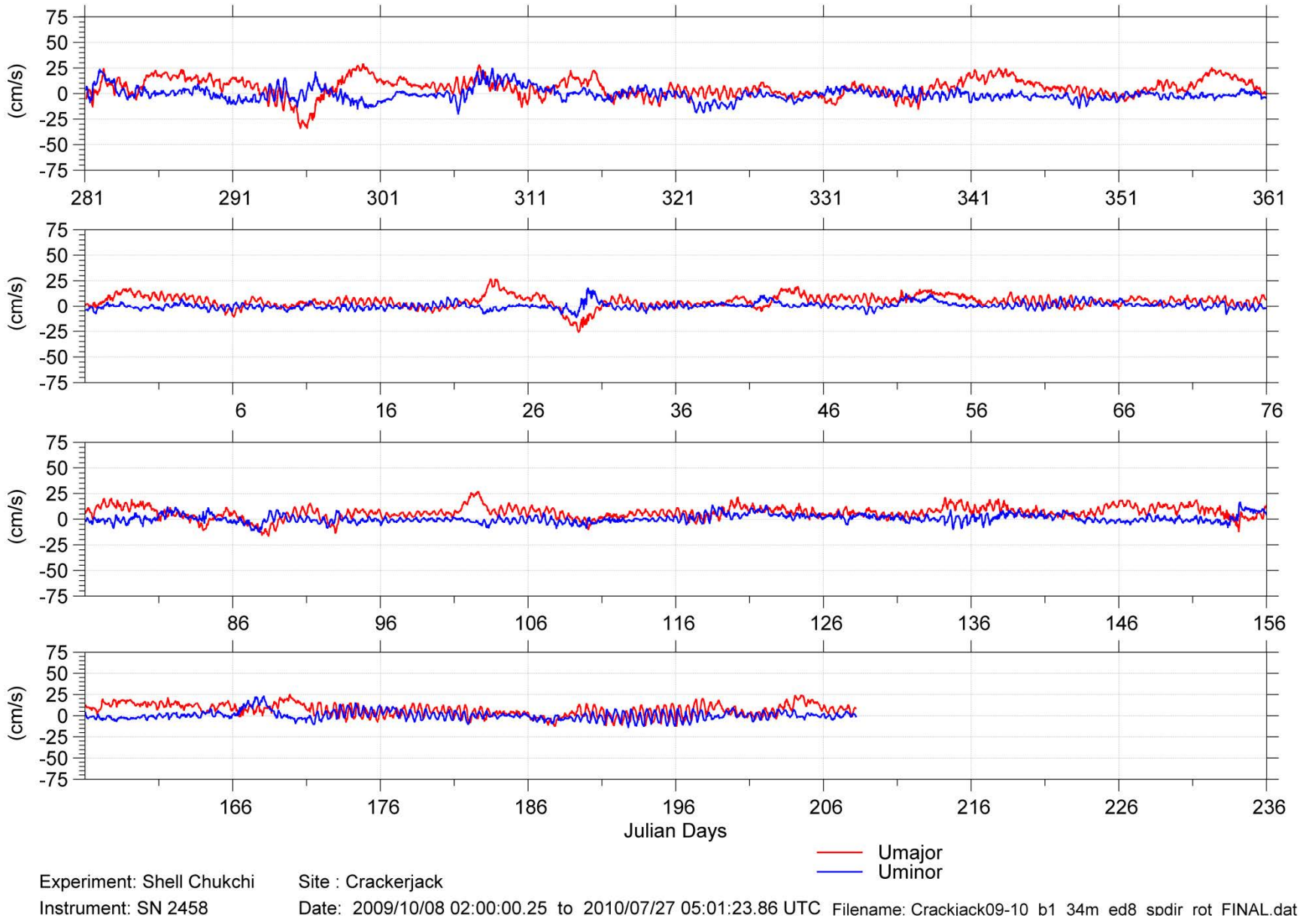

Figure 3-20. Plot of near bottom (34m) 30 minute current measurements at Crackerjack.

Table 3-16. Statistical summary of 30 minute current components and speeds at Burger and Crackerjack for the entire deployment.

			Annual Statistics (cm/s)												
Site	Depth (m)	chan	min	1%	5%	25%	50%	mean	75%	95%	99%	std	max	# valid	total #
Burger	Variable Near Surface	Umajor	-57.3	-39.6	-20.3	-6.2	0.7	-0.3	6.1	18.6	25.6	11.8	34.0		
		Uminor	-26.6	-16.5	-9.8	-2.6	1.3	1.7	5.6	15.1	20.8	7.3	41.0		
		Speed	0.1	0.9	1.9	5.3	9.1	11.2	15.3	26.7	41.6	8.3	60.4	13164	13165
	22	Umajor	-52.2	-31.5	-15.9	-3.3	3.0	2.2	8.1	18.8	25.7	10.6	35.1		
		Uminor	-22.6	-13.8	-9.0	-2.7	1.0	1.2	4.7	13.0	19.2	6.4	26.1		
		Speed	0.1	1.0	2.3	5.5	8.8	10.5	13.9	24.1	34.6	7.1	53.8	13165	13165
	34	Umajor	-48.5	-29.1	-14.5	-2.5	3.5	2.8	8.8	18.2	24.7	10.0	30.6		
		Uminor	-24.6	-13.9	-8.6	-3.0	0.5	0.7	4.1	10.8	16.9	5.9	24.8		
		Speed	0.1	1.0	2.3	5.4	8.6	10.0	13.1	22.5	31.4	6.5	49.0	13165	13165
Crackerjack	Variable Near Surface	Umajor	-43.8	-17.8	-9.3	-0.2	4.2	4.7	9.8	19.5	25.5	8.7	39.7		
		Uminor	-31.7	-17.4	-10.0	-2.5	0.7	1.1	4.4	13.8	21.7	7.1	36.7		
		Speed	0.1	0.8	1.8	4.6	8.4	10.0	13.9	23.4	31.1	7.0	50.6	14023	14023
	22	Umajor	-40.1	-14.7	-5.9	1.8	5.9	6.0	10.5	18.2	23.6	7.5	33.4		
		Uminor	-21.5	-13.2	-7.4	-2.3	0.4	0.7	3.2	10.0	17.9	5.4	29.3		
		Speed	0.1	0.9	2.2	5.0	8.3	9.4	12.6	20.3	26.8	5.8	41.9	14023	14023
	34	Umajor	-34.5	-14.0	-5.6	1.8	5.9	5.9	10.4	17.7	23.0	7.3	29.3		
		Uminor	-20.3	-11.6	-7.1	-2.5	-0.2	0.2	2.5	8.4	15.2	4.8	25.1		
		Speed	0.1	1.0	2.2	5.0	8.1	9.1	12.3	19.1	25.0	5.4	34.5	14023	14023

Table 3-17. Summary of 30 minute ocean current quarterly statistics for Burger at the near-surface.

		min	1%	5%	25%	50%	mean	75%	95%	99%	std	max	# valid	total #
Time		cm/s												
07-Oct-2009	Umajor	-50.6	-42.0	-25.0	-7.8	1.7	1.0	11.1	23.4	28.5	14.7	34.0	4090	4090
-	Uminor	-26.6	-18.7	-12.8	-4.9	-0.3	0.4	4.9	16.0	22.2	8.5	41.0		
31-Dec-2009	Speed	0.2	1.4	3.2	7.5	12.5	14.4	20.1	30.3	43.6	8.9	52.8		
01-Jan-2010	Umajor	-57.3	-43.8	-19.0	-5.4	0.4	-1.7	4.1	9.8	18.4	10.1	31.0	4320	4320
-	Uminor	-22.6	-16.5	-7.9	-2.2	0.5	0.4	3.3	9.0	12.9	5.2	18.3		
31-Mar-2010	Speed	0.1	0.6	1.4	3.5	6.4	8.4	10.7	21.5	44.2	7.8	60.4		
01-Apr-2010	Umajor	-56.9	-35.7	-15.9	-6.4	0.1	-0.8	5.2	14.4	22.1	10.0	29.8	4368	4368
-	Uminor	-18.2	-10.7	-6.0	0.2	3.9	4.7	8.9	17.5	22.0	7.0	28.4		
30-Jun-2010	Speed	0.1	0.9	2.4	5.9	9.4	11.0	14.7	23.1	38.4	7.2	57.2		
01-Jul-2010	Umajor	-10.5	-7.6	-4.4	1.2	5.6	6.8	11.8	20.5	27.4	7.8	31.3	386	387
-	Uminor	-20.6	-17.9	-13.8	-7.4	-3.3	-3.9	0.1	3.7	5.7	5.3	8.3		
09-Jul-2010	Speed	0.2	0.9	1.9	5.6	9.7	10.5	14.4	22.2	28.8	6.4	32.2		

Table 3-18. Summary of 30 minute ocean current quarterly statistics for Burger at mid-depth (22 m).

		min	1%	5%	25%	50%	mean	75%	95%	99%	std	max	# valid	total #
Time		cm/s												
07-Oct-2009	Umajor	-45.8	-36.3	-21.1	-4.7	5.7	4.0	14.4	23.2	29.2	13.7	35.1	4090	4090
-	Uminor	-22.6	-14.6	-10.6	-4.4	-0.2	0.5	4.8	14.6	20.8	7.5	26.1		
31-Dec-2009	Speed	0.1	1.3	3.4	7.9	13.1	14.1	19.1	28.1	38.1	7.9	46.0		
01-Jan-2010	Umajor	-52.2	-39.4	-18.2	-4.2	1.1	-0.4	5.5	11.6	19.5	9.9	32.4	4320	4320
-	Uminor	-21.0	-14.9	-6.7	-1.4	1.5	1.4	4.2	10.0	14.3	5.2	19.8		
31-Mar-2010	Speed	0.1	0.8	1.7	4.2	6.9	8.7	10.8	20.7	42.3	7.1	53.8		
01-Apr-2010	Umajor	-31.4	-15.7	-9.5	-2.1	3.5	2.8	7.5	14.6	21.7	7.5	28.5	4368	4368
-	Uminor	-18.2	-11.7	-7.9	-1.8	1.6	2.1	5.5	14.1	19.1	6.4	25.8		
30-Jun-2010	Speed	0.3	1.1	2.6	5.5	8.2	9.2	12.1	18.8	24.1	5.1	33.5		
01-Jul-2010	Umajor	-3.9	-3.1	-1.3	3.1	5.7	5.9	8.7	12.7	14.5	4.1	16.3	387	387
-	Uminor	-13.7	-12.0	-9.4	-6.9	-3.4	-3.5	-0.9	3.4	5.6	4.0	7.6		
09-Jul-2010	Speed	0.9	1.2	3.2	6.1	8.3	8.3	10.2	13.5	15.2	3.2	17.0		

Table 3-19. Summary of 30 minute ocean current quarterly statistics for Burger at near-bottom (34 m).

		min	1%	5%	25%	50%	mean	75%	95%	99%	std	max	# valid	total #
Time		cm/s												
07-Oct-2009	Umajor	-38.7	-32.2	-20.0	-3.6	5.8	4.3	13.9	22.6	27.6	12.9	30.6	4090	4090
-	Uminor	-24.6	-16.3	-10.1	-4.6	-0.4	0.3	4.3	13.7	19.9	7.3	24.8		
31-Dec-2009	Speed	0.2	1.7	3.7	7.9	12.7	13.7	18.4	26.8	33.8	7.2	38.8		
01-Jan-2010	Umajor	-48.5	-35.3	-16.2	-3.0	1.7	0.4	5.8	11.8	19.2	9.0	28.0	4320	4320
-	Uminor	-20.1	-15.4	-6.4	-1.2	1.7	1.6	4.5	9.8	13.8	5.1	17.9		
31-Mar-2010	Speed	0.1	0.8	1.8	4.3	7.0	8.4	10.5	19.1	35.5	6.3	49.0		
01-Apr-2010	Umajor	-26.2	-16.1	-8.8	-1.5	4.0	3.4	8.3	14.5	19.2	7.3	26.5	4368	4368
-	Uminor	-17.6	-11.6	-7.8	-2.9	0.2	0.5	3.8	9.3	14.2	5.2	18.9		
30-Jun-2010	Speed	0.1	0.9	2.2	5.0	7.8	8.4	11.2	16.9	21.4	4.6	29.2		
01-Jul-2010	Umajor	-2.1	-1.8	-0.6	4.9	7.3	7.0	9.6	13.0	15.0	3.7	16.2	387	387
-	Uminor	-12.2	-11.2	-8.5	-4.9	-3.2	-3.1	-1.4	2.7	4.3	3.2	5.8		
09-Jul-2010	Speed	0.8	2.4	3.8	6.8	8.6	8.6	10.4	13.4	15.7	2.8	16.6		

Table 3-20. Summary of 30 minute ocean current quarterly statistics for Crackerjack at the near-surface.

		min	1%	5%	25%	50%	mean	75%	95%	99%	std	max	# valid	total #
Time		cm/s												
08-Oct-2009	Umajor	-43.8	-28.5	-12.1	-2.5	5.4	5.0	13.0	21.6	27.2	11.1	35.8	4076	4076
-	Uminor	-31.7	-20.7	-13.0	-4.6	0.0	0.3	5.2	14.7	24.1	8.5	35.1		
31-Dec-2009	Speed	0.1	1.4	2.9	7.1	11.5	12.8	17.6	26.6	34.9	7.5	50.6		
01-Jan-2010	Umajor	-30.0	-17.6	-8.9	-0.4	2.6	2.7	6.0	12.5	25.0	6.9	39.7	4320	4320
-	Uminor	-12.8	-7.4	-5.0	-1.4	0.6	1.3	3.1	10.2	16.1	4.6	28.8		
31-Mar-2010	Speed	0.1	0.6	1.3	3.2	5.4	6.9	9.2	16.7	28.7	5.4	39.8		
01-Apr-2010	Umajor	-18.7	-11.0	-4.2	2.4	5.8	6.6	10.8	19.2	24.2	6.9	31.6	4368	4368
-	Uminor	-20.2	-11.5	-6.8	-1.3	1.4	2.5	5.3	15.6	23.1	6.6	34.4		
30-Jun-2010	Speed	0.1	0.8	1.9	4.7	8.2	9.9	13.8	22.8	29.8	6.7	39.6		
01-Jul-2010	Umajor	-23.6	-15.5	-11.6	-3.5	3.0	3.5	10.3	19.5	23.6	9.4	31.6	1259	1259
-	Uminor	-27.8	-23.0	-16.4	-7.1	-1.5	-1.1	4.7	14.4	24.1	9.4	36.7		
27-Jul-2010	Speed	0.1	1.2	3.1	7.5	11.4	12.2	15.9	23.6	30.8	6.4	38.1		

Table 3-21. Summary of 30 minute ocean current quarterly statistics for Crackerjack at the mid-depth (22m).

		min	1%	5%	25%	50%	mean	75%	95%	99%	std	max	# valid	total #
Time		cm/s												
08-Oct-2009	Umajor	-40.1	-27.6	-8.8	0.1	6.5	6.3	13.1	21.0	24.8	9.7	33.4	4076	4076
-	Uminor	-21.5	-16.3	-10.9	-4.3	-0.7	-0.3	2.9	11.9	20.7	6.8	28.0		
31-Dec-2009	Speed	0.2	1.2	2.6	6.2	10.4	11.6	16.1	23.8	31.3	6.9	41.9		
01-Jan-2010	Umajor	-27.7	-16.6	-8.1	1.3	4.6	4.5	8.2	15.0	21.2	6.8	32.3	4320	4320
-	Uminor	-10.5	-6.8	-4.3	-1.3	0.7	1.0	2.8	8.1	12.6	3.8	19.8		
31-Mar-2010	Speed	0.2	0.9	1.8	4.0	6.4	7.6	10.1	17.3	23.7	4.9	32.6		
01-Apr-2010	Umajor	-11.4	-6.3	-1.6	3.9	7.1	7.3	10.7	16.1	21.0	5.4	27.1	4368	4368
-	Uminor	-17.8	-9.6	-5.7	-1.5	0.9	1.6	3.9	11.3	18.0	5.2	29.3		
30-Jun-2010	Speed	0.1	1.2	2.5	5.6	8.8	9.4	12.6	18.2	24.0	4.9	30.9		
01-Jul-2010	Umajor	-15.0	-10.4	-5.7	0.7	4.9	5.2	9.8	16.9	24.9	7.1	28.4	1259	1259
-	Uminor	-15.1	-12.5	-9.9	-3.7	-0.2	-0.6	3.0	7.3	9.2	5.0	12.9		
27-Jul-2010	Speed	0.5	0.7	1.6	4.7	7.7	8.7	11.8	18.1	25.6	5.3	28.5		

Table 3-22. Summary of 30 minute ocean current quarterly statistics for Crackerjack at the near-bottom (34m).

		min	1%	5%	25%	50%	mean	75%	95%	99%	std	max	# valid	total #
Time		cm/s												
08-Oct-2009	Umajor	-34.5	-24.2	-8.3	0.4	6.0	6.0	12.1	20.3	24.2	9.1	29.3	4076	4076
-	Uminor	-20.3	-14.7	-9.6	-4.0	-1.2	-0.8	1.8	10.8	18.2	6.0	25.1		
31-Dec-2009	Speed	0.1	1.1	2.5	5.8	9.5	10.7	14.6	22.7	28.8	6.3	34.5		
01-Jan-2010	Umajor	-26.0	-16.1	-6.3	1.3	4.7	4.6	8.5	14.3	19.1	6.5	27.0	4320	4320
-	Uminor	-13.1	-8.6	-5.0	-1.8	0.3	0.5	2.4	7.4	10.3	3.7	18.3		
31-Mar-2010	Speed	0.1	0.9	1.9	4.2	6.6	7.5	10.0	16.3	21.6	4.5	27.3		
01-Apr-2010	Umajor	-14.0	-6.3	-1.4	3.8	7.2	7.6	11.3	17.1	21.7	5.7	27.2	4368	4368
-	Uminor	-10.6	-7.7	-4.9	-2.0	0.2	1.0	3.3	9.6	14.6	4.5	23.8		
30-Jun-2010	Speed	0.1	1.2	2.6	5.6	8.6	9.4	12.6	17.9	22.5	4.8	27.4		
01-Jul-2010	Umajor	-12.9	-11.3	-7.5	-0.8	3.8	4.3	9.0	17.2	22.1	7.3	24.7	1259	1259
-	Uminor	-14.3	-11.5	-8.6	-3.2	-0.4	-0.7	2.3	6.4	8.0	4.3	10.0		
27-Jul-2010	Speed	0.1	0.8	1.8	4.5	7.6	8.2	11.2	17.8	22.2	4.8	24.9		

The current speeds are further illustrated through compass plots (Figure 3-21), which show the speed and direction joint frequency distribution. The color of each segment denotes its speed interval. The radial length of each segment denotes the proportion of measurements

within the illustrated speed and direction interval. The mean and maximum are illustrated through the second radial scale as the green and red lines respectively.

Burger: Near-Surface

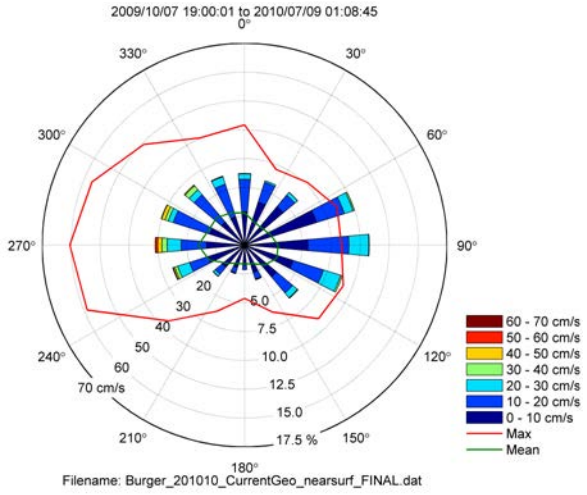

Crackerjack: Near-Surface

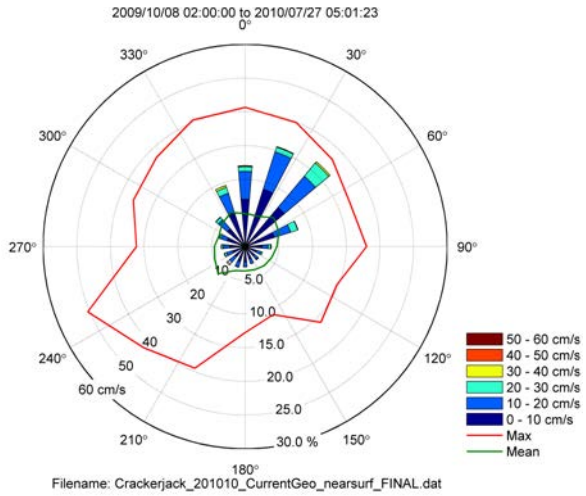

Burger: Mid-Depth

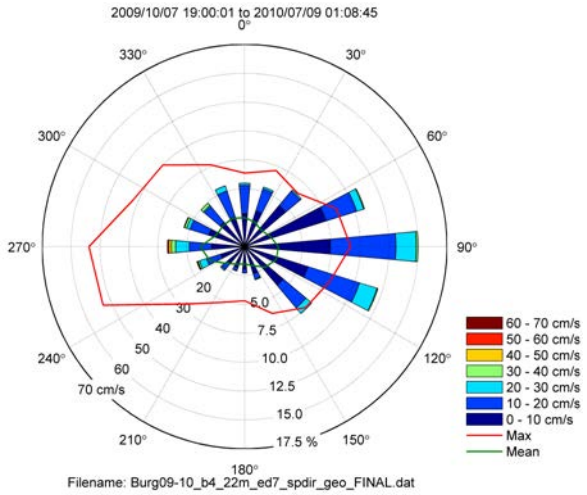

Crackerjack: Mid-Depth

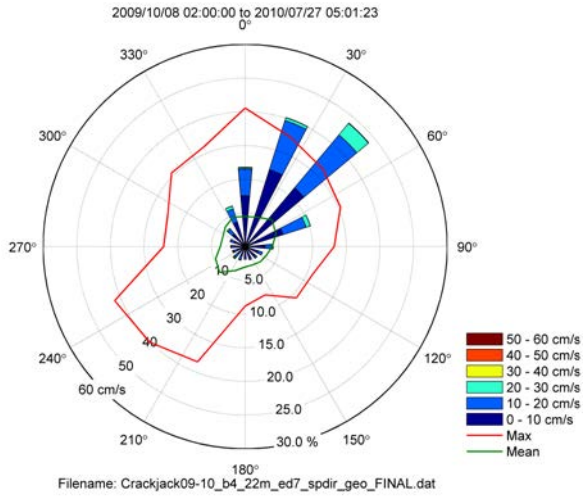

Burger: Near-Bottom

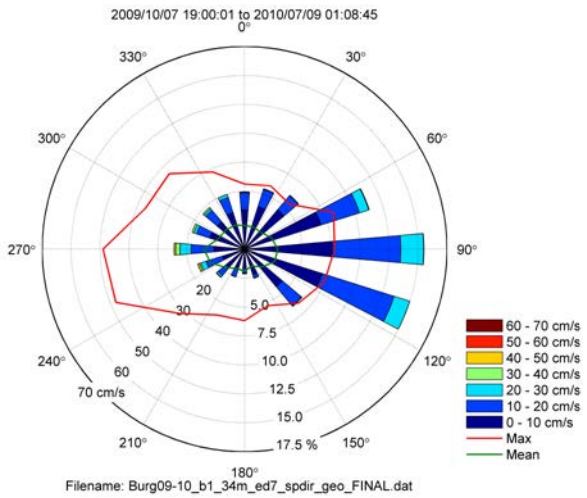

Crackerjack: Near-Bottom

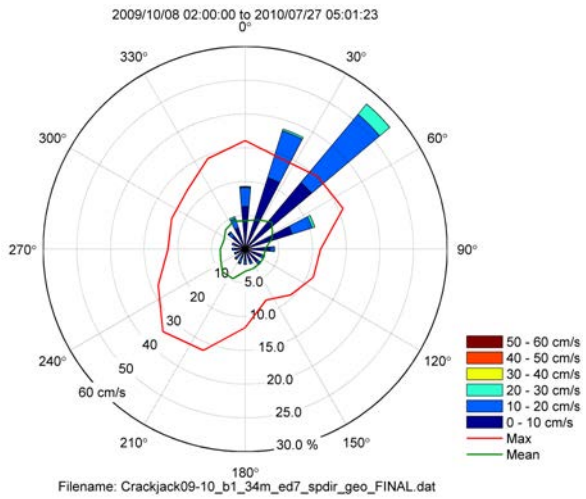

Figure 3-21. Compass plots of the directional distribution at the near-surface, mid-depth, and near-bottom at Burger and Crackerjack for the entire deployment period.

3.4.3 SUMMARY OF OCEAN CURRENTS

Continuous measurements of ocean current profiles were obtained at Burger and Crackerjack for approximately 10 months at 30 minute measurement intervals. Measurements at Burger were recorded from October 7th, 2009 to July 9th, 2010, and at Crackerjack were recorded from October 8th, 2009 to July 27th, 2010. The instrument at Burger failed 11 days prior to instrument recovery due to corrosion of the cable between the ADCP and its external battery. The instrument at Crackerjack functioned properly for the entire deployment and the quality of the data at both sites was reasonably high with a small number of gaps where the instrument rejected data due to low backscatter amplitudes or inconsistencies between the beams.

The ocean currents were characterized by occasional events of large currents, such as on October 22nd, 2009, where the speed was at 52.8 cm/s near the surface at Burger, and up to 50.6 cm/s on the same day at Crackerjack. This event corresponds to wind speeds of around 9 m/s at Point Lay and Wainwright. The maximum recorded current speed of 60.4 cm/s occurred at Burger on January 29th, 2010 while the maximum speed on the same day at Crackerjack was only 31.3 cm/s. This event corresponds to wind speeds of over 8 m/s at Wainwright. Wind speed data from Point Lay was not available for this day.

The average and maximum currents are somewhat larger at near-surface levels than at mid-depth and near-bottom levels. The average current speeds (and maximum speeds) at Burger are 11.2 (60.4) cm/s at near-surface, 10.5 (53.8) cm/s at 22 m depth and 10.0 (49.0) cm/s at 34 m depth. At Crackerjack the average (and max) current speeds are slightly lower at 10.0 (50.6) cm/s at near-surface, 9.4 (41.9) cm/s at 22 m depth, and 9.1 (34.5) cm/s at 34 m depth. The directions of the ocean currents are bi-modal at Burger with flows slightly more prevalent in the eastern rather than the western direction, particularly for the mid-depth and near bottom currents. The flows at Crackerjack were predominately to the northeast, with the near-bottom flows being more tightly distributed than the near-surface current. The current directions reflect the influence of the local bathymetry and the inflow of Pacific waters.

Current speed varied with the season, and was generally larger in magnitude in the fall at both sites. At Burger, the mean and 95th percentile speeds were largest in the fall and weakest in the winter; however, the maximum speed was highest in the winter due to a single event. Mid-depth and near-bottom speeds both had greater means and 95th percentiles in the fall than in the winter. Again the same single energetic event produced maximum speeds at mid-depth and near-bottom in the winter. At Crackerjack, maximum speed was highest in the fall season, with winter and spring maximums being similar in magnitude. The mean current speeds weakened through the winter and increased again in spring. The larger speeds in the fall may reflect a greater occurrence of winds and the prevalence of storms. In the fall and summer, when ice concentrations are reduced or zero, twice daily variations in the currents are clearly evident (see Figure 3-13 through Figure 3-20). These variations are inertial oscillations with typical speeds of 10-15 cm/s

3.5 BOTTOM TEMPERATURES, SALINITY AND DENSITY

The ADCP instruments were equipped with temperature sensors from which time series measurements of near bottom temperatures are available. A RBR XR-420 CT instrument, attached to the IPS-5 mooring cage at Crackerjack. This instrument provided bottom temperature and conductivity data which could be used to derive a salinity and density time series. The ADCP and CT data sets required truncation of data values immediately after the instruments were deployed and on recovery to limit the time series to the in-water part of the deployment where the sensors were in thermal equilibrium with the ambient water.

Temperature records at both sites show similar seasonal trends (Figure 3-22 and Figure 3-23). By early October when the records begin, the near-bottom waters are approximately 2 °C with ongoing cooling until the freezing point temperature is reached in early November 2009 at both sites. Temperatures consistently stayed at or near the freezing point at both measurement sites until late June 2010. The salinity and density measurements at Crackerjack (Figure 3-22) reveal increasing salinities through late winter and spring, which is related to horizontal advection of different water masses through the measurement area.

Table 3-23. Record-length statistics computed for the near-bottom temperature data at Sites Burger and Crackerjack.

Site	Instrument	Instrument Depth (m)	Water Depth (m)	Sample Interval (min)	Mean (°C)	Standard Deviation (°C)	Min (°C)	Max (°C)
Cj	RBR XR-420 15282	42	45	5	-0.98	1.40	-1.84	3.05
Bu	ADCP WH 11189	43	45	30	-1.34	1.13	-1.91	2.66
Cj	ADCP WH 2458	43	45	30	-1.10	1.36	-1.92	2.92

Table 3-24: Near bottom temperature, salinity and density statistics computed from the RBR XR-420 at Crackerjack.

08-Oct-2009 01:55:00 to 27-Jul-2010 05:45:00												
Depth (m)	Crackerjack	min	1%	5%	25%	50%	mean	75%	95%	99%	std	max
41	Temperature (°C)	-1.837	-1.827	-1.812	-1.778	-1.736	-0.98	-0.78	2.435	2.874	1.395	3.05
	Salinity (psu)	29.078	31.456	31.684	31.954	32.14	32.426	32.839	33.644	33.834	0.642	34.001
	Density (kg/m^3)	1023.4	1025.42	1025.56	1025.83	1026	1026.252	1026.62	1027.27	1027.43	0.547	1027.57

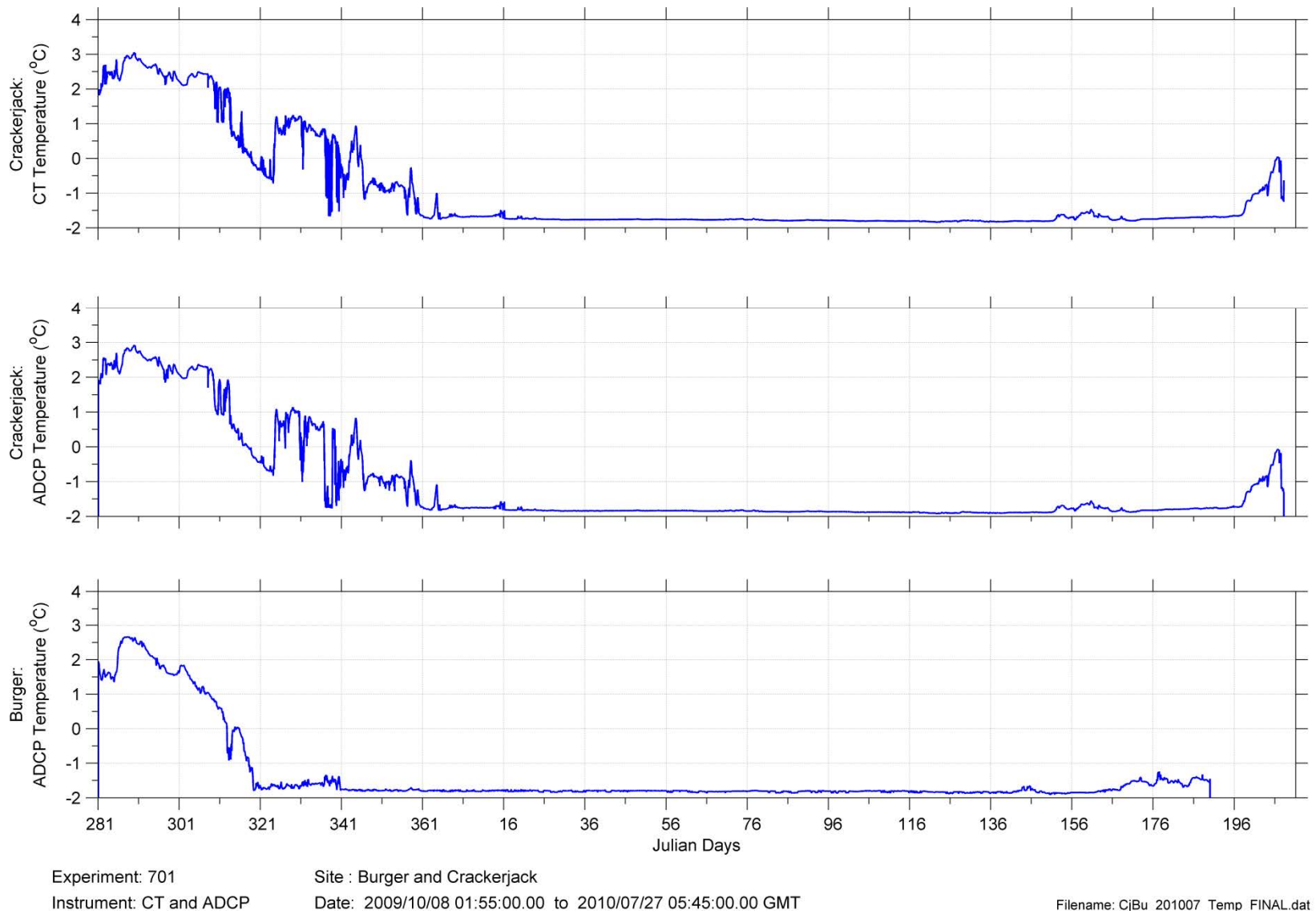

Figure 3-22: Near-bottom temperature data measured by ADCP and CT sensors at Burger and Crackerjack.

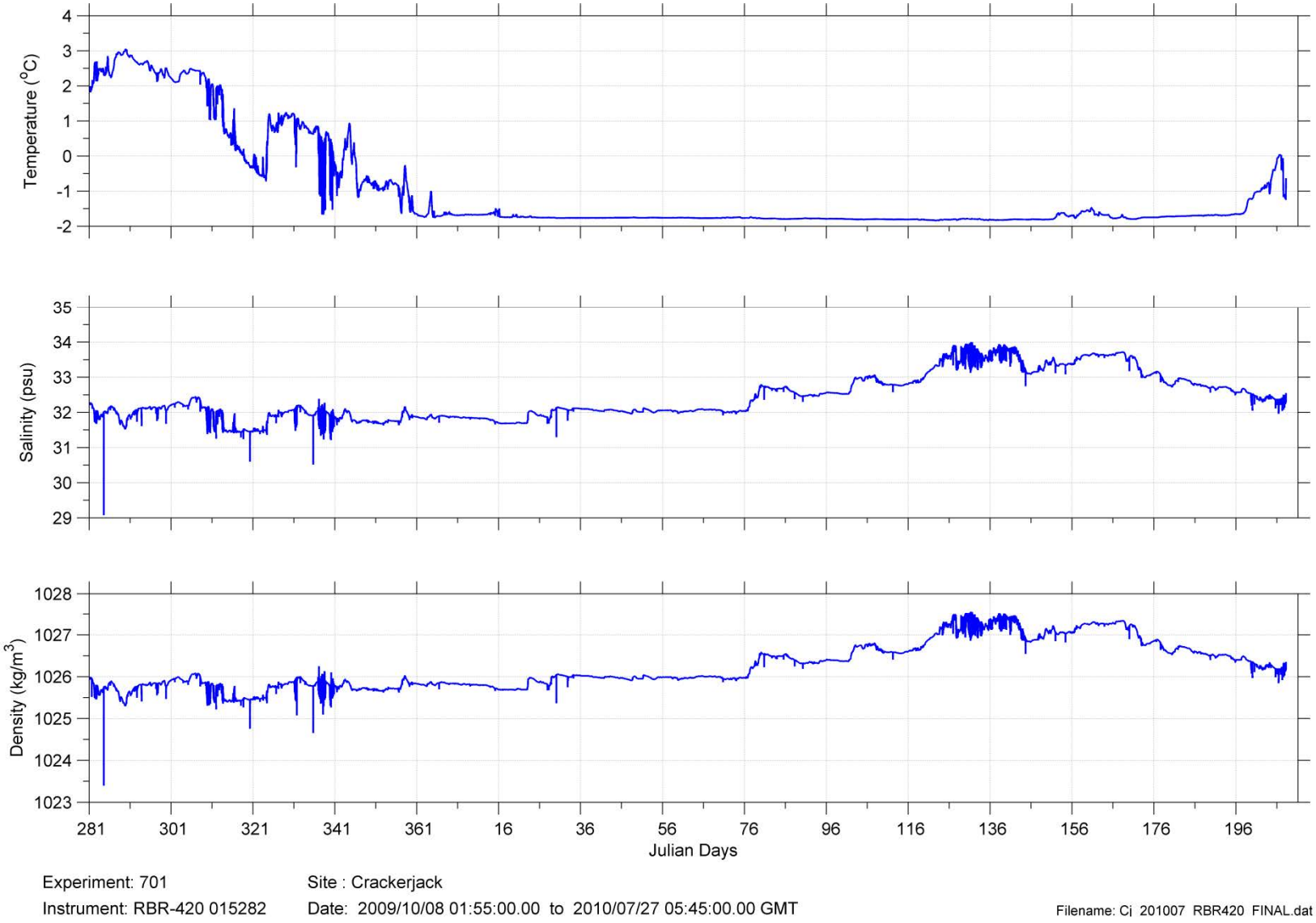

Figure 3-23: Near bottom temperature, salinity, and density measured by the CT sensor at Crackerjack.

3.6 METEOROLOGICAL DATA

Meteorological station measurements were obtained from Point Lay, and Wainwright, Alaska.

All of the measurements were obtained from the Weather Underground online weather service (*http://www.wunderground.com*). The wind data represents the standard 10 m anemometer height and represents mean wind values (1 minute or longer sampling duration) reported at hourly intervals.

The data from this site contained hourly- time series measurements of:

- atmospheric pressure (dbar)
- air temperature (°C)
- wind direction (°)
- wind speed ($m \cdot s^{-1}$)

The daily observations of wind speed and air temperature are shown in Figure 3-24. The meteorological observations were used to assist in interpreting and classifying ice keel features at the measurement site. The sea level pressure measurements (not illustrated) were also required to provide quantitative values for the purposes of computing ice drafts (equation 1 in section 3.1.2.1) for processing the ice profiling sonar data. Note that the wind data measurements are missing for Point Lay from day 303 (2009) to day 36 (2010).

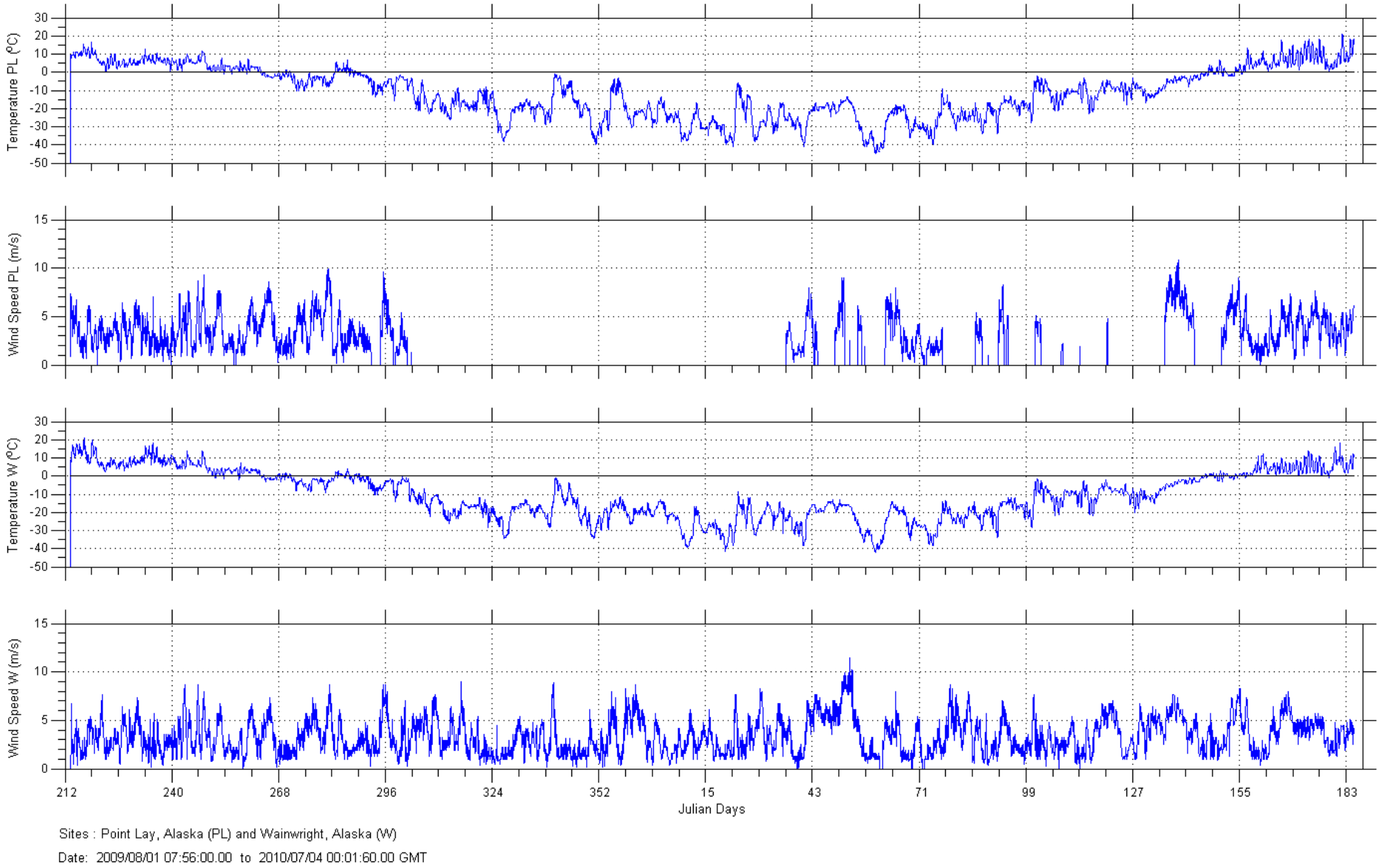

Figure 3-24. Daily air temperature and wind speed as observed at Point Lay and Wainwright weather stations from August 2009 to July 2010.

3.7 OTHER ICE DATA SETS

In addition to the underwater profiling measurements of ice keels collected at the measurement sites over the October 2009 to July 2010 period, other ice data were also obtained:

1. Weekly ice charts prepared by the U.S. National Ice Service (http://www.natice.noaa.gov/) from the week of July 31, 2009 to the week of July 29, 2010.
2. Daily SSM/I passive microwave ice concentration data provided by NOAA (http://polar.ncep.noaa.gov/seaice/Analyses.html) from July 27, 2009 to July 31, 2010.

These ice data sets were used to assist in interpretation of the ice profiling sonar data set; in particular, for determining if very thin ice or open water was present to assist in making corrections for variations to the ice drafts due to changing sound speeds in the ocean.

A source book was created using all the above data types, as well as the weather measurements. It was circulated among ASL's in-house scientific analysts to aid in interpretation and verification of ice movements in the region and, specifically, at the monitoring sites.

3.8 DATA ARCHIVE

All data sets collected directly as part of the present study are provided on a FTP site or via CD-ROM (upon request). The organization of the data, plots and other documentation is;

ANCILLARY DATA:

Crackerjack Site
- IPS
- ADCP

Burger Site
- IPS
- ADCP

Data are provided in ASL Standard Format: one data file, and header file pair for each dataset. The header file has the file extension '.hdr' and is a text file contains metadata for the data in the data file. The data file has the file extension '.dat' and is a text file that contains columns of data.

4 ANALYSIS RESULTS

4.1 OVERVIEW OF SEA ICE CONDITIONS IN 2009-2010

For the fourth year in a row, the fall season in Arctic Ocean was characterized by a major retreat north of the edge of the pack ice (Figure 4-1). The Arctic Ocean ice extent was at a historic low in 2007, with the second, third and fourth lowest values occurring in 2008, 2010 and 2009, respectively. The retreat of the minimal sea ice extent was particularly pronounced in the western Arctic Ocean in all four years.

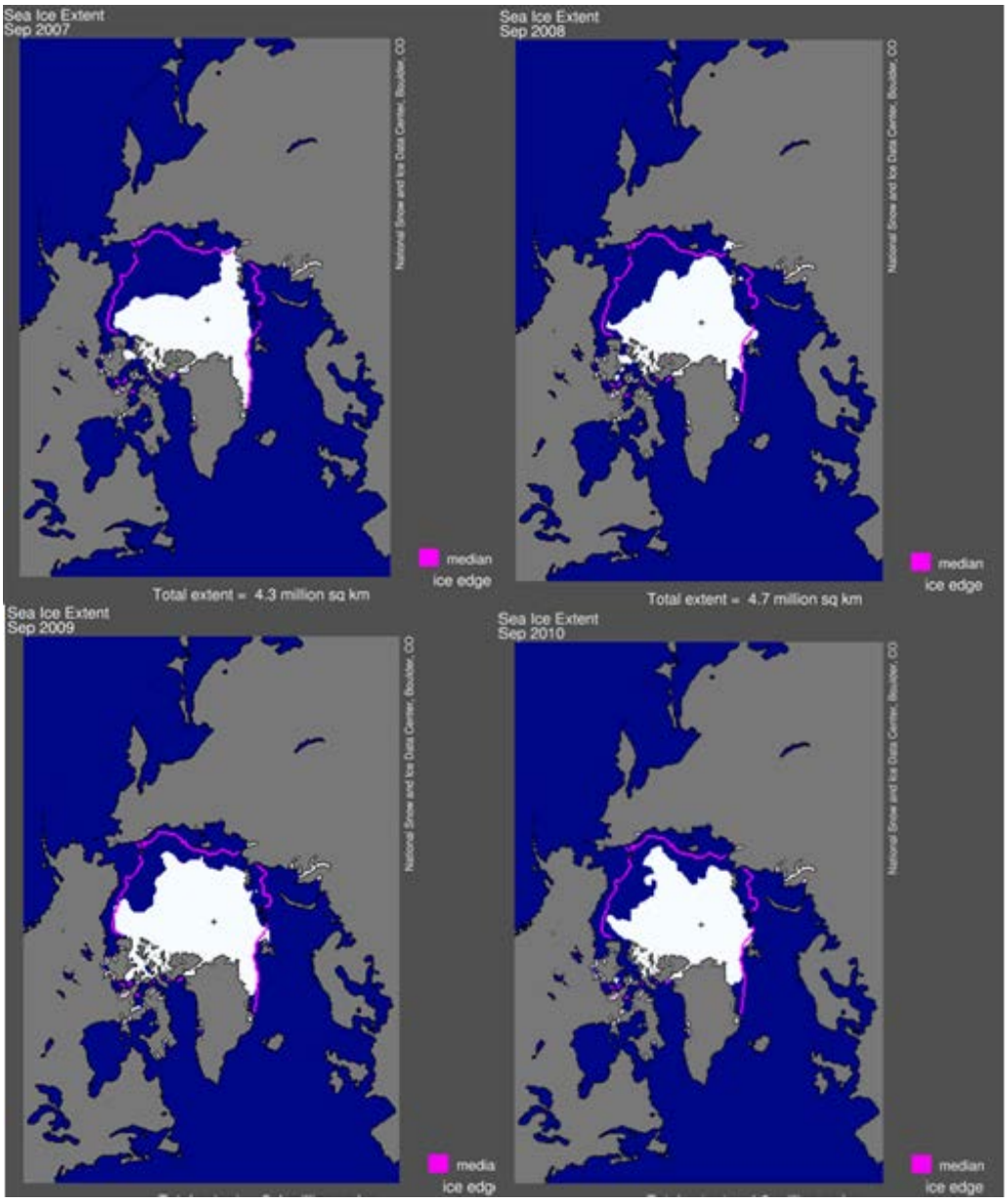

Figure 4-1. September sea ice extent concentrations for 2007 to 2010. (http://nsidc.org/).

4.1.1 FREEZE-UP PATTERNS: OF FALL 2009

In the fall of 2009, pack ice was for the most part located well offshore in the northern Chukchi Sea with the ice edge extending well beyond the continental shelf and slope waters to northerly latitudes rivaling late summer 2007; however the open water did not extend as far west off East Siberia as experienced in the last three years. (Figure 4-2 and Figure 4-3.)

Ice formation began along the coast in mid October 2009 following the usual seasonal pattern. While some new ice, at concentrations of 1 to 5 tenths, is present in the vicinity of the Burger site in the Nov 16-20 ice chart, it was not until Nov. 23-27 that the ice concentrations attained values of 9+ tenths for both the Crackerjack and Burger sites. By this time, the ice charts indicate that the ice is made up of mainly young ice with ice free waters remaining in close proximity to the Crackerjack site. The first few days of December represented the transitional time when there were no more ice-free regions in the Chukchi Sea.

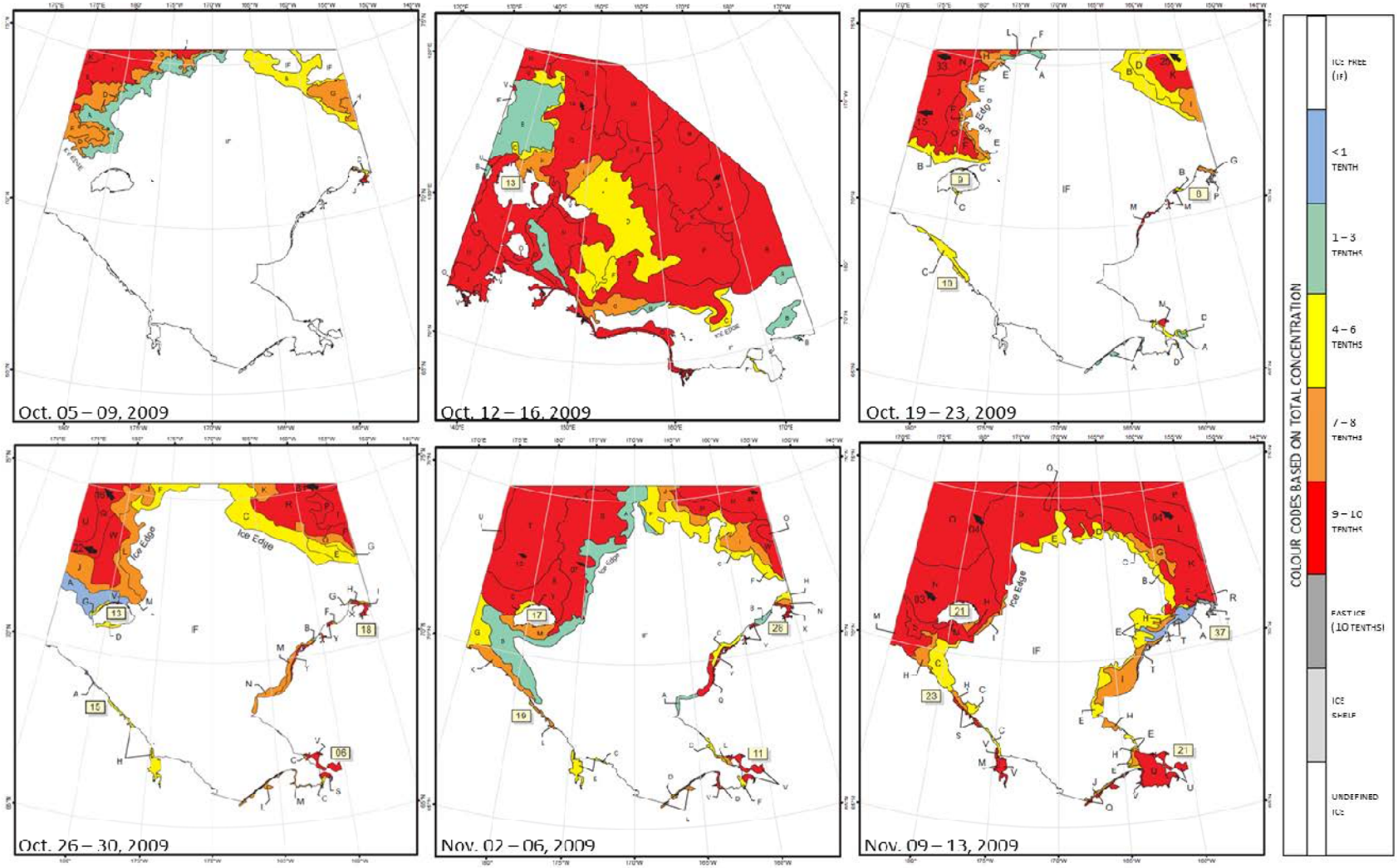

Figure 4-2. Fall 2009 freeze-up patterns. Ice charts are presented for the period of Oct. 5-9 to Nov. 9-13 in the Chukchi Sea. Crackerjack is located at 71°10'N, 166°45'W and Burger is at 71°14'N, 163°17'W.

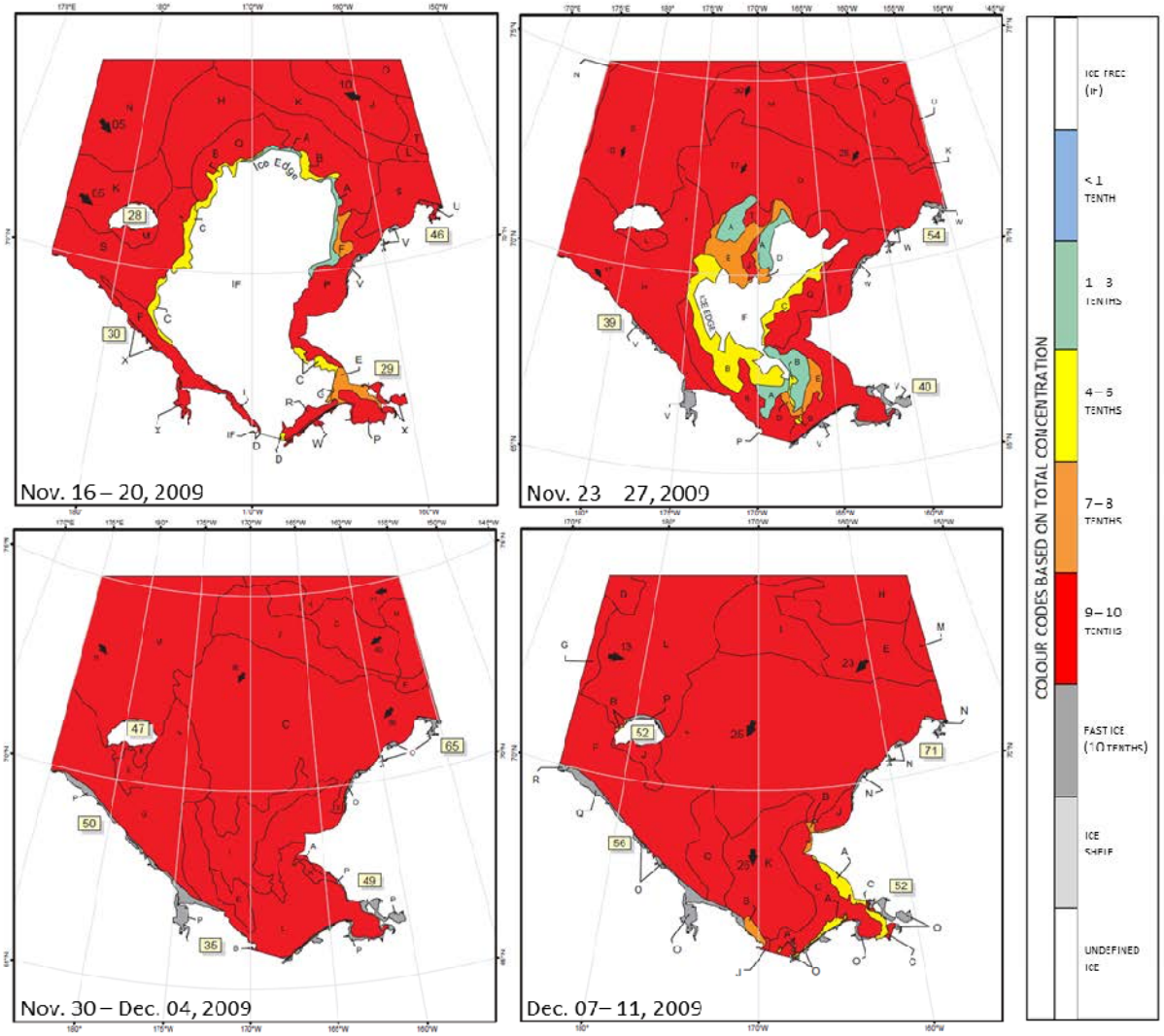

Figure 4-3. Fall 2009 freeze-up patterns. Ice charts are presented for the period of Nov. 16-20 to Dec. 7-11 in the Chukchi Sea. Crackerjack is located at 71°10'N, 166°45'W and Burger is at 71°14'N, 163°17'W.

4.1.2 BREAK-UP PATTERNS: SUMMER 2010

In the summer of 2010 (Figure 4-4 through Figure 4-6), ice began to clear along the Alaskan coastline in the first week of May with an extensive flaw lead present from south of Nome to Pt. Barrow. This area of low ice concentrations persisted throughout May, reaching the Burger site in the third week of May and expanding by the first week of June to the more offshore Crackerjack site. Occasional ice floes originating to the north from the pack ice edge (just north of 72°N) continued to pass the measurement sites until well into July. The clearing of the sea ice in the eastern Chukchi Sea was approximately 3 to 5 weeks earlier in 2010 than in the year 2009. However, the ice conditions in the northern and western Chukchi Sea were comparable, or had more ice in 2010, than in 2009 through to the end of July

.

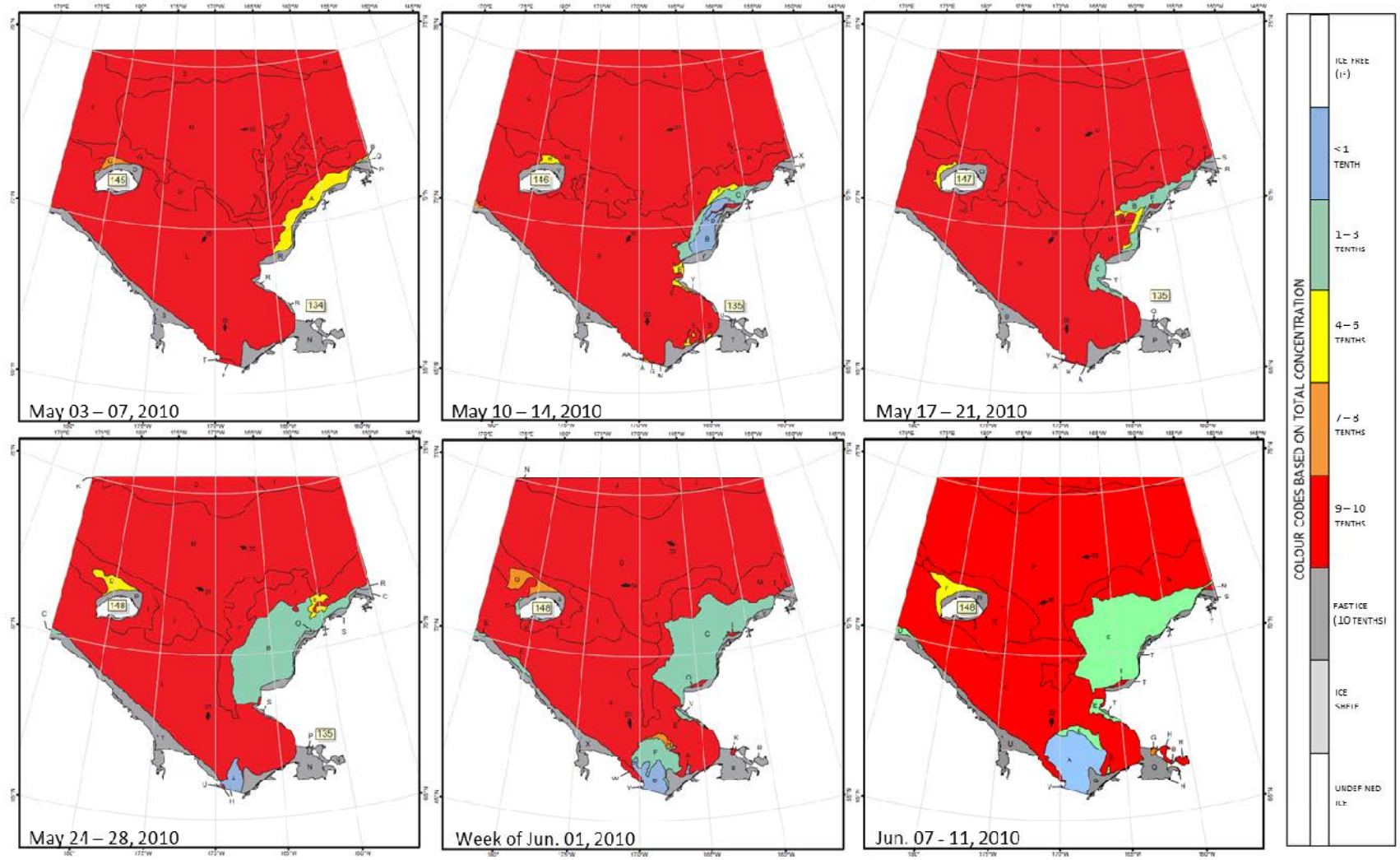

Figure 4-4. Summer 2010 break-up patterns. Ice charts are presented for the period of May 3-7 to June 7-11 in the Chukchi Sea. Crackerjack is located at 71°10'N, 166°45'W and Burger is at 71°14'N.

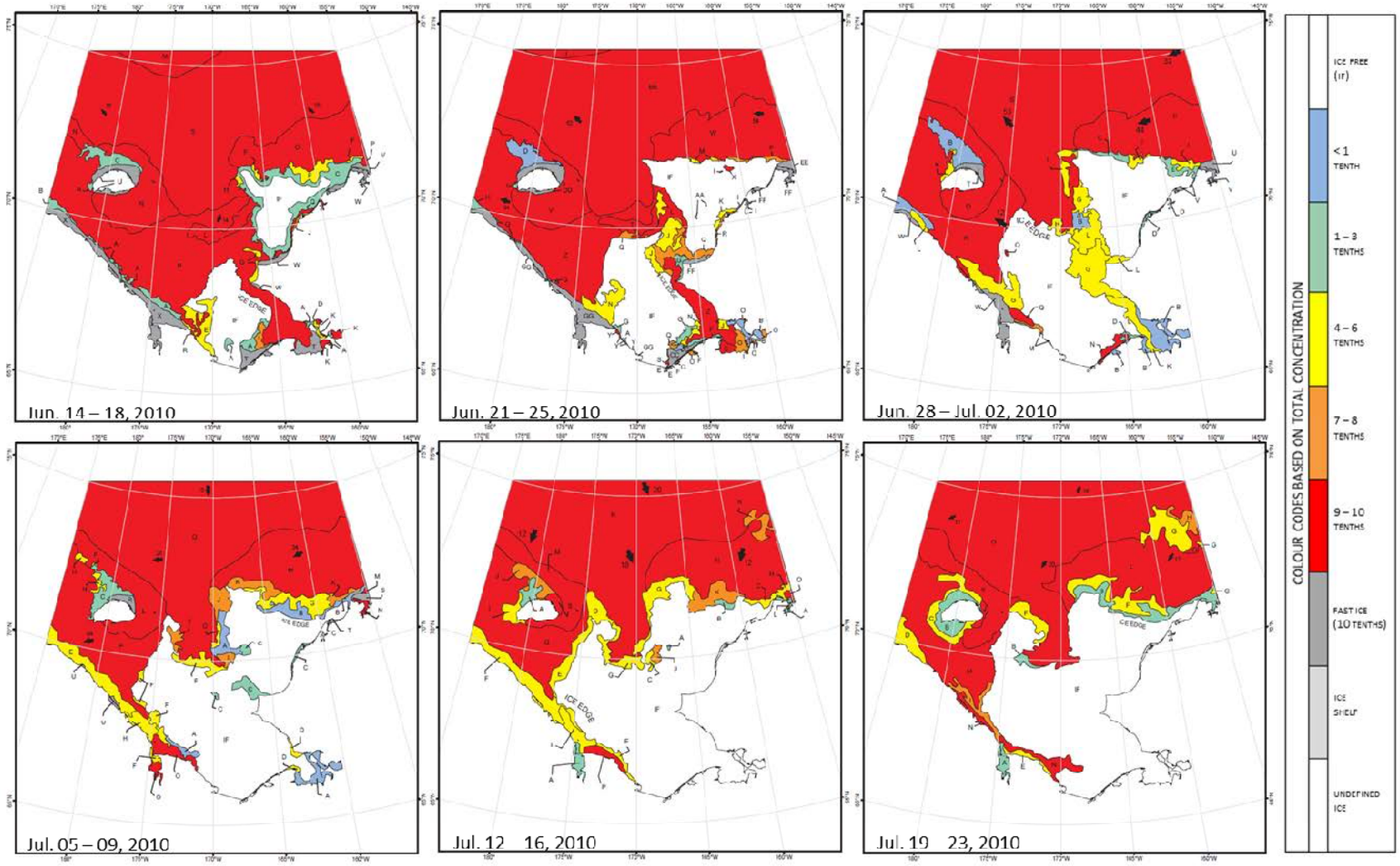

Figure 4-5. Summer 2010 break-up patterns. Ice charts are presented for the period of June 14-18 to July 19-23 in the Chukchi Sea. Crackerjack is located at 71°10'N, 166°45'W and Burger is at 71°14'.

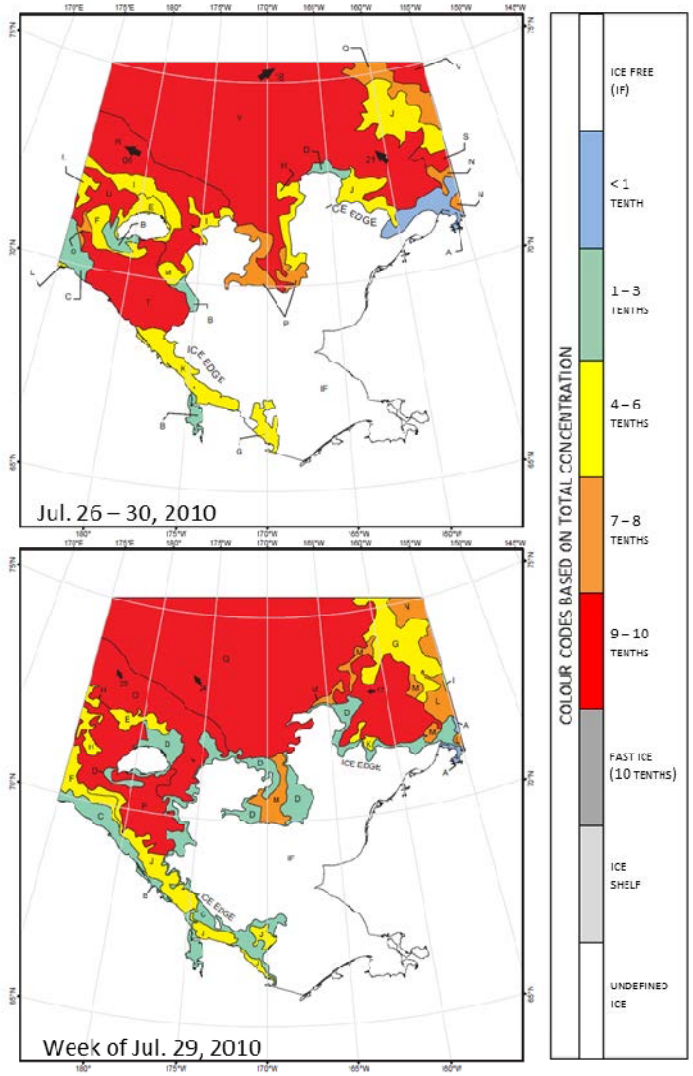

Figure 4-6. Summer 2010 break-up patterns. Ice charts are presented for the period of July 26-30 to July 29-Aug. 2 in the Chukchi Sea. Crackerjack is located at 71°10'N, 166°45'W and Burger is at 71°14'

4.2 ICE KEEL STATISTICS

4.2.1 METHODOLOGY FOR IDENTIFYING ICE KEELS

Ice keels that exceeded 5, 8, and 11 m were identified using either a Rayleigh criterion (α = 0.5), or a lower threshold of 2 m to end a feature. The keel detection algorithm was based on "Criterion A" as described in Vaudrey (1987). The algorithm found the start and end of individual ice features using three thresholds, as shown in Figure 4-7. For illustrative purposes, a 13 m starting threshold was used. A keel started, shown as "Start Point" in the figure, once the draft exceeded the "Start Threshold". The keel ended if it crossed the "End Threshold" at 2m, or if it reversed slope at a point less than a threshold given by (1 - α)*Maximum Draft, where α = 0.5 is the Rayleigh criterion.

The beginning of the keel is then found by scanning backwards from the previously designated "Start Point". The earlier keel start was found at a point that crossed the "End Threshold," or reversed slope, at a point less than the threshold given by (1 - α)*Maximum Draft.

Unlike the forward search to find the keel endpoint, the maximum draft was not updated; instead the value found for the forward search was used.

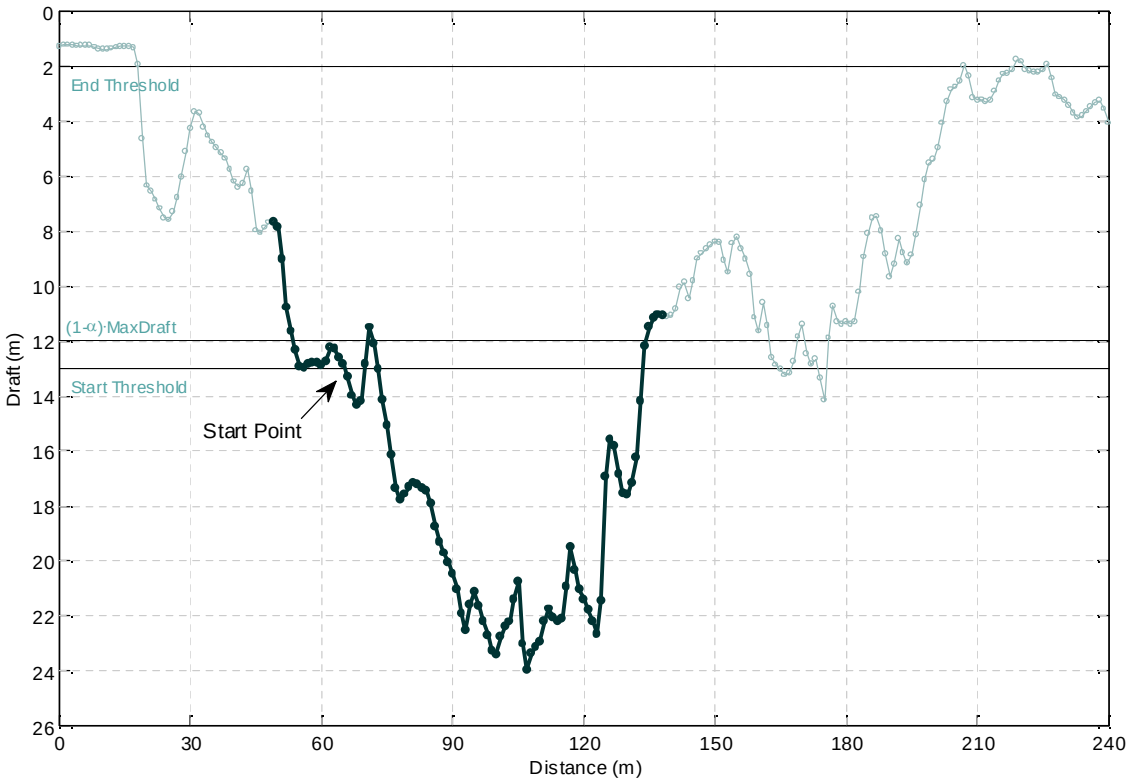

Figure 4-7. An example of the thresholds used by the keel identification algorithm. The keel was found using a 13 m start threshold, 2 m end threshold, and α equal to 0.5

4.2.2 OVERLAPPING FEATURES

The backwards search technique used to find the start of a keel can result in overlapping keel features when a keel with a larger maximum draft was followed by one with a lower maximum draft. In the backwards search on the second lower draft keel, the beginning of the keel can extend past the beginning of the first keel since the lower draft means a lower α threshold. It is also possible that the second keel can overlap with more than one previous feature. After the preliminary keels were selected, they were re-processed and the overlapping features were combined into a single event by using the start of the first keel in the overlap and the end of the last keel in the overlap.

An example of this type of overlap and the resulting combined feature is shown in Figure 4-8. For illustrative purposes, a 13 m starting threshold was used and applied to the ice keel shown in Figure 4-7. Figure 4-8 shows an overlap with the feature in Figure 4-7, and the effect of combining the two features.

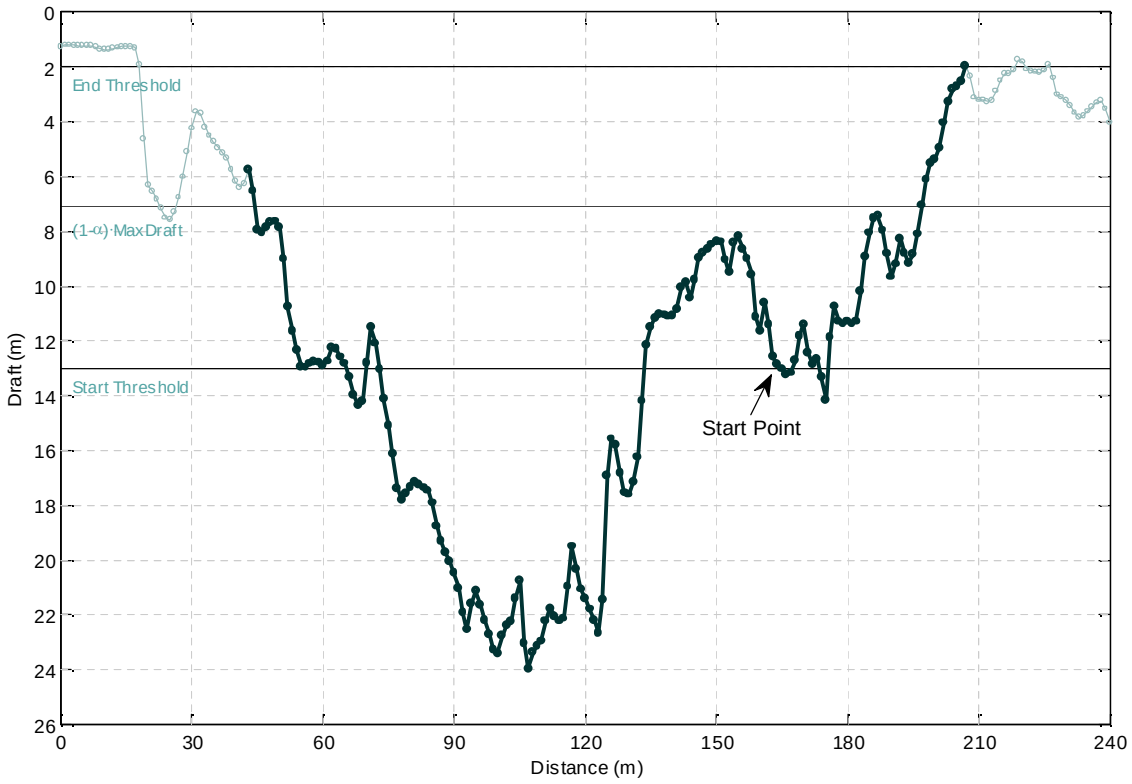

Figure 4-8. An example of a keel feature extending from the “Start Point” beyond the feature shown in Figure 4-7.

4.2.3 DESCRIPTION OF THE DATABASE OF KEEL FEATURES

A database of keel features was constructed using starting thresholds of 5, 8, and 11 m, an end threshold of 2 m and a Rayleigh criterion (α = 0.5). For each site and starting threshold, a data file was created containing the start time, end time, start distance, end distance, width, mean draft, maximum draft, minimum draft and the standard deviation of the draft for each keel feature. A description of each of the fields is provided in Table 4-1.

Statistical results are given over monthly and ice season time periods. For each starting threshold, a data file was created containing the start time of the statistic segment, the end time of the statistic segment, the minimum, mean, maximum and standard deviation of the maximum draft, the mean and standard deviation of the mean draft, the minimum, mean, maximum and standard deviation of the width, the total ice distance (sum of all ice distances for the time period), the total waves in ice and open water distance (sum of all waves in ice + open water distances for the time period), the total distance (sum of all ice + open water + data flagged as bad distances for this time period), the sum of all keel widths for this time period, the sum of all keel areas (sum of the product of each keel segment width and mean draft) and the number of keels in this time period. If a keel feature occurred on the boundary of consecutive monthly time segments, the keel was considered to be in the month where it had the greatest width. A description of each of the fields is provided in Table 4-2. In the ice keel statistical results, the average keel width is typically over 30 m. The widest keels may represent an amalgamation of individual keels or a rubbled ice field.

Table 4-1. A description of each field in the keel feature data file.

Name	Description
Start Time	The start time of the segment
End Time	The end time of the segment
Start Distance	The keel start distance (km)
End Distance	The keel end distance (km).
Width	The width of the keel feature (m).
Mean Draft	The mean draft value of the keel feature (m).
Maximum Draft	The maximum draft value of the keel feature (m).
Minimum Draft	The minimum draft value of the keel feature (m).
Std Dev of Draft	The standard deviation of the draft of the keel feature (m).

Table 4-2. A description of each field in the keel statistics (monthly and ice season) data file.

Name	Description
Start Time	The start time of the statistic segment.
End Time	The end time of the statistic segment.
Min of Max Draft	The minimum of all the maximum keel segment drafts in the time period (m).
Mean of Max Draft	The mean of all the maximum keel segment drafts in the time period (m).
Max of Max Draft	The maximum of all the maximum keel segment drafts in the time period (m).
Std of Max Draft	The standard deviation of all the maximum keel segment drafts in the time period (m).
Mean of Mean Draft	The mean of all the mean keel segment drafts in the time period (m).
Std of Mean Draft	The standard deviation of all the mean keel segment drafts in the time period (m).
Min Width	The minimum of all the keel segment widths in the time period (m).
Mean Width	The mean of all the keel segment widths in the time period (m).
Max Width	The maximum of all the keel segment widths in the time period (m).
Std of Width	The standard deviation of all the keel segment widths in the time period (m).
Total Ice Distance	The total distance of ice covered for the time period (km). This total distance includes all non-flagged data (ice).
Total O/W + Waves in Ice Dist	The total distance of waves in ice and open water covered for the time period (km). This total distance includes data flagged as open water (-200) and data flagged as waves in ice (-500).
Total Distance	The total distance covered for the time period (km). This total distance includes ice, data flagged as open water (-200), data flagged as waves in ice (-500) and data flagged as bad (-9999).
Sum of Keel Widths	The sum of the keel widths for the time period (km).
Sum of Keel Areas	The sum of the keel areas for the time period ($x10^3$ m^2). The area is calculated from the sum of the product of the mean draft and the width of each segment.
Number of Keels	The number of keel features in the time period.

Some statistical results from the ice keel feature database are presented as plots, including:

- the **daily** statistics of the number of keels and the total keel area for the 5, 8 and 11 m thresholds are shown in Figure 4-9 and Figure 4-10. Note that the large episodic variations in the number of ice keels and daily ice keel area are very strongly related to the episodic nature of daily ice movement distance;
- **monthly** histograms of maximum ice drafts using the 5m threshold are shown in Figure 4-11 and Figure 4-12.
- histograms of maximum ice drafts for the full ice **season** using the 5m threshold are shown in Figure 4-13 and Figure 4-14.
- Statistics for keels detected with the 5, 8 and 11 m thresholds are presented in Table 4-3 through Table 4-10.

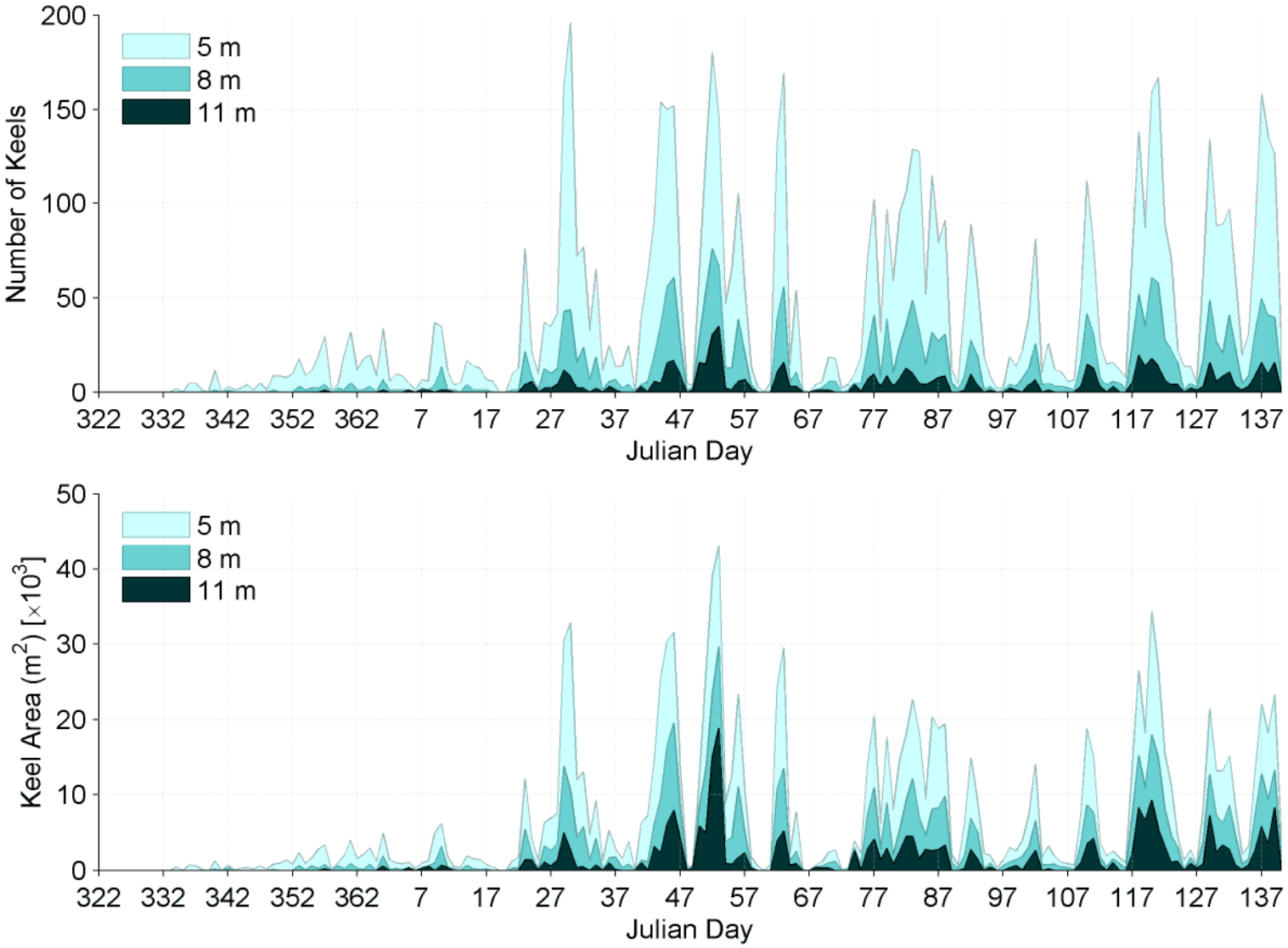

Figure 4-9. Daily numbers of keel features (top) and daily keel area (bottom) found using the 5m, 8m, and 11m thresholds at Burger.

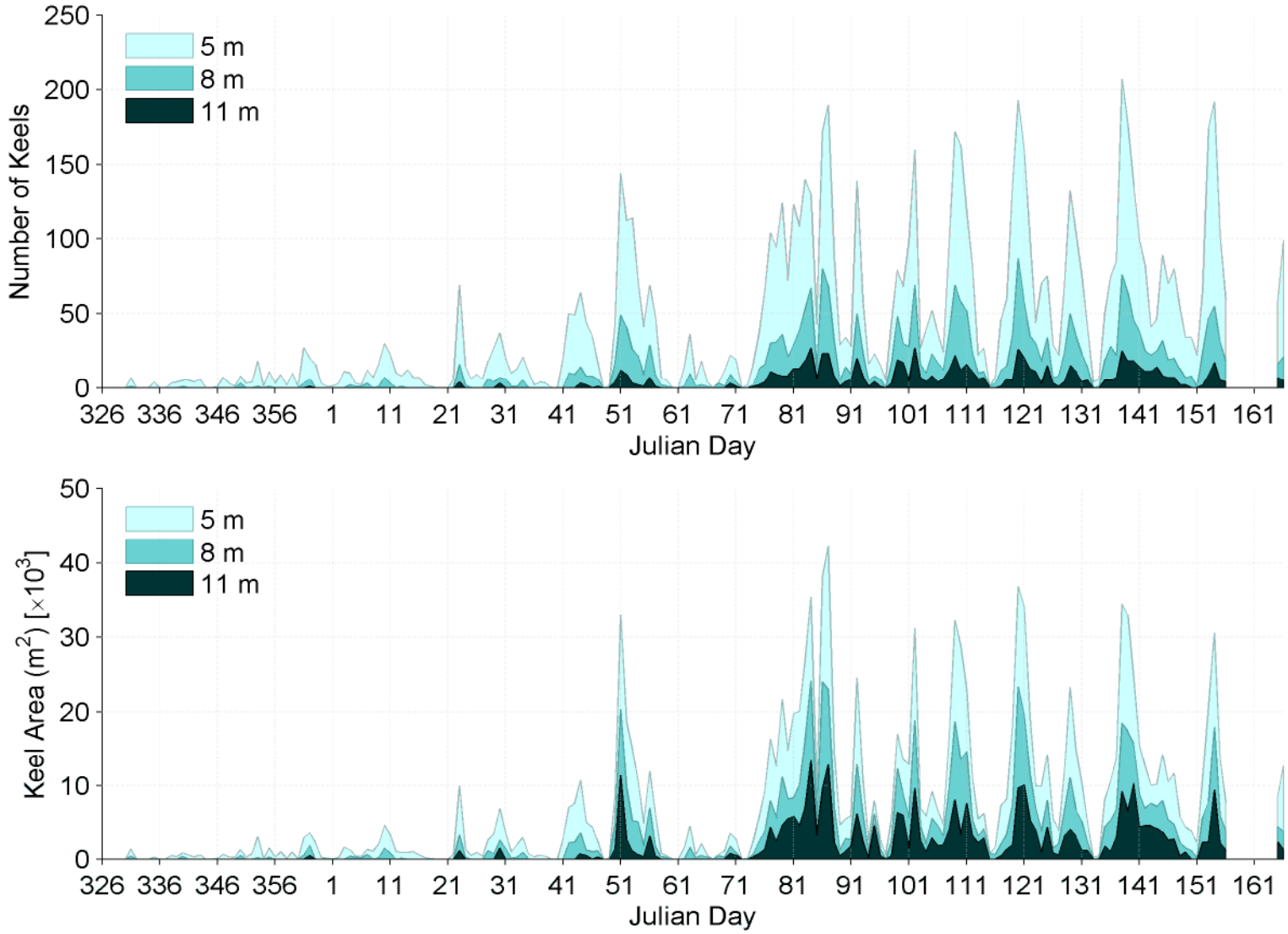

Figure 4-10. Daily numbers of keel features (top) and daily keel area (bottom) found using the 5m, 8m, and 11m thresholds at Crackerjack.

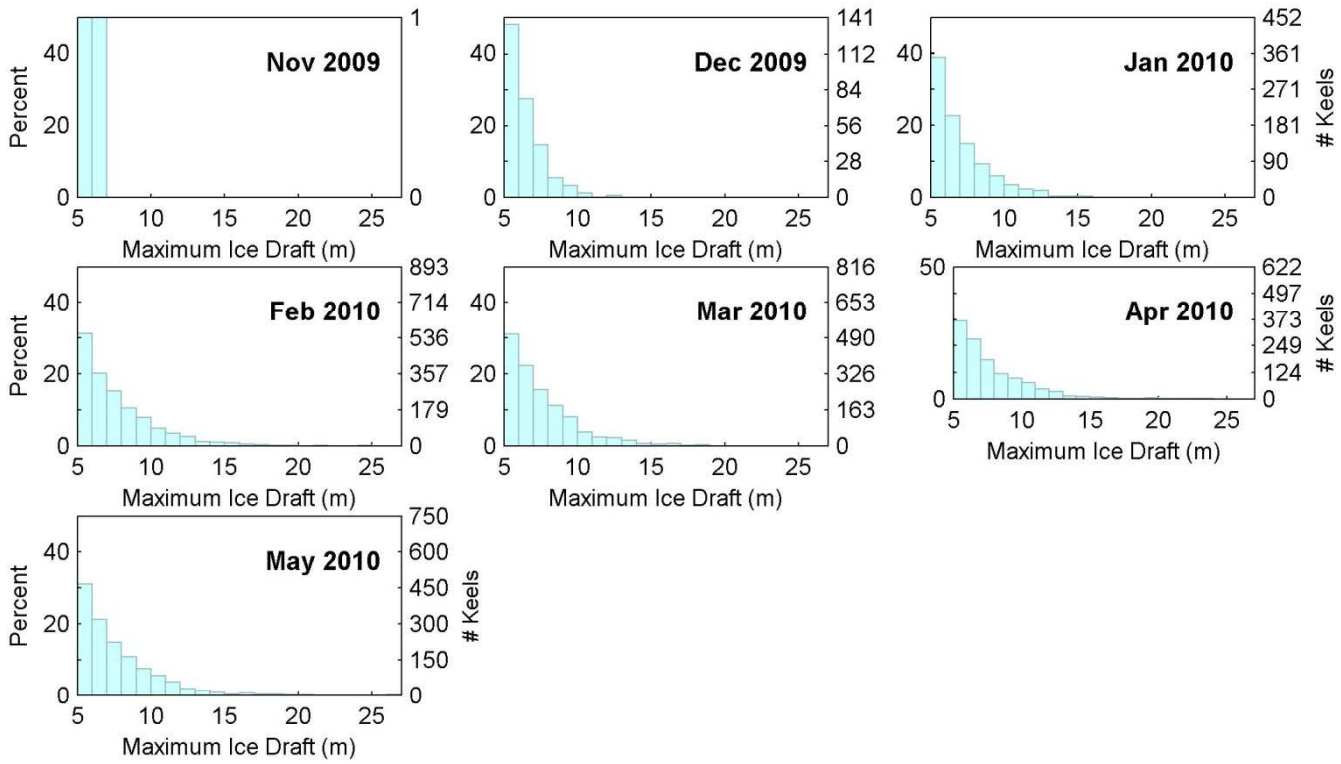

Figure 4-11. Monthly histograms of maximum ice draft for keels found using the 5 m threshold at Burger.

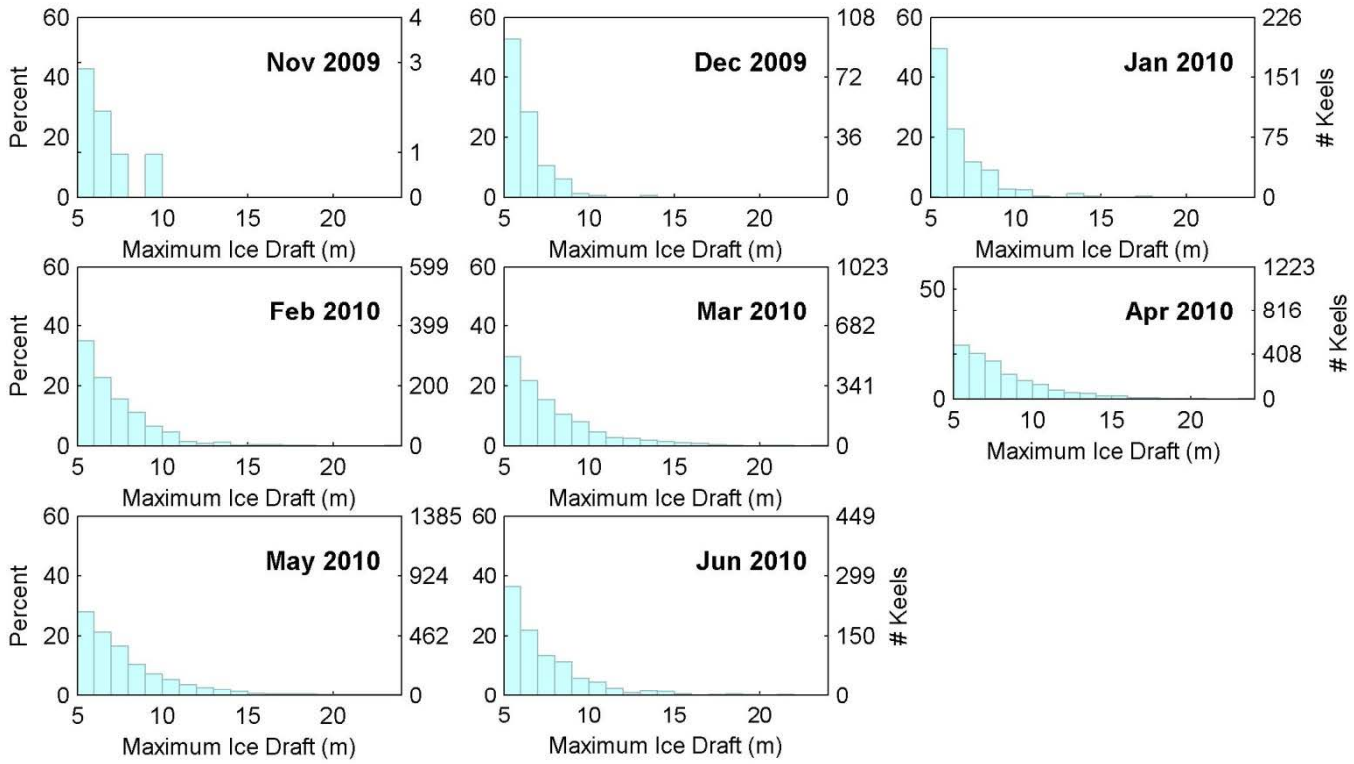

Figure 4-12. Monthly histograms of maximum ice draft for keels found using the 5 m threshold at Crackerjack.

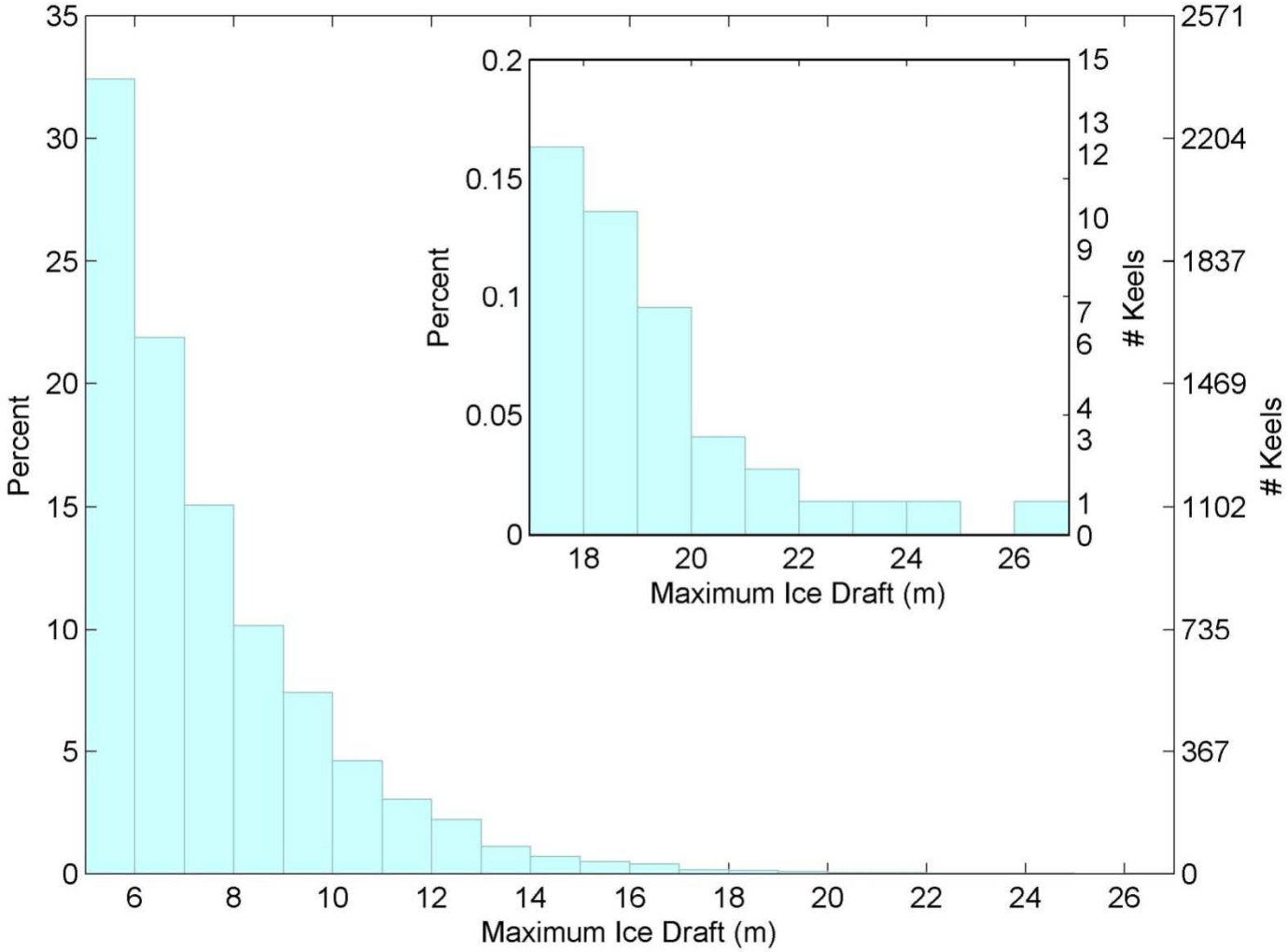

Figure 4-13. Full ice season histogram of the maximum ice draft for keels found using the 5 m threshold at Burger.

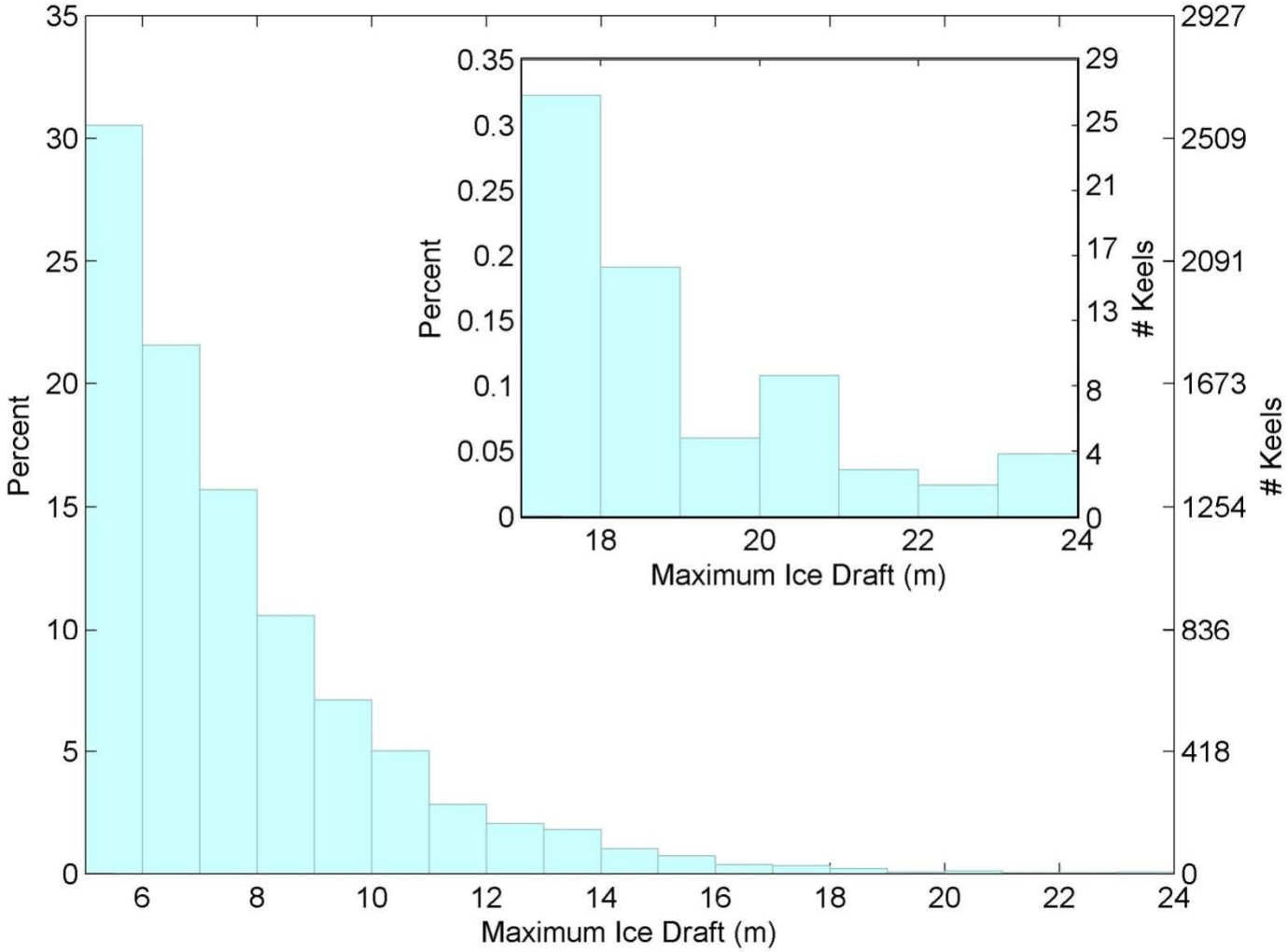

Figure 4-14. Full ice season histogram of the maximum ice draft for keels found using the 5 m threshold at Crackerjack.

Table 4-3. Burger monthly statistics of keel features for the 5m threshold level.

Burger 2009-2010: 5 m Threshold																
Month	Maximum Draft				Mean Draft		Width				Distance			Keels		
	Min (m)	Mean (m)	Max (m)	StdDev (m)	Mean (m)	StdDev (m)	Min (m)	Mean (m)	Max (m)	StdDev (m)	Total Ice (km)	Total O/W (km)	Total Ice + O/W (km)	Sum of Width (km)	Sum of Area ($\times 10^3$ m^2)	Number
November	5.02	5.83	6.64	1.15	4.36	1.02	42.00	45.50	49.00	4.95	191.86	1.67	193.52	0.09	0.40	2
December	5.00	6.35	12.09	1.22	4.36	0.79	4.00	26.78	75.00	13.63	495.10	3.15	498.25	7.53	34.50	281
January	5.00	7.03	15.58	1.90	4.74	1.11	2.00	31.42	194.00	21.38	375.23	0.00	375.23	28.37	147.42	902
February	5.00	7.63	24.56	2.51	5.11	1.51	2.00	34.00	273.00	24.61	315.46	0.00	315.46	60.69	349.59	1785
March	5.01	7.48	18.73	2.28	4.99	1.36	2.00	32.11	265.00	26.21	280.03	0.00	280.03	52.41	289.04	1632
April	5.00	7.69	23.15	2.54	5.14	1.49	3.00	31.21	273.00	24.74	240.49	0.00	240.49	38.80	221.08	1243
May	5.00	7.58	26.06	2.43	5.12	1.52	2.00	25.93	223.00	21.47	193.79	6.80	200.58	38.89	228.86	1500

Table 4-4. Crackerjack monthly statistics of keel features for the 5m threshold level.

Crackerjack 2009-2010: 5 m Threshold																
Month	Maximum Draft				Mean Draft		Width				Distance			Keels		
	Min (m)	Mean (m)	Max (m)	StdDev (m)	Mean (m)	StdDev (m)	Min (m)	Mean (m)	Max (m)	StdDev (m)	Total Ice (km)	Total O/W (km)	Total Ice + O/W (km)	Sum of Width (km)	Sum of Area ($\times 10^3$ m^2)	Number
November	5.25	6.59	9.87	1.63	5.04	1.24	15.00	34.71	67.00	21.87	208.52	3.57	212.09	0.24	1.32	7
December	5.00	6.23	13.42	1.18	4.31	0.85	4.00	27.38	106.00	16.58	524.02	4.32	528.34	4.93	22.68	180
January	5.00	6.53	17.30	1.66	4.50	1.01	2.00	28.01	111.00	16.15	390.47	0.49	390.96	10.56	51.16	377
February	5.00	7.21	23.30	2.10	4.88	1.33	2.00	29.10	238.00	21.61	247.24	0.00	247.24	29.04	157.92	998
March	5.00	7.71	23.29	2.57	5.18	1.55	2.00	31.38	241.00	25.65	236.21	0.00	236.21	53.50	316.41	1705
April	5.00	8.02	23.26	2.70	5.33	1.61	2.00	29.67	234.00	23.33	206.67	0.00	206.67	60.50	365.57	2039
May	5.00	7.76	23.66	2.57	5.21	1.57	2.00	28.31	262.00	23.72	268.20	4.81	273.01	65.36	388.40	2309
June	5.00	7.26	21.51	2.30	4.92	1.40	3.00	24.49	209.00	21.86	112.95	14.99	127.94	18.32	105.01	748

Table 4-5. Burger monthly statistics of keel features for the 8m threshold level.

Burger 2009-2010: 8 m Threshold																
Month	Maximum Draft				Mean Draft		Width				Distance			Keels		
	Min (m)	Mean (m)	Max (m)	StdDev (m)	Mean (m)	StdDev (m)	Min (m)	Mean (m)	Max (m)	StdDev (m)	Total Ice (km)	Total O/W (km)	Total Ice + O/W (km)	Sum of Width (km)	Sum of Area ($\times 10^3$ m^2)	Number
November	-	-	-	-	-	-	-	-	-	-	191.86	1.67	193.52	0.00	0.00	0
December	8.09	9.15	12.09	0.87	6.10	0.78	7.00	32.39	67.00	15.63	495.10	3.15	498.25	0.91	5.77	28
January	8.01	9.85	15.58	1.65	6.74	1.20	2.00	36.95	152.00	20.03	375.23	0.00	375.23	7.91	55.61	213
February	8.00	10.44	24.56	2.35	7.16	1.64	2.00	38.74	223.00	23.72	315.46	0.00	315.46	23.20	178.62	599
March	8.00	10.19	18.73	2.10	7.00	1.50	4.00	34.56	183.00	22.54	280.03	0.00	280.03	17.77	132.62	514
April	8.01	10.53	23.15	2.36	7.20	1.63	4.00	33.48	244.00	23.12	240.49	0.00	240.49	14.10	108.69	421
May	8.00	10.32	26.06	2.28	7.13	1.53	4.00	31.95	195.00	22.34	193.79	6.80	200.58	15.91	123.42	498

Table 4-6. Crackerjack monthly statistics of keel features for the 8m threshold level.

Crackerjack 2009-2010: 8 m Threshold																
Month	Maximum Draft				Mean Draft		Width				Distance			Keels		
	Min (m)	Mean (m)	Max (m)	StdDev (m)	Mean (m)	StdDev (m)	Min (m)	Mean (m)	Max (m)	StdDev (m)	Total Ice (km)	Total O/W (km)	Total Ice + O/W (km)	Sum of Width (km)	Sum of Area ($\times 10^3$ m^2)	Number
November	9.87	9.87	9.87	0.00	7.49	0.00	55.00	55.00	55.00	0.00	208.52	3.57	212.09	0.05	0.42	1
December	8.21	9.10	13.42	1.38	6.58	1.27	15.00	35.40	71.00	13.73	524.02	4.32	528.34	0.53	3.66	15
January	8.04	9.57	17.30	1.86	6.63	1.38	8.00	31.93	78.00	14.39	390.47	0.49	390.96	1.92	13.30	60
February	8.00	9.94	23.30	2.09	6.87	1.53	4.00	34.48	238.00	24.65	247.24	0.00	247.24	9.21	68.97	267
March	8.00	10.55	23.29	2.42	7.27	1.66	4.00	36.29	215.00	26.19	236.21	0.00	236.21	21.12	167.60	582
April	8.01	10.70	23.26	2.47	7.37	1.65	3.00	32.97	225.00	22.92	206.67	0.00	206.67	25.98	205.47	788
May	8.00	10.56	23.66	2.40	7.28	1.64	3.00	32.47	252.00	24.25	268.20	4.81	273.01	26.01	207.18	801
June	8.00	10.14	21.51	2.35	7.00	1.65	4.00	29.82	164.00	23.00	112.95	14.99	127.94	6.32	49.54	212

Table 4-7. Burger monthly statistics of keel features for the 11m threshold level.

Burger 2009-2010: 11 m Threshold																
Month	Maximum Draft				Mean Draft		Width				Distance			Keels		
	Min (m)	Mean (m)	Max (m)	StdDev (m)	Mean (m)	StdDev (m)	Min (m)	Mean (m)	Max (m)	StdDev (m)	Total Ice (km)	Total O/W (km)	Total Ice + O/W (km)	Sum of Width (km)	Sum of Area ($\times 10^3$ m^2)	Number
November	-	-	-	-	-	-	-	-	-	-	191.86	1.67	193.52	0.00	0.00	0
December	12.09	12.09	12.09	0.00	7.22	0.00	25.00	25.00	25.00	0.00	495.10	3.15	498.25	0.02	0.19	1
January	11.06	12.40	15.58	1.20	8.49	1.05	14.00	40.89	98.00	18.97	375.23	0.00	375.23	1.92	16.57	47
February	11.01	13.29	24.56	2.24	9.30	1.80	6.00	44.33	223.00	25.37	315.46	0.00	315.46	8.02	77.98	181
March	11.02	13.16	18.73	1.78	9.29	1.48	7.00	39.02	162.00	22.97	280.03	0.00	280.03	5.27	50.67	135
April	11.11	13.33	23.15	2.46	9.25	1.70	6.00	38.58	195.00	28.09	240.49	0.00	240.49	4.82	46.97	125
May	11.02	13.18	26.06	2.40	9.18	1.86	4.00	37.90	190.00	24.25	193.79	6.80	200.58	5.19	51.41	137

Table 4-8. Crackerjack monthly statistics of keel features for the 11m threshold level.

Crackerjack 2009-2010: 11 m Threshold																
Month	Maximum Draft				Mean Draft		Width				Distance			Keels		
	Min (m)	Mean (m)	Max (m)	StdDev (m)	Mean (m)	StdDev (m)	Min (m)	Mean (m)	Max (m)	StdDev (m)	Total Ice (km)	Total O/W (km)	Total Ice + O/W (km)	Sum of Width (km)	Sum of Area ($\times 10^3$ m^2)	Number
November	-	-	-	-	-	-	-	-	-	-	208.52	3.57	212.09	0.00	0.00	0
December	13.42	13.42	13.42	0.00	9.96	0.00	49.00	49.00	49.00	0.00	524.02	4.32	528.34	0.05	0.49	1
January	11.36	13.88	17.30	1.78	9.76	1.86	17.00	37.29	68.00	17.55	390.47	0.49	390.96	0.26	2.63	7
February	11.09	13.65	23.30	2.44	9.59	1.89	12.00	47.64	207.00	36.18	247.24	0.00	247.24	2.14	22.59	45
March	11.03	13.53	23.29	2.11	9.49	1.57	7.00	44.04	215.00	30.26	236.21	0.00	236.21	8.06	80.64	183
April	11.01	13.52	23.26	2.20	9.43	1.70	4.00	36.19	202.00	22.37	206.67	0.00	206.67	9.55	94.33	264
May	11.02	13.30	23.66	2.25	9.44	1.78	3.00	37.76	211.00	24.94	268.20	4.81	273.01	9.78	98.25	259
June	11.02	13.55	21.51	2.36	9.57	1.85	8.00	41.20	134.00	26.85	112.95	14.99	127.94	2.02	20.96	49

Table 4-9. Burger ice season statistics of keel features for the three thresholds (5, 8 and 11 m).

Burger 2009-2010																
Threshold	Maximum Draft				Mean Draft		Width				Distance			Keels		
	Min (m)	Mean (m)	Max (m)	StdDev (m)	Mean (m)	StdDev (m)	Min (m)	Mean (m)	Max (m)	StdDev (m)	Total Ice (km)	Total O/W (km)	Total Ice + O/W (km)	Sum of Width (km)	Sum of Area ($\times 10^3$ m^2)	Number
5	5.00	7.47	26.06	2.36	5.02	1.42	1.00	30.87	273.00	23.85	2201.51	19.78	2221.29	226.77	1270.89	7345
8	8.00	10.30		2.22	7.07	1.55	1.00	35.09	244.00	22.75				79.79	604.73	2273
11	11.01	13.18		2.18	9.20	1.69	4.00	40.34	223.00	24.83				25.25	243.79	626

Table 4-10. Crackerjack ice season statistics of keel features for the three thresholds (5, 8 and 11 m).

Crackerjack 2009-2010																
Threshold	Maximum Draft				Mean Draft		Width				Distance			Keels		
	Min (m)	Mean (m)	Max (m)	StdDev (m)	Mean (m)	StdDev (m)	Min (m)	Mean (m)	Max (m)	StdDev (m)	Total Ice (km)	Total O/W (km)	Total Ice + O/W (km)	Sum of Width (km)	Sum of Area ($\times 10^3$ m^2)	Number
5	5.00	7.61	23.66	2.50	5.12	1.52	2.00	28.99	262.00	23.27	2194.29	28.17	2222.46	242.46	1408.47	8363
8	8.00	10.48		2.39	7.22	1.64	3.00	33.43	252.00	24.08				91.14	716.14	2726
11	11.01	13.46		2.22	9.47	1.72	3.00	39.44	215.00	26.44				31.87	319.88	808

4.3 ESTIMATION OF EXTREME KEELS DRAFTS

4.3.1 EXTREME ICE KEELS

The 10 largest keels observed at Burger and Crackerjack are listed in Table 4-11 and Table 4-12. At Burger, the maximum depths of the listed exceptional keels ranged from 19.95 to 26.06 m. At Crackerjack, the maximum depths ranged from 20.86 to 23.66 m. All told, 9 keels at Burger and 18 keels at Crackerjack were observed with depths in excess of 20 m.

Table 4-11. List of keels with the ten largest drafts observed at Burger. The draft values are provided as the maximum and mean (average) draft computed for each of the 10 largest individual ice keels.

Burger		
Date/ Time	**Max Draft (m)**	**Mean Draft (m)**
19-May-2010 06:17:03	26.06	17.76
16-Feb-2010 02:00:01	24.56	13.76
29-Apr-2010 23:14:32	23.15	11.97
12-Apr-2010 14:34:06	22.62	14.26
29-Apr-2010 00:22:02	21.76	11.38
22-Feb-2010 12:17:08	21.68	15.91
10-May-2010 03:57:50	20.92	14.98
19-May-2010 14:33:01	20.36	13.98
30-Apr-2010 21:24:18	20.24	13.88
29-Apr-2010 08:16:00	19.95	13.54

Table 4-12. List of keels with the ten largest drafts observed at Crackerjack. The draft values are provided as the maximum and mean (average) draft computed for each of the 10 largest individual ice keels.

Crackerjack		
Date/ Time	**Max Draft (m)**	**Mean Draft (m)**
02-May-2010 04:28:30	23.66	14.86
20-Feb-2010 06:38:29	23.30	15.59
28-Mar-2010 02:27:11	23.29	14.34
15-Apr-2010 16:31:20	23.26	17.09
25-May-2010 07:11:07	22.77	14.73
26-May-2010 14:17:14	22.46	17.91
28-Mar-2010 02:10:20	21.55	14.49
03-Jun-2010 12:24:35	21.51	16.22
08-May-2010 23:02:34	21.26	13.24
21-Apr-2010 13:27:44	20.86	12.28

4.3.2 METHODOLOGY FOR EXTREMAL ANALYSIS

Limitations on maximum measurable draft imposed by the depth of the IPS transducers and, as well, by the limited duration of our measurement program dictate reliance on statistical procedures for estimation of probabilities for extreme keel depth occurrences. The parameter most relevant to such estimates is the 100-year return draft value, D_{100}, which is representative of the largest keel depth likely to be encountered in 100 years at a given sites.

Preliminary 100-year exceedance values were derived by fitting the high draft end of the empirical keel probabilities to a three-parameter Weibull probability distribution. Since these preliminary values are based on only two years of data, they are not considered to be sufficiently statistically stable and therefore are not presented here. As data collection spans more years, these results will become more statistically robust.

4.3.3 SELECTION OF FEATURES OF EXTREME DRAFT

The selection of ice keels for inclusion in our analyses of extreme draft probabilities followed a two-step process (ASL, 2000):

1. The largest individual ice keels were selected for each site from the final version of the 1 m smoothed spatial data set, by selecting individual big keel segments having a maximum ice draft above a chosen threshold level. The threshold was set to eventually allow selection of roughly 100 or more extreme keel values as representatives of the largest ice keel drafts observed at a given site.

2. Each of the ice keel data segments, as selected (as per item 1) were plotted and manually reviewed. In a few cases, two or more individual keels were combined into a single keel of greater horizontal extent. The final set of the largest ice keels by site are presented as individual plots of ice draft *vs*. horizontal distance in Appendix 3.

4.3.4 STATISTICAL ANALYSIS

The distributions of maximum keel draft values in 2009-2010 for keels with maximum drafts above the 13 m threshold are presented in Table 4-13 for Burger and Crackerjack.

Table 4-13. Ice draft distributions in 2009-2010 for ice keels exceeding 13.0 m maximum draft.

	Number of Keels	
Draft (m)	**Burger**	**Crackerjack**
13.0 - 13.5	38	83
13.5 - 14.0	44	67
14.0 - 14.5	29	53
14.5 - 15.0	23	32
15.0 - 15.5	24	31
15.5 - 16.0	12	30
16.0 - 16.5	18	18
16.5 - 17.0	11	13
17.0 - 17.5	5	15
17.5 - 18.0	7	12
18.0 - 18.5	6	11
18.5 - 19.0	4	5
19.0 - 19.5	1	2
19.5 - 20.0	6	3
20.0 - 20.5	2	6
20.5 - 21.0	1	3
21.0 - 21.5	0	1
21.5 - 22.0	2	2
22.0 - 22.5	0	1
22.5 - 23.0	1	1
23.0 - 23.5	1	3
23.5 - 24.0	0	1
24.0 - 24.5	0	0
24.5 - 25.0	1	0
25.0 - 25.5	0	0
25.5 – 26.0	0	0
26.0 – 26.5	1	0

To provide an appreciation of the character of the largest ice keels, plots of spatial profiles are provided in Figure 4-15 and Figure 4-16 for the widest and deepest keels encountered at each site. Arguably, the widest keels in the entire data sets could be considered to be part of rubble ice fields. Note, however, that the detected keels in the ice keel database are defined according to the quantitative criteria specified above in section 4.2.1 for large ice keels. More advanced analysis methods to distinguish between different ice deformation processes such as singular large keels and rubbled and/or hummocky ice are recommended for further investigation of these very extensive Ice Profiler data sets.

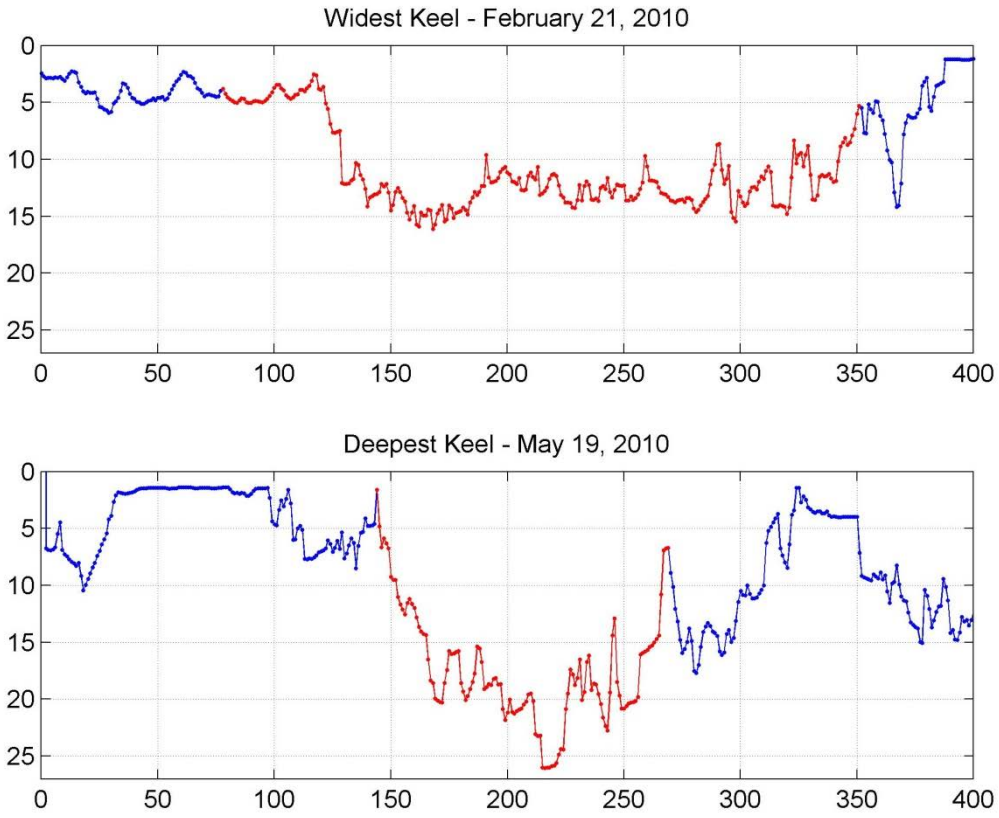

Figure 4-15. The widest keel (273 m, *top*) observed at Burger occurred on February 21, 2010. The deepest keel (26.06 m, *bottom*) occurred on May 19, 2010.

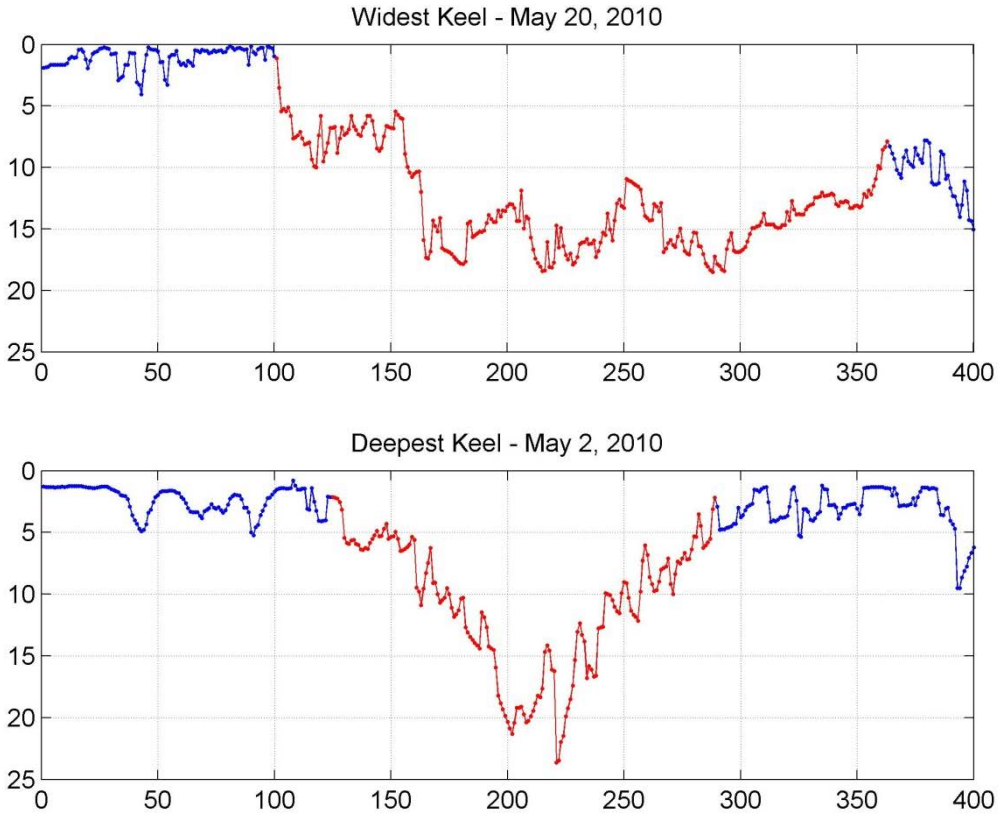

Figure 4-16. The widest keel (262 m, *top*) observed at Crackerjack occurred on May 20, 2010. The deepest keel (23.66 m, *bottom*) occurred on May 2, 2010.

4.4 ICE MOTION: EPISODES OF LARGE MOVEMENT AND NO MOVEMENT

The ice velocity measurements (Section 3.3) and the resulting distances of ice movement measured were subjected to further analyses to identify the episodes of alternately large and then negligible ice movements for the winter and spring of 2009-2010 at the Burger and Crackerjack sites where ice velocity measurements were made.

Each episode of large ice movement was identified using a criterion of having an average speed exceeding 19 cm/s over a minimum duration of 12 hours. The episodes of large ice movement are presented in Table 4-14 and Table 4-15 for Burger and Crackerjack respectively. Information on the winds (direction from and maximum wind speed) is also presented for each episode of large ice movement. As mentioned in Section 3.3, the episodes of large ice movements occur at approximately the same times as do the episodes of little or no ice movement. The importance of the underlying wind forcing in causing the large ice movements is clearly evident in these statistical results. One consequence of the wind forcing is that the events occur nearly simultaneously among the two measurement sites.

Table 4-14. Large ice motion events at Burger ordered according to the average ice speed over the event duration.

Start Date/Time	Stop Date/Time	Duration (days)	Distance Travelled (km)	Average Speed (cm/s)	Maximum Speed (cm/s)	Net Ice Dir (degT)	Maximum Wind Speed (m/s)	Wind Direction (from)
28-Jan-10 02:33	30-Jan-10 16:33	2.58	125.78	56.4	86.9	254	8.3	E
25-Dec-09 17:32	28-Dec-09 13:32	2.83	93.7	38.3	50.9	248	8.6	E
24-Mar-10 01:35	25-Mar-10 15:35	1.58	48.53	35.5	52.5	259	8	E
22-Jan-10 16:03	24-Jan-10 02:03	1.42	40.2	32.8	49	29	7.7	E
05-Dec-09 15:31	06-Dec-09 09:01	0.73	20.05	31.8	42.7	258	8.9	E
10-Feb-10 09:04	11-Feb-10 19:04	1.42	38.15	31.2	47.5	263	7	E
03-Mar-10 08:34	04-Mar-10 16:34	1.33	35.18	30.5	42.7	243	5.1	E
24-Nov-09 16:01	28-Nov-09 09:31	3.73	97.12	30.1	50.1	234	5.4	E
06-Dec-09 14:01	07-Dec-09 22:31	1.35	33.64	28.8	41.7	89	5.1	W
21-Dec-09 10:02	22-Dec-09 18:32	1.35	32.21	27.5	33.4	306	7.5	E
11-Apr-10 16:05	12-Apr-10 08:35	0.69	15.82	26.6	33.5	55	5.7	E
26-Mar-10 19:35	29-Mar-10 03:05	2.31	52.97	26.5	37.9	231	5.4	E
12-Feb-10 17:04	14-Feb-10 03:34	1.44	32.53	26.2	32.1	267	7.7	E
19-Feb-10 23:04	22-Feb-10 20:34	2.9	65.09	26	33.9	289	11.5	E
30-Nov-09 12:01	01-Dec-09 01:31	0.56	12.61	26	33.1	230	4.8	E
02-Feb-10 17:03	03-Feb-10 15:03	0.92	20.3	25.6	32	139	6.7	W
08-Dec-09 17:31	10-Dec-09 17:32	2	44	25.5	29.8	110	3.2	E
14-Feb-10 10:34	16-Feb-10 04:04	1.73	37.2	24.9	29	253	6.7	E
17-May-10 22:07	20-May-10 09:37	2.48	53.14	24.8	34.2	287	7.4	E
30-Apr-10 20:06	02-May-10 07:06	1.46	31.3	24.8	30.7	287	7	E
02-Apr-10 08:05	03-Apr-10 04:05	0.83	17.29	24	32.1	247	7	E
29-Nov-09 02:01	29-Nov-09 21:01	0.79	16.39	24	29.2	155	4.2	W
15-Dec-09 12:02	16-Dec-09 01:02	0.54	10.73	22.9	24.7	215	6.1	E
21-Mar-10 22:35	22-Mar-10 21:35	0.96	18.47	22.3	25.2	290	6.7	E
26-Jan-10 11:33	27-Jan-10 01:03	0.56	10.79	22.2	26	108	5.4	W
01-Jan-10 11:02	02-Jan-10 08:02	0.88	16.51	21.8	24.3	132	5.7	W
02-Dec-09 20:01	03-Dec-09 11:31	0.65	11.93	21.4	24.1	203	5.1	W
	Total of Events	40.02	1031.63					

Table 4-15. Large ice motion events at Crackerjack ordered according to the average ice speed over the event duration.

Start Date/Time	Stop Date/Time	Duration (days)	Distance Travelled (km)	Average Speed (cm/s)	Maximum Speed (cm/s)	Net Ice Dir (degT)	Maximum Wind Speed (m/s)	Wind Direction from (deg)
22-Jan-10 11:30	24-Jan-10 16:30	2.21	88.44	46.4	63.7	13	7.7	E
28-Jan-10 05:30	30-Jan-10 15:30	2.42	83.38	39.9	58.8	244	8.3	E
05-Dec-09 13:30	06-Dec-09 13:30	1	33.04	38.2	55.6	268	8.9	E
23-Nov-09 21:30	28-Nov-09 22:00	5.02	149.99	34.6	56.8	200	5.4	E
08-Dec-09 12:30	10-Dec-09 03:00	1.6	44.52	32.1	39.1	33	3.2	E
24-Dec-09 18:30	28-Dec-09 18:30	4	108.45	31.4	42.2	261	8.6	E
01-Jun-10 14:01	04-Jun-10 22:31	3.35	86.3	29.8	36.6	285	8.3	E
15-Dec-09 08:30	16-Dec-09 01:30	0.71	18.25	29.8	34.6	181	6.1	E
21-Dec-09 10:30	22-Dec-09 22:00	1.48	36.08	28.2	32.7	296	7.4	E
14-Jun-10 16:01	15-Jun-10 12:31	0.85	20.63	28	34.3	329	7	E
29-Nov-09 00:00	29-Nov-09 23:00	0.96	22.34	27	32.8	168	4.2	W
01-Dec-09 13:30	03-Dec-09 02:00	1.52	35.29	26.9	34.8	181	5.1	E
24-Mar-10 10:30	25-Mar-10 11:00	1.02	23.74	26.9	32.3	253	8	E
13-Dec-09 12:30	14-Dec-09 21:00	1.35	31.13	26.6	32.6	124	2.3	W
11-Apr-10 20:30	12-Apr-10 12:30	0.67	15.07	26.2	33.3	38	3.5	E
10-Feb-10 10:00	11-Feb-10 13:00	1.13	25.21	25.9	34.3	285	7	E
21-Mar-10 22:30	23-Mar-10 01:00	1.1	24.1	25.3	29	316	6.7	E
19-Feb-10 23:00	22-Feb-10 19:00	2.83	61.65	25.2	33.1	293	11.5	E
30-Apr-10 21:00	02-May-10 06:30	1.4	29.86	24.8	29.9	300	7	E
27-Mar-10 03:30	29-Mar-10 10:00	2.27	47.59	24.3	31.1	188	5.4	E
26-Jan-10 09:30	27-Jan-10 00:00	0.6	12.56	24.1	29.9	104	5.4	W
17-Dec-09 10:30	18-Dec-09 16:30	1.25	25.68	23.8	32.2	228	3.8	E
17-Mar-10 17:00	18-Mar-10 08:30	0.65	13.16	23.6	26.9	25	2.6	E
02-Feb-10 18:30	03-Feb-10 13:30	0.79	15.46	22.6	27.8	123	6.7	W
18-May-10 00:01	19-May-10 08:31	1.35	25.9	22.1	24.3	319	7.4	E
	Total of Events	41.53	1077.82					

4.5 OCEAN WAVE RESULTS

The time series of significant wave height (H_s) and peak period (T_p) for Burger and Crackerjack are presented in Figure 4-17 and Figure 4-23 respectively.

At Crackerjack, H_{max} (maximum wave height) was also computed. There was one storm with H_s exceeding 5 m at both sites, three events at Crackerjack with H_s greater than 4 m and six events with H_s greater than 3 m at both sites. The largest storm, which occurred between 2009/10/21 18:00 and 2009/10/25 00:00, had H_s over 5 m and T_p up to 10 s. At this time, wind speeds at Prudhoe Bay were from the east at 30-40 knots and winds at Wainwright and Barrow were from the east at 15-20 knots. This event is shown in detail in Figure 4-19. In 2008/2009, the largest storm produced waves of 4 m at 10 seconds.

Statistics and joint frequency tables of significant wave height (H_s) and peak period (T_p) for Burger and Crackerjack are presented in Table 4-16 to Table 4-19. The Burger site required more flagging due to the longer presence of high concentrations of ice. Most of the peak period data corresponding to wave heights below 0.1 m was flagged due to the autospectra's uncertainty in identifying the correct period. The joint frequency tables show that most of the waves have a period in the 4-7 second range and were 0.5-1.5 m. Phase 2 was sampled every 2 seconds (0.5 Hz) and the smallest resolvable period is 4 seconds (0.25 Hz). For this phase, the lower data sampling rate likely results in a minor underestimate of the H_s Values due to not including contributions for waves with periods of 2 to 4 seconds. It is recommended that the higher sampling rate of 1 Hz be extended later into the autumn period (i.e. start phase 2 later).

The percent exceedances of H_s are presented in Table 4-20 and Figure 4-20 for both sites. For both data sets, more than 50% of the data had H_s greater than 1 m. Burger had 4 % of the data above 3 m and Crackerjack had 7.5 %.

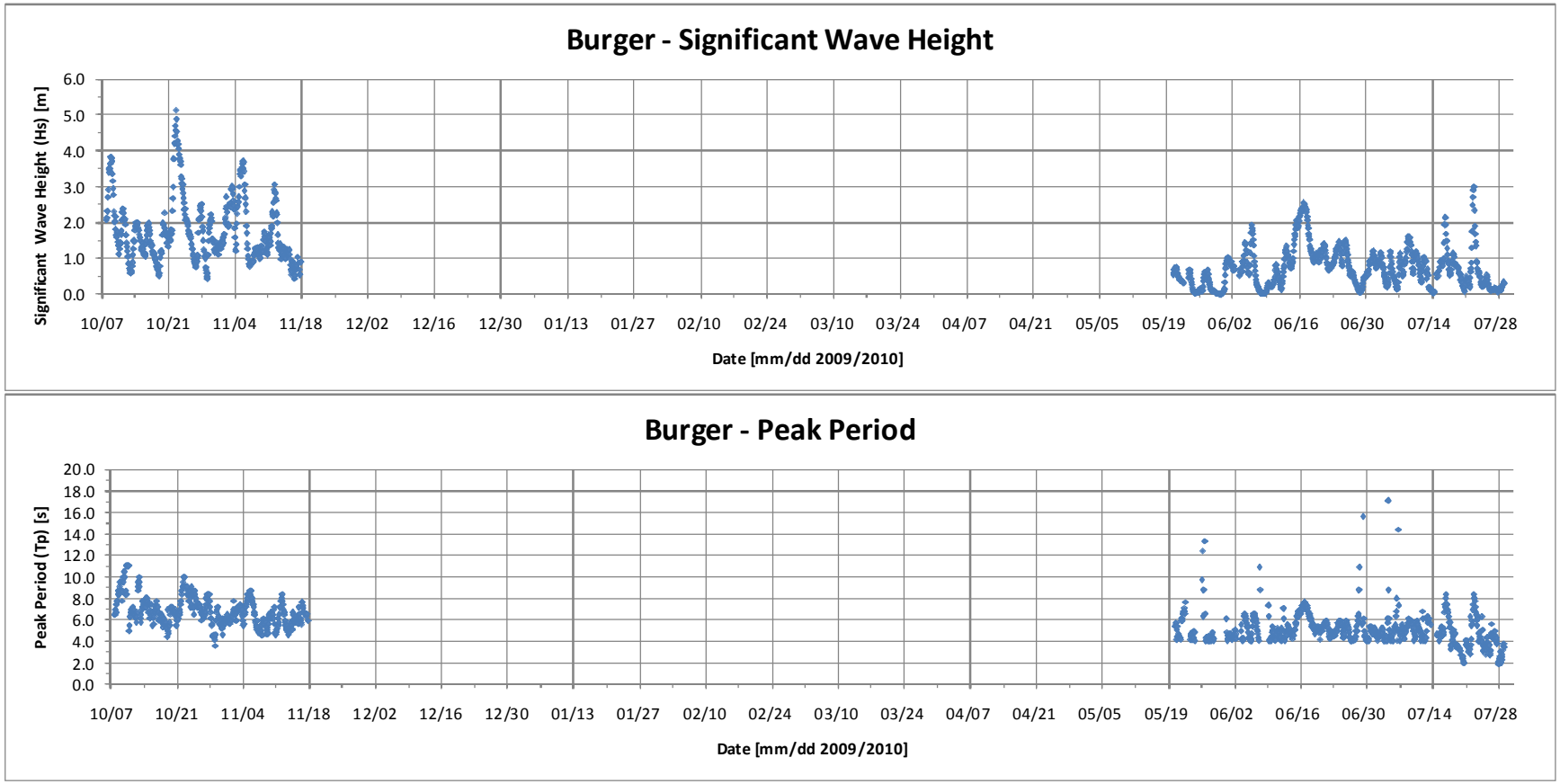

Figure 4-17. Significant wave height (H_s) and peak period (T_p) at Burger for 2009/2010.

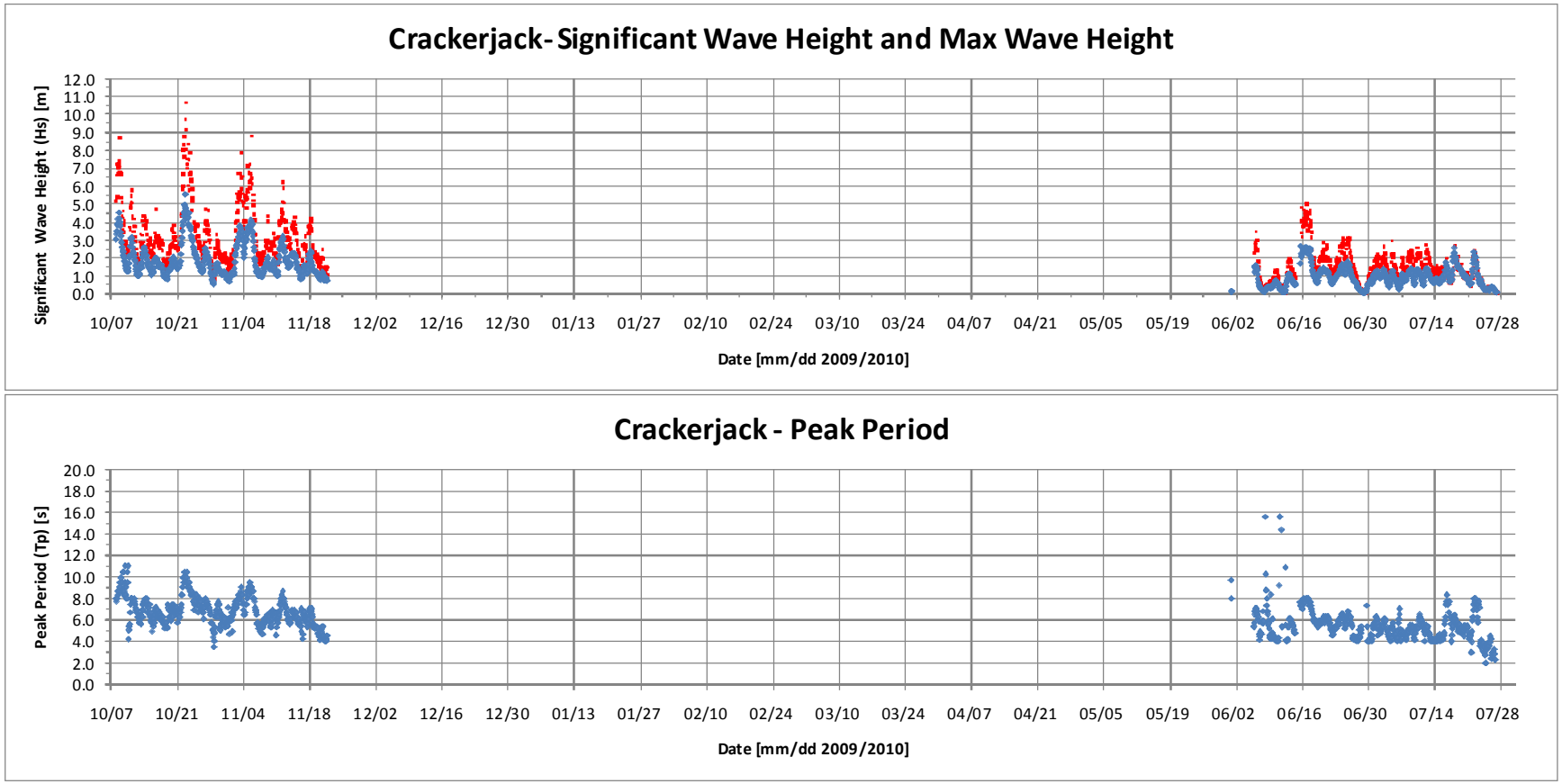

Figure 4-18. Significant wave height (Hs) (upper panel, blue marker), maximum wave height (Hmax) (upper panel, red marker) and peak period (Tp) at Crackerjack for 2009/2010.

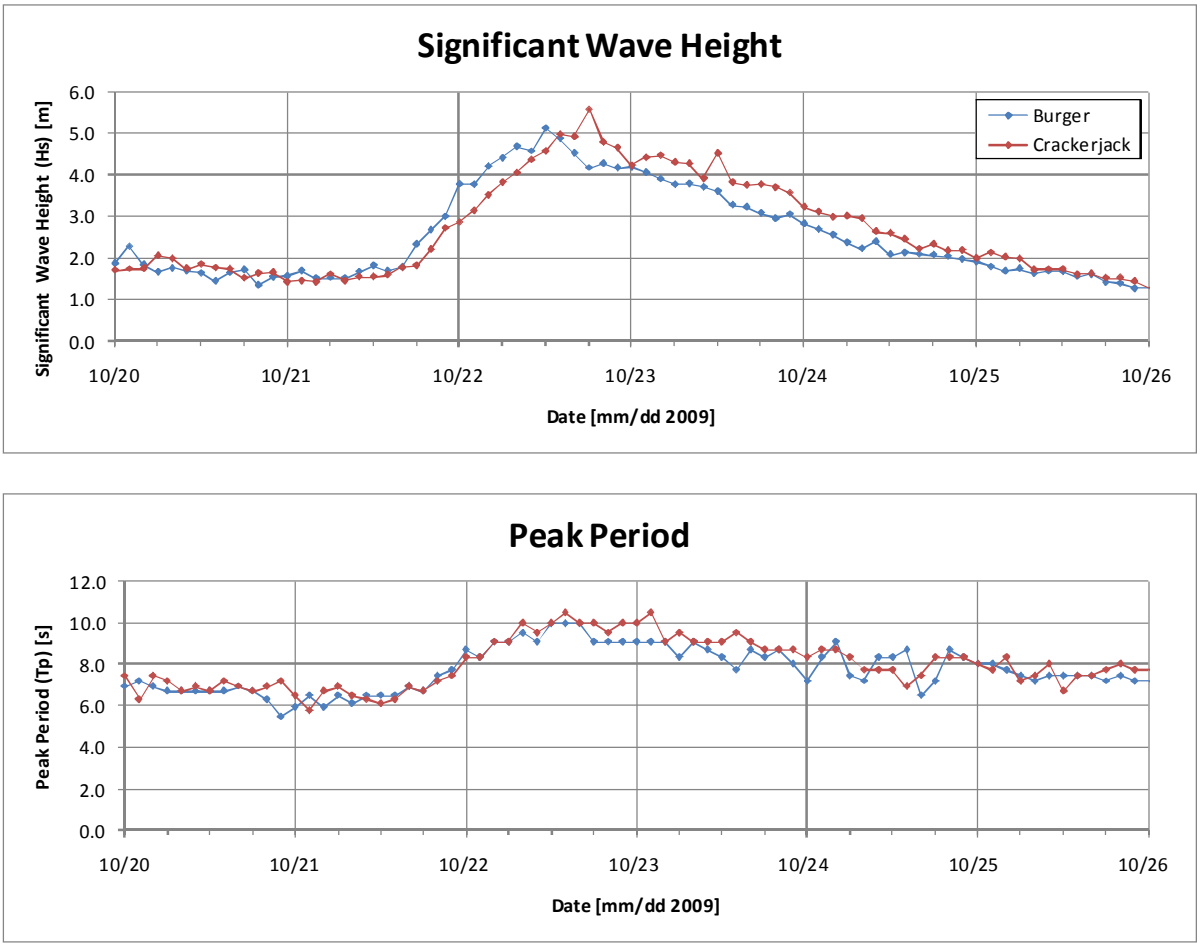

Figure 4-19. Significant wave height (Hs) and peak period (Tp) for both sites from October 20 – 26, 2009.

Table 4-16. Monthly statistics of significant wave height (Hs) and peak period (Tp) at Burger.

Date		25%	50%	mean	75%	95%	99%	max	# valid	total #
07-Oct-2009 to 31-Oct-2009	Hs (m) :	1.21	1.64	1.82	2.09	3.80	4.56	5.12	290	290
	Tp (s) :	6.1	6.9	7.1	8.0	10.0	11.0	11.0	290	290
November 2009	Hs (m) :	1.10	1.35	1.66	2.27	3.35	3.63	3.71	197	360
	Tp (s) :	5.6	6.1	6.3	6.9	8.0	8.7	8.7	197	360
December 2009	Hs (m) :								0	372
	Tp (s) :								0	372
January 2010	Hs (m) :								0	372
	Tp (s) :								0	372
February 2010	Hs (m) :								0	336
	Tp (s) :								0	336
March 2010	Hs (m) :								0	372
	Tp (s) :								0	372
April 2010	Hs (m) :								0	360
	Tp (s) :								0	360
May 2010	Hs (m) :	0.08	0.22	0.31	0.52	0.76	1.01	1.04	128	372
	Tp (s) :	4.1	4.6	5.2	5.7	7.7	12.4	13.3	77	372
June 2010	Hs (m) :	0.49	0.83	0.90	1.20	2.19	2.45	2.55	349	360
	Tp (s) :	4.4	5.1	5.3	5.7	7.3	8.8	15.6	321	360
01-Jul-2010 to 29-Jul-2010	Hs (m) :	0.29	0.63	0.70	0.94	1.58	2.70	2.99	328	337
	Tp (s) :	4.0	4.7	4.8	5.4	7.4	8.3	17.1	310	337

Table 4-17. Joint Frequency Table of H_s vs. T_p at Burger.

Location: Burger
Instrument: IPS5-052
For period: 2009/10/07 20:00:04 to 2010/07/29 02:06:35

		Hs (m)												
Tp (s)		0.00 to 0.50	0.50 to 1.00	1.00 to 1.50	1.50 to 2.00	2.00 to 2.50	2.50 to 3.00	3.00 to 3.50	3.50 to 4.00	4.00 to 4.50	4.50 to 5.00	5.00 to 5.50	5.50 to 6.00	Row Total (%)
0.00	1.00													0.00
1.00	2.00	0.42												0.42
2.00	3.00	1.59												1.59
3.00	4.00	2.85	1.76											4.60
4.00	5.00	8.12	17.57	4.35	0.25									30.29
5.00	6.00	1.76	7.28	13.39	2.26									24.69
6.00	7.00	2.18	2.93	5.44	5.19	3.43	0.33							19.50
7.00	8.00	0.50	0.42	0.92	2.43	2.59	2.09	0.50	0.08					9.54
8.00	9.00	0.33	0.08	0.17	0.84	1.09	0.92	1.00	1.09					5.52
9.00	10.00	0.08	0.59		0.08	0.25	0.08	0.08	0.33	0.59	0.33	0.08		2.51
10.00	11.00	0.17			0.25									0.42
11.00	12.00			0.50										0.50
12.00	13.00	0.08												0.08
13.00	14.00	0.08												0.08
14.00	15.00	0.08												0.08
15.00	16.00	0.08												0.08
16.00	17.00													0.00
17.00	18.00	0.08												0.08
18.00	19.00													0.00
19.00	20.00													0.00
Column Total (%)		18.41	30.63	24.77	11.30	7.36	3.43	1.59	1.51	0.59	0.33	0.08	0.00	

Filename: Burger_HsTp.dat
Max Hs: 5.12 m
Mean Hs: 1.20 m
non-flagged Hs records: 1292
non-flagged Tp records: 1195

Table 4-18. Monthly statistics of significant wave height (Hs) and peak period (Tp) at Crackerjack.

Date		25%	50%	mean	75%	95%	99%	max	# valid	total #
08-Oct-2009 to 31-Oct-2009	Hs (m) :	1.28	1.65	1.95	2.26	4.22	4.78	5.57	287	287
	Tp (s) :	6.3	6.9	7.2	8.0	9.5	10.5	11.0	287	287
November 2009	Hs (m) :	1.15	1.53	1.81	2.25	3.68	3.87	4.12	250	360
	Tp (s) :	5.6	6.3	6.4	7.2	8.7	9.1	9.5	250	360
December 2009	Hs (m) :								0	372
	Tp (s) :								0	372
January 2010	Hs (m) :								0	372
	Tp (s) :								0	372
February 2010	Hs (m) :								0	336
	Tp (s) :								0	336
March 2010	Hs (m) :								0	372
	Tp (s) :								0	372
April 2010	Hs (m) :								0	360
	Tp (s) :								0	360
May 2010	Hs (m) :								0	372
	Tp (s) :								0	372
June 2010	Hs (m) :	0.37	0.74	0.90	1.26	2.38	2.52	2.65	292	360
	Tp (s) :	4.8	5.7	5.9	6.3	8.0	10.9	15.6	267	360
01-Jul-2010 to 27-Jul-2010	Hs (m) :	0.61	0.87	0.92	1.19	1.74	2.26	2.56	314	314
	Tp (s) :	4.2	4.9	5.0	5.5	7.4	8.0	8.3	311	314

Table 4-19. Joint Frequency Table of H_s vs. T_p at Crackerjack.

Location: Crackerjack
Instrument: IPS5-049
For period: 2009/10/08 02:00:01 to 2010/07/27 04:08:49

		Hs (m)												
Tp (s)		0.00 to 0.50	0.50 to 1.00	1.00 to 1.50	1.50 to 2.00	2.00 to 2.50	2.50 to 3.00	3.00 to 3.50	3.50 to 4.00	4.00 to 4.50	4.50 to 5.00	5.00 to 5.50	5.50 to 6.00	Row Total (%)
0.00	1.00													0.00
1.00	2.00	0.18												0.18
2.00	3.00	0.99	0.09											1.08
3.00	4.00	1.70	0.63											2.33
4.00	5.00	3.68	13.45	3.32	0.09									20.54
5.00	6.00	1.97	8.43	14.71	1.97	0.27								27.35
6.00	7.00	0.54	1.52	10.31	8.07	2.51	0.45							23.41
7.00	8.00	0.45	0.81	1.43	3.86	4.57	1.97	0.45						13.54
8.00	9.00	0.18		0.36	0.27	1.52	1.17	1.97	1.52	0.18	0.09			7.26
9.00	10.00	0.18		0.18	0.18		0.18	0.27	0.90	0.81	0.45		0.09	3.23
10.00	11.00	0.18		0.09		0.18				0.09	0.09			0.63
11.00	12.00			0.09	0.09									0.18
12.00	13.00													0.00
13.00	14.00													0.00
14.00	15.00	0.09												0.09
15.00	16.00	0.18												0.18
16.00	17.00													0.00
17.00	18.00													0.00
18.00	19.00													0.00
19.00	20.00													0.00
Column Total (%)		10.31	24.93	30.49	14.53	9.06	3.77	2.69	2.42	1.08	0.63	0.00	0.09	

Filename: CJ_HsTp.dat
Max Hs: 5.57 m
Mean Hs: 1.40 m
non-flagged Hs records: 1143
non-flagged Tp records: 1115

Table 4-20. Percent exceedance tables of significant wave height (Hs) for Burger and Crackerjack.

Burger			Crackerjack		
Instrument: IPS5-052			Instrument: IPS5-049		
2009/10/07 20:00:04 to 2010/07/29 02:06:35			2009/10/08 02:00:01 to 2010/07/27 04:08:49		
# non-flagged Hs records: 1292			# non-flagged Hs records: 1143		
# non-flagged Tp records: 1195			# non-flagged Tp records: 1115		
Hs (m)	**# Exceeding**	**% Exceedance**	**Hs (m)**	**# Exceeding**	**% Exceedance**
0.00	1292	100.00	0.00	1143	100.00
0.25	1104	85.45	0.25	1074	93.96
0.50	975	75.46	0.50	1000	87.49
0.75	805	62.31	0.75	868	75.94
1.00	609	47.14	1.00	722	63.17
1.25	434	33.59	1.25	531	46.46
1.50	313	24.23	1.50	382	33.42
1.75	238	18.42	1.75	269	23.53
2.00	178	13.78	2.00	220	19.25
2.25	134	10.37	2.25	160	14.00
2.50	90	6.97	2.50	119	10.41
2.75	69	5.34	2.75	92	8.05
3.00	49	3.79	3.00	77	6.74
3.25	42	3.25	3.25	58	5.07
3.50	30	2.32	3.50	47	4.11
3.75	20	1.55	3.75	36	3.15
4.00	12	0.93	4.00	20	1.75
4.25	7	0.54	4.25	13	1.14
4.50	5	0.39	4.50	8	0.70
4.75	2	0.15	4.75	4	0.35
5.00	1	0.08	5.00	1	0.09
5.25	0	0.00	5.25	1	0.09
5.50	0	0.00	5.50	1	0.09
5.75	0	0.00	5.75	0	0.00
6.00	0	0.00	6.00	0	0.00

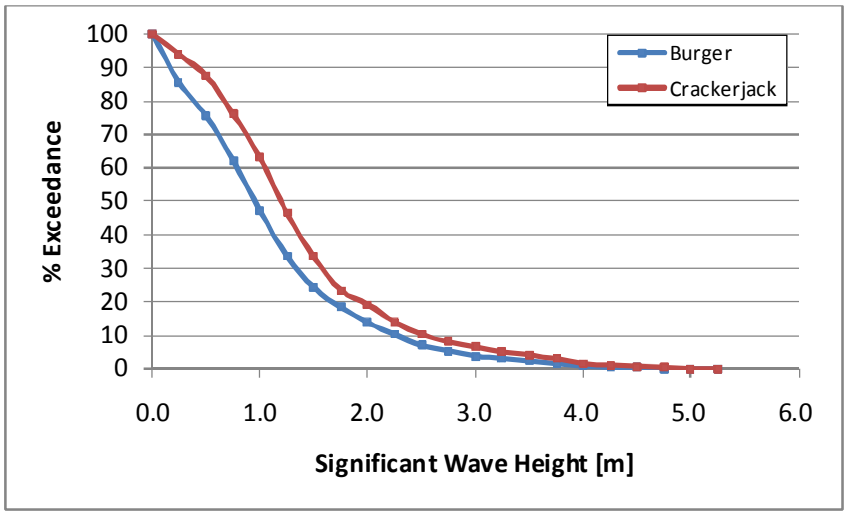

Figure 4-20. Percent exceedance plot of significant wave height (H_s) for both sites.

5 SUMMARY AND CONCLUSIONS

A program of ice keel depth and ice velocity measurements was carried out in the Chukchi Sea, within Shell's lease acreage from October 2009 to July 2010. The data collection program involved the deployment and operation of pairs of IPS5s and ADCPs at two sites in depths of approximately 45 m for nearly 10 months.

At each measurement site, an Ice Profiling Sonar (IPS5) instrument was operated to provide ice draft measurements at one- or two- second intervals. The IPS5 also provided non-directional wave measurements at 2 Hz sampling rates. Ice velocity measurements, at 30 minute sampling intervals, were obtained from Acoustic Doppler Current Profilers (ADCP), which also provided ocean current profile data.

5.1 OVERVIEW OF THE 2009-2010 ICE SEASON

Ice conditions in the region were reduced or lighter than normal with the September 2009 ice edge well north of its median position. The region has a very dynamic ice regime with ice movement occurring 97% of the time at both Burger and Crackerjack from November 2009 to June 2010. Ice features having large vertical drafts, of up to 53% and 58% the total water depth, were observed from December until May at Burger and Crackerjack, respectively. Thousands of Ice keels with horizontal dimensions of typically 30-35 m, up to a few hundred meters, were observed. The great majority of these ice keels are individual ice keel features which a few of the very widest keels representing massively deformed features. As was seen in the 2008-2009 data sets, the ice proved to be quite mobile, with only the months of January thru April for Burger and Crackerjack having more than 1% no-motion events. The greatest percentage of no-motion events for a month in this measurement period was 12% at Burger in March 2010, in contrast to 20% which happened in February 2010 at Crackerjack for the 2009-2010 measurement period.

The results from this measurement period were obtained during the two years with the historically third and fourth smallest summer ice retreat. Extensive open water conditions existed in the study area until late November 2009 and ice clearing began in late May, but some ice remained in the vicinity of Burger until early August.

5.2 DEEPEST ICE KEELS

Very deep ice keels were observed at both Burger and Crackerjack with 9 keels at Burger and 18 keels at Crackerjack measuring over 20 m ice draft. The deepest keels at Burger and Crackerjack were 26.1 m and 23.7 m respectively.

Keels exceeding 12 m ice draft were measured in all months from December 2009 to May 2010 at both sites and in June 2010 at Crackerjack. From the distance of ice passage (derived for ice velocity measurements in the November to late July period), the total distances of sea ice passing by Burger and Crackerjack were 2202 and 2194 km. Ice keels

having threshold drafts of 5, 8 and 11 m were individually identified and statistics on these were compiled. The total number of ice keels greater than 5, 8 and 11 m were 7345, 2273 and 626 respectively for Burger and 8363, 2726 and 808 for Crackerjack. The average widths of the individual ice 5, 8 and 11 m keels were 30.9, 35.1 and 40.3 m for Burger and 29.0, 33.4 and 39.4 m for Crackerjack.

By comparison to the first year of measurements, 2008-2009, there was a notable reduction in both sites for the total number of keels and the total distance of ice measured (in 2008-2009, the number of keels > 5 m ice draft were 13,628 and 12,924 and the total ice distance was 3352 and 3318 km, at Burger and Crackerjack, respectively). The maximum keel ice draft measured in 2008-2009 was 27.0 and 27.7 m at Burger and Crackerjack, respectively.

5.3 WIDEST ICE KEELS

There were occurrences of ice keels with very large horizontal dimensions of up to a few hundred meters and large maximum keel depths. Detection of keels and their beginning and ending positions are determined by objective criteria as outlined in section 4. The widest keels, using a threshold of 5 m, were 273 m for Burger and 262 m for Crackerjack. Arguably, the widest keels in the entire data sets could be considered to be part of rubble ice fields, in particular the widest keel at the Crackerjack site. More advanced analysis methods to distinguish between different ice deformation processes such as singular large keels and rubbled and/or hummocky ice are recommended for further investigation of these very extensive Ice Profiler data sets.

5.4 ICE VELOCITY

Over ten occurrences of large ice velocities were measured throughout the year with peak ice velocities 87 cm/s at Burger and 64 cm/s at Crackerjack. This is considerably less than the 2008-2009 peak ice speeds exceeding 119 cm/s at Burger and 109 cm/s at Crackerjack. The episodes of large ice velocities were associated with strong wind events having peak speeds of 5 to 9 m/s (10 to 18 knots). At both sites, the median ice drift was generally highest in November and December (17-28 cm/s) and lower (~10 cm/s) from January to July. The lone exception is June 28 cm/s for Crackerjack. The highest median speeds of the 2008-2009 data were almost twice as large at 20-50 cm/s.

5.5 OCEAN CURRENTS

Ocean currents were characterized by large events during which speeds exceeded 40 cm/s at Burger. Currents at Crackerjack were weaker than those observed at Burger with events rarely exceeding 40 cm/s. From September to late December, current speeds were typically large and associated with strong wind events that were at times greater than 8 m/s as measured at Wainwright. During January the currents were lower typically lower except for a large event late in the month. Currents then generally stayed weak for the rest of the ice season. As was seen in the ice velocities, the currents during the 2008-2009 measurement

period were generally larger, with a number of events greater than 50 cm/s observed at both Burger and Crackerjack.

Surface current direction at Burger aligned along an E-W axis, were more variable than the surface currents at Crackerjack which were predominantly to the NE. Mid-depth and near-bottom current directions were less variable than the surface and were predominately towards the ESE and NE for Burger and Crackerjack respectively. The same directionality was observed with the 2008-2009 data sets. These current directions are likely influenced by the local topography, the inflows from the Pacific Ocean and by offshore winds. The current directions at Burger and Crackerjack are similar to the mean flows observed by Weingartner et al. (2009) where the main water flow coming in from the Pacific bifurcates and flows around the west and southern parts of Hanna Shoal.

Inertial oscillations are present in the ocean current data during the times of reduced or zero ice concentrations. These twice-daily ocean current variations produced a peak to trough current variation of up to 35 cm/s, and they appeared to be more prevalent at Crackerjack.

5.6 OCEAN WAVES

The acoustic range data from the ASL Ice Profiler was used to derive information on ocean waves when sea ice was not present. In October 2009, there were three storms when the significant wave heights approached or exceeded 4 m. The largest wave heights occurred between 2009/10/21 and 2009/10/24, where the wave heights at the Crackerjack site reached a maximum significant wave height value of 5.6 m (10.9 m maximum individual wave height) with a corresponding peak period of 10s. At the Burger site, the maximum significant wave height was measured at 5.1 m. During this event, wind speeds at Point Lay exceeded 19 knots for several hours. For all non-ice measurement times, the average wave heights were 1.2 m at Burger and 1.4 m at Crackerjack.

5.7 RECOMMENDATIONS

Further analyses of this one year data set may be useful to extract further information on the properties of the sea ice regime in the Eastern Alaskan Beaufort Sea lease areas. Possibilities for further analysis are provided below:

(1) **Additional wave analysis using a combined analysis of winds** (NCEP-2 Reanalysis winds along with the Point Lay and Wainwright weather stations) and the measured non-directional wave parameters and wave spectra to estimate wave directions and to examine the fetch and duration scales applicable to the generation of the measured waves.

(2) **Compute the frequency and properties of Rubbled and Hummocky Ice from the ice distance series.** Rubbled and hummocky ice can pose operational threats that are comparable to those presented by large ice ridges and keels. The statistics of rubbled and hummocky ice will be derived using existing software developed for this purpose.

(3) **Prepare Joint-Bivariate Distributions of ice keel drafts (e.g. > 5m, > 8 m, > 11 m) and ice speeds, for each site.**
An important factor is statistics on ice drift direction persistence and the rates of change in ice drift direction (i.e.: the radius of curvature), for example, for tanker loading and supply vessel offloading considerations. This can be readily done for the full record, and by individual months using software that already available. It is also proposed to investigate whether the occurrence of deep-draft features is statistically independent of drift speed. From a statistical test of the null hypothesis that deep-draft features are not dependent on ice drift speed, using the data compiled for this task, the hypothesis will be tested.

(4) **Compute the radius of curvature of ice drift from the x- and y-displacement values derived from the vector velocity time series.**
From these x- and y-displacement values, the radius of curvature can be computed as a function of time. Occurrences of events for the radius of curvature values, ranging from being comparable to the vessel length to an order of magnitude greater than the hull length, will be identified and statistics on the frequency of occurrence and persistence of such events will be prepared by radius categories. An analysis of joint-bivariate distributions of radius of curvature and drift speed will also be prepared; it will be useful to examine if they have a negative correlation, and make the offloading operations manageable**.**

6 LITERATURE CITED

Amundrud, T., H. Melling and R. Ingram. 2004. Geometrical constraints on the evolution of ridged sea ice. *Journal of Geophysical Research* 109(C6): doi: 10.1029/2003JC002251. issn: 0148-0227.

ASL Environmental Sciences Inc., 2000. Analyses of Ice Keel and Ice Velocity Data Sets (1996 to 1999) from Offshore Sakhalin Island, D.B. Fissel, ed. Report for Sakhalin Energy Investment Company Ltd., by ASL Environmental Sciences Inc., Sidney, B.C. Canada. ix +124p.

Barber, D. G., R. Galley, M. G. Asplin, R. De Abreu, K.-A. Warner, M. Pućko, M. Gupta, S. Prinsenberg, and S. Julien (2009), Perennial pack ice in the southern Beaufort Sea was not as it appeared in the summer of 2009, Geophys. Res. Lett., 36, L24501, doi:10.1029/2009GL041434.

Barnes, P.W., J.L. Asbury, D.M. Rearic and C.R Ross. 1987. Ice erosion of a sea-floor knickpoint at the inner edge of the stamukhi zone, Beaufort Sea, Alaska. *Marine Geology*, 76(3): 207-222.

Barrett, S.A., and W.J. Stringer. 1978. Growth Mechanisms of "Katie's Floeberg". *Arctic and Alpine Research*, 10(4): 775-783.

Belliveau, D.J., G.L. Bugden, B.M. Eid and C.J. Calnan, 1990. Sea ice velocity measurements by upward-looking Doppler current profilers. *J. Atmos. Oceanic Technol.*, 7(4): 596-602.

Fissel, D.B., J.R. Marko and H. Melling, 2008. Advances in Upward Looking Sonar Technology for Studying the Processes of Change in Arctic Ocean Ice Climate. Paper to be published in the Journal of Operational Oceanography and presented at the Oceanology International Conference, London UK, 12 March 2008.

Fissel, D.B., J.R. Marko, T. Mudge, E. Ross, A. Kanwar, J. Lawrence, K. Borg, M. Martínez de Saavedra Álvarez, and D. Billenness, 2009. Analysis of Ice Keel Depth, Ice Velocity and Ocean Current Profile Measurements Offshore of Camden Bay, N.E. Alaska, 2007-2008. Report for Shell Alaska Exploration, Houston TX, USA, and IMV Projects, Calgary AB, Canada by ASL Environmental Sciences Inc., Sidney, B.C. Canada. xiii + 140 p. + appendices.

Garrison G.R., R.E. Francois and T. Wen. 1991. Acoustic reflections from Arctic ice at 15-300 kHz. *J. Acoust. Soc. Amer.* 90(2): 973-984.

Hudson, R.D., G.R. Pilkington, and M. Metge, 1981. Extreme ice features along the northwest edge of the Canadian Arctic Archipelago. Workshop on ice action on shores, J.C. Dionne ed., National research Council, pp.15-34.

Kovacs, A., and M. Mellor. 1974. Sea ice morphology and ice as geological agent in the southern Beaufort Sea. In: *The Coast and Shelf of the Beaufort Sea,* 113-161. Proceedings of a Symposium on Beaufort Sea and Shelf *Research*. J.C. Reed and J.A. Sater, Ed. The Arctic Institute of North America: Virginia.

Melling, H., P.H. Johnston and D.A. Riedel, 1995. Measurements of the underside topography of sea ice by moored subsea sonar. *J. Atmospheric and Oceanic Technology,* 13(3): 589-602.

Melling, H. 2008. Science Cruise Report – CCGS Sir Wilfrid Laurier, September – October, 2008. Unpublished report, Institute of Ocean Sciences, Department of Fisheries and Oceans, Sidney B.C.

Melling, H. 2009. Science Cruise Report – CCGS Sir Wilfrid Laurier, September – October, 2009. Unpublished report, Institute of Ocean Sciences, Department of Fisheries and Oceans, Sidney B.C.

Myers, J.J., C.H. Holm and R.F. McAllister, Ed. 1969. *Handbook of Ocean and Underwater Engineering*. New York: McGraw-Hill Book Co.

Norton and Gaylord, 2004. Drift Velocities of Ice Floes in Alaska's Northern Chukchi Sea Flaw Zone: Determinants of Success by Spring Subsistence Whalers in 2000 and 2001. *Arctic,* 57 (4), 347-362.

Stringer, W.J., and J.E. Groves. 1991. Local and Areal Extents of Polynyas in the Bering and Chukchi Seas. *Arctic*, 44(1): 164-171.

Urick, R.J., 1983. *Principles of Underwater Sound,* Third Edition. New York: McGraw-Hill, Inc. 423 p.

Vaudrey, K., 1987. 1985-86 Ice Motion measurements in Camden Bay, AOGA Project 328, Vaudrey & Associates, Inc. San Luis Obispo, CA.

Weingartner, T., K. Aagaard, D. Cavalieri, S. Danielson, M. Kulakov, V. Pavlov, A. Roach, Y. Sasaki, K. Shimada, T. Whitledge, and R. Woodgate, 2009. Chukchi Sea Circulation. *http://www.ims.uaf.edu/chukchi/*

Woodgate, R.A., K. Aagaard, J.H. Swift, K.K. Falkner and W.M. Smethie Jr, 2005. Pacific Ventilation of the Arctic Ocean's Lower Halocline by Upwelling and Diapycnal Mixing Over the Continental Margins. *Geophys. Res. Lett.*, 32, L18609, doi:10.1029/2005GL023999.